MAGNETIC RESONANCE STUDIES OF THE BINDING SITE INTERACTIONS BETWEEN ^{19}F LABELLED NITROPHENYL HAPTENS AND SPECIFIC MOUSE MYELOMA IMMUNOGLOBULIN MOPC-315

I. GENERAL INTRODUCTION

II. CHEMICAL SHIFT AND BINDING STUDIES OF THE INTERACTION BETWEEN ^{19}F LABELLED NITROPHENYL HAPTENS AND MOUSE MYELOMA IMMUNOGLOBULIN MOPC-315

III. PERTURBATION MIXING AS A TECHNIQUE FOR STUDYING BINDING DYNAMICS IN BIOLOGICAL SYSTEMS. INTERACTION OF MOPC-315 WITH ^{19}F LABELLED NITROPHENYL HAPTENS

IV. pH AND DOUBLE RESONANCE STUDIES OF ^{19}F LABELLED NITROPHENYL HAPTENS BINDING TO MOUSE MYELOMA IMMUNOGLOBULIN MOPC-315

Thesis by

Dale A. Kooistra

In Partial Fulfillment of the Requirements

for the Degree of

Doctor of Philosophy

California Institute of Technology

Pasadena, California

1978

(submitted October 12, 1977)

ACKNOWLEDGEMENT

I would like to gratefully acknowledge my research advisor, Professor John H. Richards. I would like to thank him for the freedom to explore my own capabilities, and for encouragement and intellectual guidance when I needed them.

I would like to thank the members of this research group for creating an environment that was both enjoyable and stimulating. A special thanks to Dr. Stephen Smallcombe for his advice on NMR theory and techniques. A word of appreciation to Dave Collier and Jack Welch for their assistance, and to Professor Michael Raftery for allowing me to use his fluorescence spectrophotometer.

Finally, I would like to acknowledge the National Institutes of Health and California Institute of Technology for their financial support.

Part I ABSTRACT

This section presents an introduction and brief review of the literature on immunoglobulin structure and their binding to antigens (haptens). This section also presents some general comments about the approach and objectives of this thesis.

Part II

ABSTRACT

The interactions between MOPC-315, a mouse myeloma protein with specificity for nitrophenyl haptens, and ^{19}F substituted haptens have been investigated using nuclear magnetic resonance (NMR) spectroscopy. The haptens studied are mono- or dinitrophenyl derivatives of γ-aminobutyric acid, lysine, or glycine that have trifluoromethyl groups attached to the phenyl rings. Upon binding to immunoglobulin, the ^{19}F nucleus experiences a downfield shift whose magnitude depends on the position of the trifluoromethyl group on the phenyl ring but is independent of other structural changes in the hapten such as the number of nitro groups attached to the phenyl ring. Further, the chemical shift of bound hapten is not influenced by the amount of the constant region attached to the binding site; we accordingly conclude that the presence of the distal, constant regions of the immunoglobulin molecule does not influence binding site interactions.

Part III

ABSTRACT

We have studied the dynamics of binding of ^{19}F labelled haptens by mouse plasmacytoma antibody MOPC-315, a protein which shows specificity for nitrophenyl haptens. The off rates for the dissociation of hapten from MOPC-315 proteins (7S, Fab' and Fv) were determined by the application of a novel technique, perturbation mixing, which allows the direct determination of the rate of exchange of nuclei between magnetically non-equivalent sites without requiring prior knowledge of intrinsic line widths. Used in conjunction with independently determined data on line widths, chemical shifts, and binding affinities these studies show that the rates for hapten association to, or dissociation from, the intact 7S, the Fab' fragment, and the Fv fragment of MOPC-315 are essentially the same. They also indicate the presence, probably in the Fv region, of a low affinity ($K_a \sim 10^3\ M^{-1}$) site(s) for hapten binding. The mobility of the hapten combining site decreases as the size of the protein increases (Fv > Fab' > 7S). These rate data, which were determined at relatively high protein concentrations, (up to 40 mg/ml) agree with on rates determined at much lower protein concentrations ($\leq$ 1 mg/ml); we therefore conclude that protein aggregation if it does occur it does not significantly affect binding in these systems.

Part IV ABSTRACT

Fluorine nuclear magnetic resonance (NMR) is used to explore the binding site of MOPC-315 immunoglobulin. The pH dependence of the chemical shift of bound haptens shows the immunoglobulin to contain one or two groups that cause a reversible loss of binding ability when deprotonated above pH 9. Studies at low pH are hampered by precipitation of both the protein and hapten. However, the nonreversible decrease in NMR signal shows that the precipitated immunoglobulin probably contains bound hapten.

Two double resonance techniques were used to explore the chemical shift of protons near the fluorine nuclei: (i) Comparison of the chemical shift of the fluorine and proton nuclei of a CHF_2 labelled nitrophenyl hapten when bound to protein shows an upfield shift for the proton and a downfield shift for the fluorine nuclei. Thus the major cause of fluorine chemical shift cannot be diamagnetic ring currents. (ii) NOE data of DNTP-GABA and NTP-GABA bound to the Fv fragment of MOPC-315 indicate that the aromatic protons shift upfield upon binding. When used in conjunction with T_1 and T_2 relaxation times the NOE data show that there is no internal rotation for the trifluoromethyl group of DNTP-GABA and that there is slow internal rotation for the trifluoromethyl group of NTP-GABA. Studies in deuterium oxide buffer indicate

that there are no hydrogen bonds between the fluorines of DNTP-GABA and the protein binding site.

ABSTRACTS OF THE PROPOSITIONS

PROPOSITION I

A method for examining the effects of environment on the chemotactic receptors of neutrophils is proposed.

PROPOSITION II

A fluorine and proton nuclear magnetic resonance study on the contribution of the light chain to hapten binding in mouse myeloma protein MOPC-315 immunoglobulin is proposed.

PROPOSITION III

A study on reptile venom factors that interact with the first component of complement is proposed.

PROPOSITION IV

A study on the catalytic mechanism of dioldehydratase by using the kinetic isotope effect of ^{13}C labelled substrate and coenzyme.

PROPOSITION V

A method for investigating conformational changes in antibody structure due to antigen binding is proposed.

TABLE OF CONTENTS

PART I.

Page

Immunoglobulin Structure..... 2

Studies with Heterogeneous Antibodies..... 7

- Specificity of Antibody Binding..... 7
- Energetics of Binding..... 10
- Hapten Binding to Fab Fragments..... 12
- Affinity Labelling..... 13
- Other Physical Studies of Antibody Hapten Binding..... 13

Studies with Homogeneous Antibodies..... 14

- Major Sources of Homogeneous Antibodies..... 14
- Binding Specificity..... 14

General Strategies and Objectives of this Thesis..... 22

References..... 24

PART II.

Introduction..... 33

Materials and Methods..... 34

- Maintenance of MOPC-314 Plasmacytoma..... 34
- Preparation of a Nitrophenyl-Sepharose Affinity Column..... 34
- Purification of MOPC-315 Immunoglobulin..... 35
- Preparation of Fab' and Fv fragments of MOPC-315 37
- Recycling Used Protein..... 38
- Preparation of NMR Samples..... 38
- γ-N-(2,6,-Dinitro-4-trifluoromethylphenyl) aminobutyric acid, DNTP-GABA..... 40
- 2-Nitro-4-trifluoromethylchlorobenzene, NTCB.... 41
- γ-N-(2-Nitro-4-trifluoromethylphenyl) aminobutyric acid, 2NTP-GABA..... 41

Page

γ-N-(4-Nitro-2-trifluoromethylphenyl) amino-butyric acid, NTP-GABA..... 42
α-N-(2,6-Dinitro-4-trifluoromethylphenyl) amino-butyric acid, DNTP-Gly..... 43
ε-N-(4-Nitro-2-trifluoromethylphenyl)-L-lysine, NTP-Lys..... 44
ε-N-(2,6-Dinitro-4-trifluoromethylphenyl)-L-lysine, DNTP-Lys..... 45
ε-N-(2-Nitro-4-trifluoromethylphenyl)-L-lysine, 2NTP-Lys..... 46
Determination of Binding Affinities..... 46
Fluorescence Quenching..... 46
NMR Binding Determinations..... 50

Results..... 52

Binding Affinities..... 52
Chemical Shift..... 55

Discussion..... 57

Binding Affinities..... 57
Environment of Bound Ligand..... 60

References..... 67

PART III.

Introduction..... 71

General Theory..... 74

Chemical Shift-Line Width..... 74
Perturbation Mixing..... 76

Materials and Methods..... 81

Binding Affinities..... 81
Perturbation Mixing..... 84

Results..... 90

DNTP-GABA..... 90
2NTP-GABA..... 93
NTP-GABA..... 94

Page

Discussion..... 94

DNTP-GABA..... 95
2NTP-GABA..... 99
NTP-GABA..... 100
General..... 101

References..... 104

PART IV

Introduction..... 107

Materials and Methods..... 109

pH Studies..... 110
Calibration of the Decoupler..... 110
NOE Studies..... 111
Proton NMR Spectra..... 113
CHF_2-GABA..... 114
Fluorescence Quenching..... 114
γ-N-(2,6-dinitro-4-methylphenyl) aminobutyric acid, DNMP-GABA..... 115
4-Chloro-3,5-dinitrobenzyl alcohol..... 116
4-Chloro-3,5-dinitrobenzaldehye..... 117
4-Difluoromethyl-2,6-dinitrochlorobenzene..... 118
γ-N-(4-difluoromethyl-2,6-dinitrophenyl) amino-butyric acid, CHF_2-GABA..... 119

Theory..... 121

NOE..... 121

Results..... 131

pH Studies..... 131
NOE Studies..... 145
CHF_2-GABA..... 162
Fluorine Chemical Shifts in D_2O..... 165

Discussion..... 168

pH Studies..... 168
Assignment of Chemical Shifts..... 176
CHF_2- GABA..... 180
NOE..... 183
Fluorine Chemical Shifts in Deuterium Oxide..... 197

Page

Conclusion..... 199

References..... 201

PROPOSITIONS

Proposition I..... 204

Proposition II..... 208

Proposition III..... 213

Proposition IV..... 218

Proposition V..... 222

LIST OF TABLES

Part	Table	Title	Page
II	I	Binding Affinity of Fluorinated Haptens for MOPC-315 Immunoglobulin Determined by Fluorescence Quenching and NMR Spectroscopy.....	53
	II	Total Chemical Shift, Δ, of Fluorinated Haptens Bound to MOPC-315 Immunoglobulin and its Proteolytic Fragments.....	56
III	I	Binding Affinities of Various Fluorinated Haptens for MOPC-315, 7S, and Fv Fragment Measured by Fluorescence Quenching.....	83
	II	Relaxation Data and Rate Constants for Several CF_3 Labelled Nitrophenyl Haptens Binding to MOPC-315 Proteins (7S, Fab', and Fv).....	91

Part	Figure	Title	Page
I	1	Generalized Structure of an Immunoglobulin Molecule.....	6
II	1	Structure and Abbreviations of Fluorinated Nitrophenyl Haptens.....	48
	2	^{19}F NMR Spectra of DNTP-GABA Plus MOPC-315 Protein (7S, Fab', and Fv..	66
III	1	Comparison of Observed ^{19}F NMR Spectra for DNTP-GABA Bound to MOPC-315 (7S, Fab', and Fv) with Calculated Line Shapes Used to Determine Intrinsic Line Widths of Bound and Free Hapten.....	86
	2	^{19}F NMR Spectra of DNTP-GABA Plus MOPC-315 Fv Used to Determine Off Rates from Perturbation Mixing Experiment.....	88
IV	1	Energy Level Diagram for Two Spin 1/2 Nuclei that are Coupled by a Dipolar Mechanism.....	123
	2	^{19}F NMR Spectra of DNTP-GABA Plus MOPC-315 7S Monomer at Different Basic pH Values.....	133
	3	^{19}F NMR Spectra of DNTP-GABA Plus MOPC-315 7S Monomer at Different Acidic pH Values.....	135
	4	^{19}F NMR Spectra of DNTP-GABA Plus MOPC-315 Fv Fragment at Different Basic pH Values.....	137
	5	^{19}F NMR Spectra of DNTP-GABA Plus MOPC-315 Fv Fragment of Different Acidic pH Values.....	139

Part	Figure	Title	Page
	6	Variation in the Observed Chemical Shift, δ, of the ^{19}F NMR Spectra of NTP-GABA Plus MOPC-315 7S Monomer at Different pH Values.....	143
	7	NOE of an Excess of DNTP-GABA Plus the Fv Fragment of MOPC-315 when Various Regions of the Proton NMR Spectra are Saturated with a Second Radio Frequency.....	147
	8	NOE of DNTP-GABA Plus the Fv Fragment of MOPC-315 when Various Regions of the Proton NMR Spectra are Saturated with a Pulse from the Decoupler.....	149
	9	NOE of DNTP-GABA Plus the Fv Fragment of MOPC-315 in D_2O Buffer when Various Regions of the Proton NMR Spectra are Saturated with a Pulse from the Decoupler.....	151
	10	NOE of NTP-GABA Plus the Fv Fragment of MOPC-315 when Various Regions of the Proton NMR Spectra are Saturated with a Pulse from the Decoupler.....	155
	11	NOE of NTP-GABA Plus the Fv Fragment of MOPC-315 in D_2O Buffer when Various Regions of the Proton NMR Spectra are Saturated with a Pulse from the Decoupler.....	157
	12	^1H NMR Spectra (100 MHz) of MOPC-315 Fv Fragment Plus Increasing Amounts of DNMP-GABA.....	159
	13	^1H NMR Spectra (220 MHz) of MOPC-315 Fv Fragment Plus Increasing Amounts of DNMP-GABA.....	161

Part	Figure	Title	Page
	14	^{1}H NMR Spectra (100 MHz) of MOPC-315 Fv Fragment Plus Increasing Amounts of DNTP-GABA.....	164
	15	Change in Line Wdith of the Fluorine NMR Specta of CHF_2-GABA Bound to the Fv Fragment of MOPC-315 when Different Regions of the Proton Spectra are Saturated with a Second Radio Frequency.....	166

PART I

General Introduction

INTRODUCTION

I. Immunoglobulin Structure

In the late 1950's Edelman (Edelman, 1959; Edelman and Poulek, 1961) began the studies that elucidated the molecular composition of antibodies. By studying the effects of reducing agents on antibody structure, Edelman (Edelman, 1973) showed that immunoglobulins are composed of four peptide chains, two identical light (L) chains (M.W. $\sim$ 25,000) and two identical heavy (H) chains (M.W. 50,000-70,000). The heavy chains are divided into five types, α, γ, δ, ε, and μ, that determine the class to which an immunoglobulin belongs (IgA, IgG, IgD, IgE, and IgM) (Edelman and Gall, 1969). There are two major types of light chains (λ and κ), and they are distributed throughout the immunoglobulin classes.

The heavy chains are composed of four or five homology units each consisting of about 110 amino acids and containing an internal disulfied bond. The N-terminal homology unit, or domain, contributes the heavy chain's portion to the binding site. This N-terminal domain is termed the variable region because its amino acid sequence varies for antibodies with different specificities. The other three or four domains are constant for a given class and subclass and are known as constant regions. The light chains have only two domains. The N-terminal, is again variable in amino acid sequence and comprises part

of the binding pocket, while the C-terminus is constant within a light chain class. Several regions of the variable domain of both the heavy and light chains show greater amino acid heterogenity. These three to four regions (5-10 amino acids per region) per chain of increased variability are known as hypervariable regions (Wu and Kabat, 1970; Capra and Kehoe, 1975). X-ray structure data have shown that the amino acids of the hypervariable regions line the hapten (antigen) binding pocket.

Porter (Porter, 1959) approached immunoglobulin structure by using papain in the presence of crysteine to obtain limited cleavage fragments. He used ion exchange chromatography to separate the digest products into three fractions.[1] Two of these fractions have a molecular weight of 45,000 and contain the binding site of the native antibody. These fractions, which make up approximately two-thirds of the original immunoglobulin, are called Fab fragments for fragment antibody binding. The other fraction, which accounts for one-third of the immunoglobulin mass, has a molecular weight of 50,000, and is called Fc, fragment crystallizable because it is

---

[1]Three fractions are obtained because of charge differences in the Fab fragments derived from heterogeneous antibodies.

easily crystallized.

Nisonoff (Nisonoff et al., 1960b) treated antibody molecules with pepsin and obtained a 100,000 molecular weight fragment that contains both binding sites. When this fragment is treated with a disulfied reducing agent, monovalent antigen binding fragments are obtained. These monovalent fragments are similar to the Fab fragments produced by papain digestion, but they have slightly larger molecular weight. This bivalent fragment obtained from the pepsin digest is called $F(ab')_2$, and the monovalent fragment obtained after reduction is called Fab' after the corresponding papain fragment.

The area between the Fab and Fc fragments, which is highly susceptible to proteolytic cleavage, is called the hinge region.

The cross reactivity of antibodies directed against the Fc and Fab fragments with light and heavy chains led Porter and co-workers (Fleischman et al., 1963) to conclude that the Fc fragment consisted of only heavy chain fragments, but the Fab fragment contained both heavy and light chain fragments. This led Porter to propose the Y shaped structure similar to the one pictured in Figure 1.

Figure 1

Generalized structure of an immunoglobulin molecule.

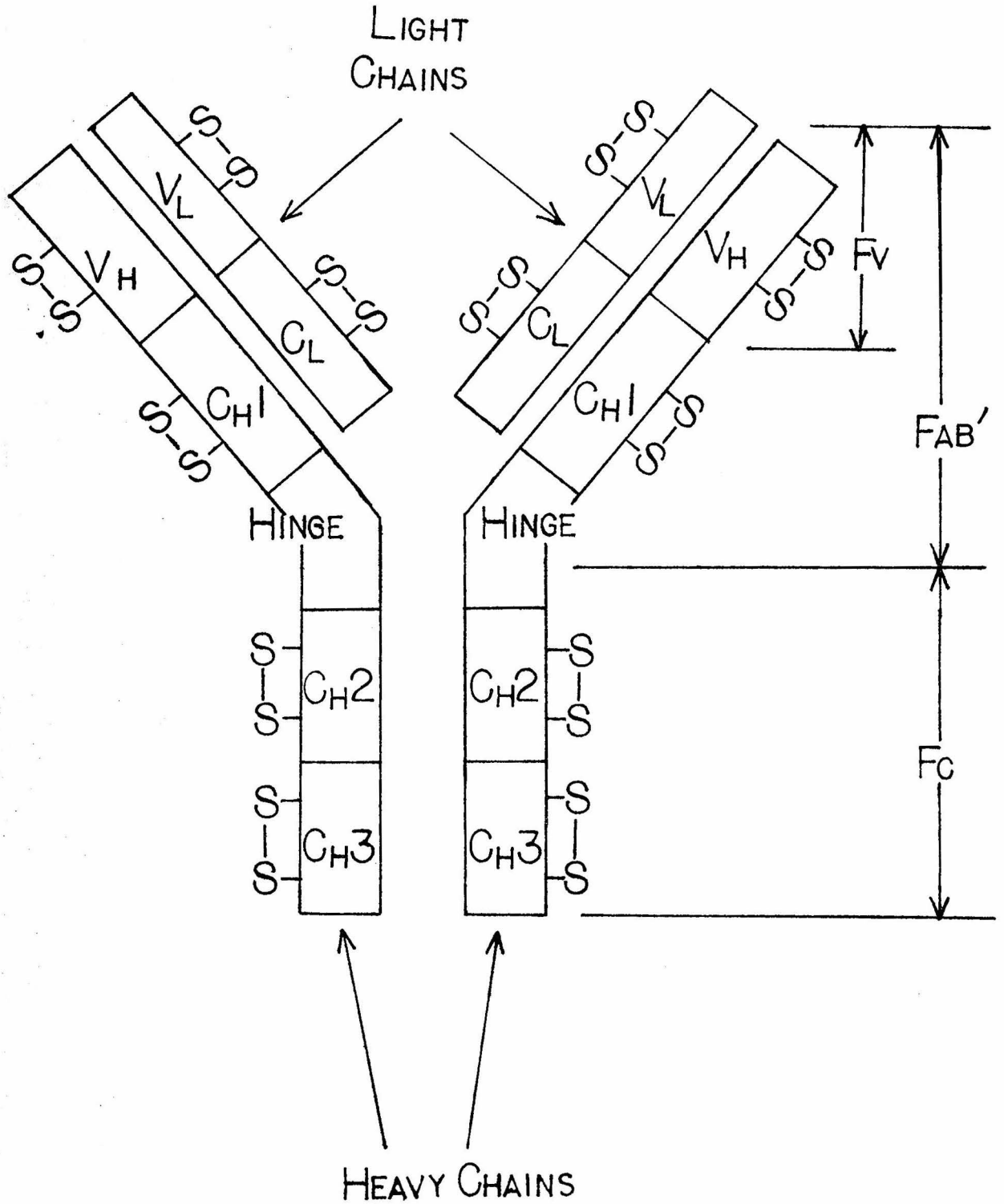
LIGHT CHAINS
S-S
VL
VH
CL
CH1
HINGE
CH2
CH3
Fv
FAB'
Fc
HEAVY CHAINS

Electron micrographs of antibodies with their antigen provide a visual picture of the Y shape (Valentine and Green, 1967) and the flexibility of the Fab arms (Feinstein and Rowe, 1965). X-ray diffraction studies (recently reviewed by Davies et al., 1974) are also consistent with this structure.

Crystallographic structure of an intact human IgG antibody Kol and human Fc fragment reveal less domain interaction then previously seen in crystallographic structures of the Fab' fragments (Huber et al., 1976). The authors suggest that this difference in domain interaction may be indicative of an antigen induced conformation change. The crystal structure of the Fab fragment having a conformation analogous to the antibody in the bound state. Further discussion of the interaction between the Fab and Fc portions of the immunoglobulin is also given in Section II-C and III-B-1.

II. Studies with Heterogeneous Antibodies

A. Specificity of Antibody Binding

Small molecules (haptens) attached to larger carrier molecules can be used to stimulate antibodies that are specific for the hapten. The interaction of these antibodies with their hapten(s) has been investigated by many of the techniques used in studying enzyme-substrate binding. The steric specificity of

antibody binding was examined in the late 1950's by Nisonoff and Pressman (1957) by studying the ability of various hapten analogues to inhibit antibody precipitation by competing for the binding site against a multivalent carrier containing the immunogenic hapten. More quantitative results on antibody specificity have been obtained by comparing the binding affinity of the antibody for its hapten and hapten analogues (Eisen and Siskind, 1964).

Results from investigations of this type on the specificity of antibody-hapten binding can be summarized as follows: (1) The ligands that bind most tightly to a given set of antibodies are those ligands that most closely resemble the haptenic groups of the immunogen. (2) Structural elements that protrude the furthest from the carrier molecule are most important in determining binding specificity and are called immunodominant. (3) The resolving power of an antibody to differentiate between haptens is similar to that found in enzymes. (4) The magnitude of the antibody-hapten binding affinity is dependent on the difference in the affinity of the solvent (solubility) and the antibody for the ligand. Antibodies to haptens that are sparingly soluble in water usually have larger binding affinities than antibodies against very soluble haptens. (5) High

affinity antibodies usually appear to be less specific than lower affinity antibodies.

1. Electrostatic Interactions between Antibodies and Charged Haptens

Investigations on the electrostatic aspects of antibody-hapten binding have centered on the study of antibodies against charged haptens. Antibodies that bind negatively charged haptens usually contain positively charged amino acids in their binding pocket and negatively charged residues are active in antibodies against positively charged haptens (Grossberg and Pressman, 1968; Freedman et al., 1968; Grossberg and Pressman, 1960; and Mayers et al., 1973).

2. Size of Antibody Binding Site

Using spacer groups of varying lengths in divalent DNP compounds, Carsen and Metzger (1974) studied the variation in the binding site of rabbit anti-DNP antibodies and found them to range between 9.7 to 12.3 Å. Halsey et al. (1975) found that antibodies fractionated according to depth of binding site differed in their ability to bind the tail of the hapten. The deeper sites show a stronger interaction with the hapten side chain than antibodies with shallower binding pockets, but they all had similar binding affinity for the nitrophenyl ring.

Studies on the ability of oligosaccharides of

various lengths to inhibit the precipitation of dextran by anti-dextran antibodies show maximum inhibition to occur with hexasaccharides (Kabat, 1960; Mage and Kabat, 1963). Measurements of this type on the size of the binding pocket agree well with those measured directly by X-ray diffraction (Davies et al., 1975).

B. Energetics of Binding

1. Thermodynamics of Hapten Binding

In addition to binding constants, other thermodynamic parameters (ΔG, ΔH, and ΔS) have also been examined in an attempt to determine the nature of the noncovalent forces involved in binding. Early determinations of ΔH were made by measuring the temperature dependence of the binding constant (using the van't Hoff equation) (Velick et al., 1960; Eisen and Siskind, 1964). This method can give erroneous values that may not represent the average ΔH of a heterogeneous set of antibodies. So, more recently, microcalorimetry (Barisas et al., 1971; Halsey and Biltonen, 1975) has been used to determine changes in enthalpy. Karush (1962) and Singer (1965) tried to relate changes in enthalpy and entropy with various types of noncovalent bonding thought to be present in antigen (hapten) binding. They proposed that hydrophobic bonding is primarily entropy driven, with little or no change in enthalpy, and that hydrophilic

interactions are primarily enthalpy controlled. They present examples of antibody binding reactions that have zero enthalpy change, but a large increase in entropy, and other antibodies that bind because they have a large decrease in enthalpy. The binding of the same hapten (DNP) to different antibody preparations can differ in relative importance of enthalpy and entropy even though the binding affinities are essentially the same (Halsey et al., 1975). These studies show that many different interactions occur between the antibody and hapten and that the sum (total ΔH and ΔS) may not be informative about the specific interactions that occur in the micro-environment.

2. Binding Kinetics

Antibody-hapten binding reactions represent some of the fastest biochemical reactions known. The rate of binding has been studied by spectrophotometric (Sturtevant et al., 1961) and fluorometric (Day et al., 1962) stopped-flow and by equilibrium perturbation (Froese et al., 1962) methods. All methods show on rates that approach the diffusion limit (10^7 to 5×10^8 M^{-1} sec^{-1}). These rapid on rates imply a low activation energy for haptens binding without any energy requiring conformational changes induced by hapten binding.

C. Hapten Binding to Fab Fragments

Antibodies and their Fab fragments have essentially the same binding affinities and Sips heterogenity index (Nisonoff et al., 1960a). This suggests that the binding sites on the same immunoglobulin do not interact with each other and are not influenced by the more distal regions of the antibody molecule. However, Kelly et al., (1971) found the on rates for hapten binding to the Fab' fragments to be about twice the rates of binding the whole immunoglobulins, but the binding affinity of the Fab fragment was only 20-50% higher. This increased rate of binding for the Fab' fragment was attributed to a more accessible binding pocket and not to a hapten induced conformational change since the temperature jump experiments showed only one exponential relaxation.

More recent experiments involving small angle X-ray scattering (Pilz et al., 1974), circular polarization of luminescence (CPL) (Jaton et al., 1975a; Schlessinger et al., 1975), and X-ray diffraction (Huber et al., 1976) reveal that there is a change in subunit interaction induced by hapten binding. The CPL experiments suggest that some of these changes are in the Fc portion, but only in the intact immunoglobulin (with no reduction and alkytation of interchain disulfied bonds) and only when the haptens (monovalent or polyvalent) was large enough to fill a major portion of the binding site.

D. Affinity Labelling

Affinity labelling techniques have been used to identify the amino acid residues lining the antigen binding site (Wofsey et al., 1962; and Givol, 1974). These studies were the first to demonstrate that the amino acid residues of the hypervariable region were intimately involved in antigen (hapten) binding.

E. Other Physical Studies of Antibody Hapten Binding

Resonance Raman Spectroscopy (RRS) has been utilized in an attempt to study the molecular interaction of rabbit anti-DNP antibodies with DNP-haptens (Carey et al., 1973). RRS showed antibody induced structural changes in the hapten spectra, but the authors could not quantitate them. ESR spectroscopy of rabbit antibodies against haptens containing spin-labels has been used to determine the mobility of the bound hapten; flexibility of the antibody arms in the 7S monomer, $F(ab')_2$, and Fab'; and the relative distance between the two binding sites (Kyaivyaryainen et al., 1974). The rotational freedom of methyl groups of quarternary amine haptens bound to rabbit antibodies was studied by NMR relaxation of the ^{1}H nuclei (Burgan et al., 1967). The NMR relaxation behavior of the ^{35}Cl nucleus has been used to determine: (1) accessibility of the bound hapten to solvent, (2) binding affinity, and (3) rotational mobility of the bound hapten (Haugland et al., 1967) in antibodies bind-

ing 2,4-dinitro-4'-(chloromercuri)-diphenylamine.

III. Studies with Homogeneous Antibodies

A. Major Sources of Homogeneous Antibodies

In the late 1960's two major sources of homogeneous antibodies with known binding specificities became available to immunologists: (1) human (Eisen et al., 1967; and Ashman and Metzger, 1969) and mouse (Potter, 1972) myelomas and (2) rabbit immunoglobulins against bacterial polysaccharides (Krause, 1970; and Bokisch et al., 1973). With these sources of homogeneous antibodies, one can compare the results of physical investigations to immunoglobulin structural data available from amino acid sequences and X-ray diffraction. It is also possible to ascertain if a single homogeneous immunoglobulin shows the same steric specificity and cross reactivity as the average of a heterogeneous group.

B. Binding Specificity

The most thoroughly investigated of these homogeneous antibodies (that have known specificities) bind one of three types of antigens: (1) Myeloma proteins that bind DNP compounds and usually cross react with other aromatic compounds, (2) Myeloma proteins that bind phosphorylcholine, and (3) Mouse myeloma and rabbit antibodies that bind polysaccharides.

1. Anti-polysaccharide Antibodies

Most of the research on anti-polysaccharide antibodies has been focused on the size of the binding site and the initiation of effector functions. The size of the binding cavity of anti-polysaccharides immunoglobulins has been measured by comparing the binding affinity of oligosaccharides of different sizes. These antibodies react best with sugars of four to six monosaccharide units (Jolley et al., 1974). Primary structure determination of several of these proteins is being performed (for example, Jaton, 1975).

Some of the most interesting work with these homogeneous rabbit antibodies against bacterial polysaccharides has been in the area of complement activation by the classical pathway. Circular polarization of luminescence (CPL) spectroscopy of rabbit anti-type III pneumococcal antibodies has detected conformational changes in antibodies induced by oligosaccharide binding. Small monovalent ligands (tetra-, hexa-, and octasaccharides) are capable of causing CPL changes in the Fab and Fc portions of the molecule. The assignment of CPL change due to the Fab and Fc portion is based on comparison of CPL spectra taken of the isolated Fab' and Fv fragments with the spectra taken of the whole immunoglobulin. Antigen binding by reduced by intact immunoglobulin shows only conformation changes isolated to

the Fab arms and not the Fc portion. More extensive conformational changes are seen in the Fc region when whole polysaccharide is used as the antigen. A ligand of minimum size of 16 sugar residues is needed to produce changes similar to those seen with the intact polysaccharide. These CPL changes are independent of antigen-antibody ratio indicating that they are induced by antigen binding and not by lattice formation (Jaton et al., 1975a).

Complement activation by these anti-type III pneumococcal antibodies occurs only when oligomers larger than 21 sugar residues are used. Antibody binding to this size oligomer produce tetrameric antigen-antibody aggregates (Jaton et al., 1976). Pentameric IgM on the other hand can fix complement when activated by a monomeric antigen (Brown and Koshland, 1975).

More work is needed to determine the relative importance of conformational or allosteric transformations to aggregate formation (Hoffman, 1976a, b, c). Rabbit anti-polysaccharides antibodies and mouse myeloma producing IgG and IgM (Weigert et al., 1974; and Leon et al., 1970) will play important roles in examining the activation of complement by the classical pathway.

2. Anti-Phosphorylcholine Antibodies

Mouse myeloma IgA immunoglobulins specific for phosphorylcholine probably represents the most extensively studied group of related antibodies (Potter and Lieberman, 1970; Hood et al., 1975; and Potter, 1972). Extensive sequence information (Hood et al., 1975; Barstad et al., 1974), idiotype information (Potter and Lieberman, 1970; Claflin et al., 1975; Claflin et al., 1974; Köhler, 1975), binding subspecificities (Leon and Young, 1971; Leon and Young, 1970; and Goetze and Richards, 1977a) and the three dimensional structure of the Fab' fragment of one of these proteins by X-ray diffraction (Segal et al., 1974) has been determined.

The extensive amount of information available on this system has allowed correlation of structure with function, comparison of the relative contribution of light and heavy chains to antigen binding, and generalization about genetic diversity of antibody formation. Some of this work is being done in this laboratory (Goetze and Richards, 1977a and b).

3. Anti-Dinitrophenyl Antibodies

a. Binding Affinities and Structural Selectivity

A number of transplantable mouse plasmacytomas are known which produce antibodies with affinity

for DNP compounds (Porter, 1972; Schubert et al., 1968; and Salk Institute for Biological Studies, 1974). Most of the research on mouse myeloma proteins with nitrophenyl binding activity has been focused on two of these proteins, MOPC-315 (Eisen et al., 1968) and MOPC-460 (Jaffe et al., 1969). This research has included the determination of the equilibrium binding affinities for various DNP compounds and other related aromatic compounds (Jaffe et al., 1971; Michaelides and Eisen, 1974; and Johnston et al., 1974). Rosenstein et al. (1972) have looked at the binding of MOPC-460 to DNP-Lys and 2-methyl-1:4-napthaquinone-thioglycollate (Men TG) under various conditions. In buffered saline these two haptens compete for the same binding site, but labelling a relatively inaccessible sulfhydryl group on the heavy chain decreases Men TG binding without affecting DNP-Lys binding. The presence of quanidine-HCl selectively reduces Men TG binding, and papain digestion of the MOPC-460 protein gives two fractions with differing specificities toward these two haptens. These results were interpreted as indicating that, even though the haptens compete with each other, there is still spatial separation between the amino acid residues that make contact with the haptens. These studies have led several investigators to consider

the general significance of antibodies having more than one specificity (Varga et al., 1973; Richards and Konigsberg, 1973; and Richards et al., 1975).

Somewhat conflicting results have been reported on the question of whether hapten/antibody binding constants depend on the concentration of antibody. One group (Underdown et al., 1971) found a decrease in the number of binding sites per 7S immunoglobulin at low antibody concentrations but no concentration dependence of the binding constant. In contrast Johnston et al. (1974) reported a large variation in binding affinity with concentration, but they always saw two binding sites.

Reconstitution to form homologous and heterologous immunoglobulins made from separated heavy and light chains have been reported for MOPC-315, MOPC-460, and two other mouse myeloma IgA proteins that lack DNP specificity. Homologous recombinations of MOPC-460 and MOPC-315 regenerated immunoglobulins that showed essentially the same binding activity, but heterologous recombinations are, in general, without significant activity (the heterologous cross between MOPC-460 heavy chain with the light chain of MOPC-315 did show some activity for DNP-ligands (Bridges and Little, 1971).

Pepsin digestion of MOPC-315 Fab' fragment produces a smaller fragment (Fv, M.W. $\sim$ 25,000) that contains the variable regions of both the light and heavy chains, the DNP-binding site with a similar binding affinity to the whole immunoglobulin, and the antigenic determinants recognized by idiotypic antibodies made against the intact protein (Inbar et al., 1972a; Hochman et al., 1973; and Wells et al., 1973). The 7S, Fab' and Fv proteins of MOPC-315 all have essentially the same binding affinity (Hochman et al., 1973). The dynamics of hapten binding by these proteins of MOPC-315 have been studied (Pecht et al., 1972a, b; and Hochman et al., 1972). The on rates are 1-3 x 10^8 M^{-1} sec^{-1} with the on rate and off rate of the Fab' fragment slightly faster than the 7S monomer.

b. Structural Features

Partial sequence data for MOPC-460 (Haimovich et al., 1972; Lifter et al., 1974; and Hood et al., 1976) and MOPC-315 (Dugen et al., 1973; and Francis et al., 1974) have been determined. Affinity labelling has been used to identify some of the amino acid residues that participate in hapten binding (Givol, 1974).

Both NMR and ESR spectroscopy have been used to examine the binding site of MOPC-315 (Dwek et al., 1975). Using different sized nitroxide spin labels attached to a

DNP ring and observing the resulting ESR spectra of these haptens bound to MOPC-315, they mapped the size of the binding site as 11 Å x 9 Å x 6 Å. These spin labels were found to shift the NMR signals of about 30 aliphatic and 30 aromatic hydrogens.

The same group (Dwek et al., 1976) studied the time dependence of fluorescence enhancement caused by the binding of lanthanide metals. The results were interpreted as evidence for a slow conformational change of the protein. The lanthanide salts are observed to compete somewhat for the DNP binding site. A distance of 12 Å between the binding site of the lanthanide salts and DNP-nitroxide haptens is inferred from the data. The binding constants for the heavy metals shows a pH dependence ($pK_a \sim 6.0$); and they also perturb the ionization of one of the three histidine residues of the Fv fragment.

By comparing the on rates of a variety of structurally different DNP compounds a crude map of the binding site of MOPC-315 has been determined. The binding site is 6 Å wide and about 12 Å long with four different subsites: subsite 1 (about 6 Å long) binds the aromatic ring, subsite 2 (1 Å long) is a hydrophobic region, subsite 3 (3 Å long) is a second hydrophobic region, and subsite 4 (1.5 Å long) contains a positively charged amino acid (Haselkorn et al., 1974).

No X-ray diffraction data have been reported for a DNP binding myeloma protein. However, the crystal structure of the Fab' fragment of Ig New which has low affinity for several aromatic compounds has been done (Amzel et al., 1974 and Poljak et al., 1974) and the binding of DNP compounds and several other small aromatic molecules to a λ-type Bence-Jones dimer has been studied by X-ray diffraction techniques (Edmundsen et al., 1974). Different haptens are found to bind to different regions in the "binding site". Padlan et al. (1976) has proposed a three dimensional model for MOPC-315 by analogy with other known immunoglobulin structures. This model has been further modified by Dwek et al. (1977) using results of NMR and ESR spectroscopy.

IV. General Strategies and Objectives of this Thesis

The purpose of this thesis has been to study the interactions that occur when an immunoglobulin binds its hapten, to investigate the molecular energetics between the hapten and the amino acid residues in the binding site, and to determine what interactions, if any, occur between subunits that are induced by hapten binding. MOPC-315 protein was studied because it provided a high affinity homogeneous immunoglobulin that could be enzymatically split into several binding fragments for use in comparing subunit interactions. MOPC-315

immunoglobulin was a poor model for studying hapten induced conformation changes because interchain disulfied bonds were reduced and alkytated during isolation and purification. Also since MOPC-315 immunoglobulin is of the alpha class it would not be expected to activate complement by the classical pathway. There are now better sources of immunoglobulin (such as the rabbit antibodies against bacterial polysaccharides mentioned in the introduction) for investigating the existence of antigen induced conformation changes, but these antibodies were not available when this study began.

Nuclear Magnetic Resonance spectroscopy was the primary technique used in this study because it provides both structural (environmental) and dynamic information on labelled haptens.

Fluorine was used as an NMR probe because of its high sensitivity (83 percent of a proton's), its high natural abundance, low background interference from buffer and unlabelled protein, and sensitivity to local environment. A trifluoromethyl group with three identical fluorine nuclei is not only an excellent NMR probe, but it is also a relatively unperturbing substitute for a nitro group, since they are both similar in size and inductive ability. MOPC-315 protein binding to trifluoromethyl substituted haptens are comparable to their nitrophenyl analogues.

REFERENCES

Ashman, R.F. and Metzger, H. (1969), J. Biol. Chem. 244, 3405.

Amzel, L.M., Poljak, R.J., Saul, F., Varga, J.M., and Richards, F.F. (1974), Proc. Natl. Acad. Sci. 71, 1427.

Barisas, B.G., Sturtevant, J.M., and Singer, S.J. (1971), Biochemistry 10, 2816.

Barstad, P., Rudikoff, S., Potter, M., Cohn, M., Konigsberg, W., and Hood, L. (1974), Science 183, 962.

Bokisch, V.A., Chiao, J.W., Burnstein, D., and Krause, R.M. (1973), J. Exp. Med. 138, 1184.

Bridges, S.H. and Little, J.R. (1971), Biochemistry 10, 2525.

Brown, J.C. and Koshland, M.E. (1975), Proc. Natl. Acad. Sci. 72, 5111.

Burgan, A.S.V., Jardetzky, O. Metcalf, J.C., and Wade-Jardetzky, N. (1967), Proc. Natl., Acad. Sci. USA. 58, 447.

Capra, J.D. and Kehoe, J.M. (1975), Advan. Immunol. 20, 1.

Carey, P.R., Froese, A., and Schneider, H. (1973), Biochemistry 12, 2198.

Carsen, D. and Metzger, H. (1974), Immunochem. 11, 355.

Claflin, J.L., Lieberman, R., and Davie, J.M. (1974), J. Immunol. 112, 1747.

Claflin, J.L., Rudikoff, S., Potter, M., and Davie, J.M. (1975), J. Exp. Med. 141, 608.

Davies, D.R., Padlan, E.A., and Segal, D.M. (1975), A. Rev. Biochem. 44, 639.

Day, L.A., Sturtevant, J.M., and Singer, S.J. (1962), J. Amer. Chem. Soc. 84, 3768.

Dugan, E.S., Bradshaw, R.A., Simms, E.S., and Eisen, H.N. (1973), Biochemistry 12, 5400.

Dwek, R.A., Givol, D., Jones, R., McLaughlin, A.C., Wain-Hobson, S., White, A.I., and Wright, C. (1976), Biochem. J. 155, 37.

Dwek, R.A., Knott, J.C.A., Marsh, D., McLaughlin, A.C., Press, E.M., Price, N.C., and White, A.I. (1975), Eur. J. Biochem. 53, 25.

Dwek, R.A., Wain-Hobson, S., Dower, S., Gettens, P., Sutton, B., Perkins, S.J., and Givol, D. (1977), Nature 266, 31.

Edelman, G.M. (1959), J. Amer. Chem. Soc. 81, 3155.

Edelman, G.M. (1973), Science 180, 830.

Edelman, G.M. and Gall, W.E. (1969), Ann. Rev. Biochem. 38, 415.

Edelman, G.M. and Poulek, M.D. (1961), J. Exp. Med. 113, 861.

Edmundsen, A.B., Ely, K.R., Girling, R.L., Abola, E.E., Schiffer, M., Westholm, M.A., Faush, M.D., and Deutsch, H.F. (1974), Biochemistry 13, 3816.

Eisen, H.N., Little, J.R., Osterland, C.K., and Simms, E.S. (1967), Cold Spring Harbor Symp. Quant. Biol. 32, 75.

Eisen, H.N., Simms, E.S., and Potter, M. (1968), Biochemistry 7, 4126.

Eisen, H.N. and Siskind, G.W. (1964), Biochemistry 3, 996.

Feinstein, A. and Rowe, A.J. (1965), Nature (London) 205, 147.

Fleischman, J.B., Porter, R.R., and Press, E.M. (1963), Biochem. J. 88, 220.

Francis, S.H., Leslie, R.G.Q., Hood, L., and Eisen, H.N. (1974), Proc. Natl. Acad. Sci. USA 71, 1123.

Freedman, M.H., Grossberg, A.L., and Pressman, D. (1968), J. Biol. Chem. 243, 6186.

Froese, A., Sehon, A., and Eigen, M. (1962), Can. J. Chem. 40, 1786.

Givol, D. (1974), Essays Biochem. 10, 73.

Goetze, A.M. and Richards, J.H. (1977a), Proc. Natl. Acad. Sci. USA 74, 2109.

Goetze, A.M. and Richards, J.H. (1977b), Biochemistry 16, 228.

Grossberg, A.L. and Pressman, D. (1960), J. Amer. Chem. Soc. 82, 5478.

Grossberg, A.L. and Pressman, D. (1968), Biochem. 7, 272.

Haimovich, J., Eisen, H.N., Hurwitz, E., and Givol, D. (1972), Biochemistry 11, 2389.

Halsey, J.F. and Biltonen, R.L. (1975), Biochem. 14, 800.

Halsey, J.F., Cebra, J.J., and Biltonen, R.L. (1975). Biochem. 14, 5221.

Haselkorn, D., Friedman, S., Givol, D., and Pecht, I. (1974), Biochemistry 13, 2210.

Haugland, R.P., Stryer, L., Stingle, T.R., and Baldeschwieler, J.D. (1967), Biochem. 6, 498.

Hochman, J., Inbar, D., and Givol, D. (1973), Biochem. 12, 1130.

Hochman, J., Inbar, D., Wilchek, M., Pecht, I., and Givol, D. (1972), Israel J. Med. Sci. 8, 635.

Hoffmann, L.G. (1976a), Immunochemistry 13, 725.

Hoffmann, L.G. (1976b), Immunochemistry 13, 731.

Hoffmann, L.G. (1976c), Immunochemistry 13, 737.

Hood, L., Loh, E., Hubert, J., Barstad, P., Eaton, B., Early, P., Fuhrman, J., Johnson, N., Kronenburg, M., and Schilling, J. (1976), Cold Spring Harbor Symp. Quant. Biol. 41, 817.

Hood, L., Campbell, J.H., and Elgin, S.C.R. (1975), Ann. Rev. Genetics 9, 305.

Huber, R., Deisenhofer, J., Colman, P.M., Matsushima, M., and Palm, W. (1976), Nature 264, 415.

Inbar, D., Hochman, J., and Givol, D. (1973), Proc. Natl. Acad. Sci. USA. 70, 1585.

Jaffe, B.M., Simms, E.S., and Eisen, H.N. (1971), Biochemistry 10, 1693.

Jaffe, B.M., Eisen, H.N., Simms, E.S., and Potter, M. (1969), J. Immunol. 103, 872.

Jaton, J.C., Huser, H., Brown, D.G., Givol, D., Pecht, I., and Schlessinger, J. (1975a), Biochem. 14, 5312.

Jaton, J.C. (1975b), Biochem. J. 147, 235.

Jaton, J.C., Huser, H., Riesen, W.F., Schlessinger, J., and Givol, D. (1976), J. of Immunol. 116, 1363.

Johnston, M.F.M., Barisas, B.G., and Sturtevant, J.M. (1974), Biochemistry 13, 390.

Jolley, M.E., Glaudemans, C.P.J., Rudikoff, S., and Potter, M. (1974), Biochemistry 13, 3179.

Kabat, E.A. (1960), J. Immunol. 84, 82.

Karush, F. (1962), Adv. Immunol. 2, 1.

Kelly, K.A., Sehon, A.H., and Froese, A. (1971), Immunochem. 8, 613.

Köhler, H. (1975), Transplantation Rev. 27, 24.

Krause, R.M. (1970), Adv. Immunol. 12, 1.

Kyaivyaryainen, A.I., Neylin, R.S., and Vol'Kenstein, M.V. (1974), Molekulyarnaya Biologiya 8, 816.

Leon, M.A. and Young, N.M. (1970), Fed. Proc. 29, 437.

Leon, M.A. and Young, N.M. (1971), Biochem. 10, 1424.

Leon, M.A., Young, N.M., and McIntire, K.R. (1970), Biochem. 9, 1023.

Lifter, J., Hew, C.L., Yoshioka, M., Richards, F.F., and Konigsberg, W.H. (1974), Biochemistry 13, 3567.

Mage, R.G. and Kabat, E.A. (1963), Biochemistry 2, 1278.

Mayers, G.L., Grossberg, A.L., and Pressman, D. (1973), Immunochemistry 10, 37.

Michaelides, M.C. and Eisen, H.N. (1974), J. Exp. Med. 140, 687.

Nisonoff, A. and Pressman, D. (1957), J. Amer. Chem. Soc. 79, 1616.

Nisonoff, A., Wissler, F.C., and Woernly, D.L. (1960a), Arch. Biochem. Biophys. 88, 241.

Nisonoff, A., Wissler, F.C., and Lipman, L.N. (1960b), Science 132, 1770.

Padlan, E.A., Davies, D.R., Pecht, I., Givol, D., and Wright, C. (1976), Cold Spring Harbor Symp. Quant. Biol. 41, 627.

Pecht, I., Givol, D., and Sela, M. (1972a), J. Mol. Biol. 68, 241.

Pecht, I., Haselkorn, D., and Friedman, S. (1972b), FEBS Let. 24, 331.

Pilz, I., Kratky, O., and Karush, F. (1974), Eur. J. Bio-Chem. 41, 91.

Poljak, R.J., Amzel, L.M., Chen, B.L., Phizackerley, R.P., and Saul, F. (1974), Proc. Natl. Acad. Sci. USA. 71, 3440.

Porter, R.R. (1959), Biochem. J. 73, 119.

Potter,M. (1972), Physiol. Rev. 52, 631.

Potter, M. and Lieberman, R. (1970), J. Exp. Med. 132, 737.

Richards, F.F. and Konigsberg, W.H. (1973), Immunochem. 10, 545.

Richards, F.F., Konigsberg, W.H., Rosenstein, R.W., and Varga, J.M. (1975), Science 187, 130.

Rosenstein, R.W., Mussen, R.A., Armstrong, M.Y.K., Konigsberg, W.H., and Richards, F.F. (1972), Proc. Natl. Acad. Sci. USA 69, 877.

Salk Institute for Biological Studies (1974), "Catalogue of Murine Immune Related Culture and Tumor Cell Lines" available upon request from The Salk Institute for Biological Studies, Post Office Box 1809, San Diego, California 92112.

Schlessinger, J., Steinberg, I.Z., Givol, D., Hochman, J., and Pecht, I. (1975), Proc. Natl. Acad. Sci. USA 72, 2775.

Schubert, D., Jobe, A., and Cohn, M. (1968), Nature 220, 882.

Segal, D.M., Padlan, E.A., Cohn, G.E., Rudikoff, S., Potter, M., and Davies, D.R. (1974), Proc. Natl. Acad. Sci. USA 71, 4298.

Singer, S.J. (1965), The Proteins, Vol. 3, p. 269. Academic Press, N.Y.

Sturtevant, J.M., Wolsey, L., and Singer, S.J. (1961), Science 134, 1434.

Underdown, B.J., Simms, E.S., and Eisen, H.N. (1971), Biochemistry 10, 4359.

Valentine, R.C. and Green, N.M. (1967), J. Mol. Biol. 27, 615.

Varga, J.M., Konigsberg, W.H., and Richards, F.F. (1973), Proc. Natl. Acad. Sci. USA 70, 3269.

Velick, S.F., Parker, C.W., and Eisen, H.N. (1960), Proc. Natl. Acad. Sci. USA 46, 1470.

Weigert, M., Raschke, W.C., Carson, D., and Cohn, M. (1974), J. Exp. Med. 139, 137.

Wells, J.V., Fudenberg, H.H., and Givol, D. (1973), Proc. Natl. Acad. Sci. USA 70, 1585.

Wofsy, L., Metzger, H., and Singer, S.J. (1962), Biochemistry 1, 1031.

Wu, T.T. and Kabat, E. (1970), J. Exp. Med. 132, 211.

PART II

Chemical Shift and Binding Studies of the Interaction Between ^{19}F Labelled Nitrophenyl Haptens and Mouse Myeloma Immunoglobulin MOPC-315

INTRODUCTION

As a part of a program aimed at gaining a molecular understanding of the specific recognition and binding of antigen by antibody (Goetze and Richards, 1977), we have used magnetic resonance techniques to study the interactions of the MOPC-315 myeloma protein, and its binding fragments, with specific haptens containing ^{19}F as a probe for magnetic resonance observation. In particular, trifluoromethyl groups have proved to be sensitive probes of their environment when used for example to study the allosteric changes that occur on ligation of hemoglobin (Huestis and Raftery, 1972) and to probe the binding site of chymotrypsin (Smallcombe et al., 1972a; Smallcombe et al, 1972b; Gammon et al., 1972; Maddox et al., 1975).

Mouse plasmacytoma MOPC-315 grows in Balb/c mice (Eisen et al., 1968) and produces an α class immunoglobulin with a λ_2 light chain (Dugan et al., 1973). The antibody has a high affinity for ligands which incorporate a di- or trinitrophenyl group (Eisen et al., 1968; Johnston et al., 1974), and its binding specificity and affinity (Haimovich and Eisen, 1971; Johnston et al., 1974), amino acid sequence (Dugan et al., 1973; Francis et al., 1974), binding kinetics (Haselkorn et al., 1974), and fragmentation by proteolytic enzymes (Inbar et al., 1971; Inbar et al., 1972; Hochman et al., 1973) have been previously studied.

The nature of the binding pocket of MOPC-315 has also recently received attention (Dwek et al., 1977; Padlan et al., 1976).

MATERIALS AND METHODS

Maintenance of MOPC-315 Plasmacytoma. Balb/c mice injected with MOPC-315 plasmacytoma were obtained from Herman Eisen (Washington University School of Medicine, St. Louis, Mo.) and Salk Institute for Biological Studies (San Diego, Calif.). The tumor was transplanted by a subcutaneous injection into Balb/c female mice (Potter, 1972). Mice were obtained from a variety of vendors and, as long as the mice were healthy, there was no noticeable difference in tumor growth.

Preparation of a Nitrophenyl-Sepharose Affinity Column. ε-N-DNP-lysine was coupled to Sepharose 4B (Pharmacia) by a modification of the procedure given by Goetzl and Metzger (1970a). Cyanogen bromide (3-5 gm/100 ml of Sepharose) was dissolved in 5-10 ml of fresh dioxane and added rapidly to a pH 11 Sepharose-water suspension. The temperature during the activation reaction was maintained between 20-25°C, no cooling was usually necessary, and the pH was kept at 11 by the addition of sodium hydroxide.

The activation reaction was complete when the pH remained constant (10-20 min). This activated Sepharose

was rapidly filtered and washed with 3 volumes of 0.1 M $NaHCO_3$, and quickly added to 1.5 volumes of 0.1 M $NaHCO_3$ solution containing 0.67 mg/ml of ε-N-DNP-lysine hydrochloride at pH 8.5. This coupling reaction was allowed to react overnight with stirring at 4°C. The coupled Sepharose was filtered, washed with one volume of methanol, washed with eluting buffer until the effluent was clear and packed into columns. The column was wrapped in aluminum foil to prevent bleeding of the coupled DNP. Prior to protein isolation, the column was washed alternately with a half volume of 10% acetic acid and 0.1 M NaP_2O_7.

MOPC-315 7S monomer used for binding studies was further purified on a DE-52 column. The 7S monomer purified by affinity chromatography, was eluted from a DE-52 column by using a 0.03 to 0.3 M potassium phosphate gradient (pH 8.0) at 4°C. This gave a single asymmetric peak. Only fractions at the top of the peak were used. Protein purified in this manner was clearer at high concentrations, but no qualitative differences were noticed in NMR experiments.

Purification of MOPC-315 Immunoglobulin. MOPC-315 protein was initially acquired from the serum obtained by bleeding the tumor-laden Balb/c mice by the throat 20-21 days after tumor injection. The average mouse produced

0.5 ml of serum from which 8-11 mg/ml of purified protein could be obtained.

Better yields were obtained from mineral oil primed CDF (Balb/c x DBA/2) hybrid females injected intraperitoneally with screened MOPC-315 tumor cells as described by Potter (1972). These mice produced 3-5 ml of ascites per tapping, and could be tapped twice a week for 2 to 3 weeks. From the ascites 3-5 mg/ml of purified MOPC-315 immunoglobulin could be obtained.

MOPC-315 antibody content of the ascites or serum was occasionally tested by immunodiffusion on Ouchterlony plates against DNP-BGG.[1]

The MOPC-315 immunoglobulin was purified by affinity chromatography as described by Inbar et al. (1971) with only slight modification. The ascites was filtered through glass wool and diluted with one-tenth its volume of 2 M tris HCl pH 8.6. This buffered ascites was reduced with

---

[1]Abbreviations used: DNP-BGG, dinitrophenylated bovine γ-globulin synthesized as described by Eisen (1964) or purchased from Sigma; DNTP-GABA, γ-N-(2,6-dinitro-4-trifluoromethylphenyl) aminobutyric acid; NTCB, 2-nitro-4-trifluoromethylcholorbenzene; 2NTP-GABA, γ-N-(2-nitro-4-trifluoromethylphenyl) aminobutyric acid; NTP-GABA, γ-N-(4-nitro-2-trifluoromethylphenyl) aminobutyric acid; DNTP-Gly, α-N-(2,6-dinitro-4-trifluoromethylphenyl) amino-acetic acid; NTP-Lys, ε-N-(4-nitro-2-trifluoromethylphenyl)-L-lysine; EDTA, ethylenediaminetetracecetic acid; Buffer used for all protein and UV-vis spectroscopy experiments was 0.15 M NaCl, 0.01 M sodium phosphate, 0.02% sodium azide, and 0.003 M EDTA at pH 7.4. DNTP-Lys, γ-N-(2-6-dinitro-4-trifluoromethylphenyl) lysine; 2NTP-Lys, γ-N-(2-nitro-4-trifluoromethylphenyl) lysine.

0.01 M dithiothreitol for 1 hr at room temperature followed by alkylation in 0.03 M iodoacetamide for 2 hrs in an ice bath. The reduced and alkylated protein was then loaded directly onto a Sepharose column conjugated with DNP-lysine and eluted with 0.5 M DNP-glycine.

Preparation of Fab' and Fv fragments of MOPC-315. Fab' fragments were made by a 1% pepsin digest of the purified MOPC-315 antibody in 0.05 M sodium acetate buffer, pH 4.7, for 6 hrs at 37°C (Inbar et al., 1971). The fragments were purified by affinity chromatography as described above. Purification was checked by 7.5% SDS gel electrophoresis which indicated greater than 90% Fab', in agreement with Inbar et al. (1971).

Fv fragments were made by a 1% pepsin digest of the Fab' fragment in 0.1 M sodium acetate buffer, pH 3.6, for 4 hrs at 37°C (Inbar et al., 1972; Hochman et al., 1973). After purification on the DNP-lysine Sepharose column, the Fv fragments were further purified by gel filtration chromatography on a G-75 sephadex column. Purification was checked by 7.5% SDS gel electrophoresis and showed that 90% of the protein migrated as a single band. The other 10% migrated with a molecular weight similar to a normal light chain. The purified Fv fragments were dialyzed against distilled water and lyophilized.

Recycling Used Protein. Protein samples used for NMR and binding experiments could be repurified and used again after removal of hapten. Pooled hapten protein solutions (7S, Fab', and Fv proteins were kept separately) were dialyzed against several volumes of 0.5 M DNP-glycine using an Amicon Diaflow. This protein DNP-glycine solution was then diluted with buffer until the protein concentration was less than 1 mg/ml and passed down a short Dowx 1 x 8 column to remove the DNP-glycine. This faint yellow protein solution was then applied to the DNP-Lys affinity column and purified as usual. The purity of the protein was checked by electrophoresis on 7.5% SDS gels.

Preparation of NMR Samples. Purified MOPC-315 immunoglobulin, 7S monomer, was dialyzed against buffer (0.15 M NaCl, 0.01 M sodium phosphate, 0.001 M EDTA and 0.02% NaN_3 at pH 7.4; this buffer was used for all protein and UV-vis spectroscopy experiments) and concentrated to the desired concentration under pressure by ultrafiltration. Normal NMR samples had protein concentrations of 30-120 mg/ml determined from the protein's absorption at 278 nm (Abs $\frac{1cm}{0.1\%}$ at 278 nm = 1.35 mg/ml, M.W. 153,000) (Underdown et al., 1971). The fluorinated haptens were added to this protein solution in one of two ways: a small aliquot was added from a standard solution, or the protein solution was added to a centrifuge tube in which a premeasured

aliquot of the fluorinated nitrophenyl solution had been lyophilized.

NMR samples of MOPC-315 Fab' fragments were prepared in the same manner (Abs $\frac{1cm}{0.1\%}$ at 278 nm = 1.35 mg/ml, M.W. 50,000 gave the best agreement with the integrated areas of the bound and free peaks seen in ^{19}F NMR spectra with 2NTP-GABA and DNTP-GABA).

NMR samples of Fv fragments of MOPC-315 were reconstituted from the lyophilized protein. A preweighed sample of the Fv protein was added to a centrifuge tube containing 2.5 ml of buffer. The protein was dissolved in the buffer by a combination of stirring and centrifugation (all but a small amount dissolved). The supernatant was removed and the fluorinated hapten was added as described above. Concentrations of the Fv protein were determined either by assuming all dissolved or from the absorption at 278 nm (Abs $\frac{1cm}{0.1\%}$ at 278 nm = 1.5 mg/ml, M.W. 25,000) (Hochman et al., 1973). This reconstituted protein showed about 70-80% of the calculated binding activity as determined by ratio of bound to free peaks in ^{19}F NMR spectra. NMR spectra were usually determined on solutions which contained 10-30 mg/ml of Fv protein.

Fluorine NMR spectra were observed on 2.0-3.0 ml of sample in a 12 mm tube containing a 5 mm tube of D_2O for locking. The spectra were determined on a Varian XL-100-15 operating at 94.1 MHz for ^{19}F NMR.

γ-N-(2,6-Dinitro-4-trifluoromethylphenyl) aminobutyric acid, DNTP-GABA. DNTP-GABA was prepared by modification of the procedure described by Porter (1950). 3,5-Dinitro-4-chlorobenzotrifluoride (Columbia Organics) was purified by dissolving in ether, washing with 0.1 M Na_2CO_3 pH 10.5 and then removing the ether to give phenol-free 3,5-dinitro-4-chlorobenzene. γ-Aminobutyric acid (1.0 gm. 9.7 mmol) and $NaHCO_3$ (2.2 gm) were dissolved in 28 ml of water and titrated to pH 7.5. To this solution was added an ethanolic solution (54 ml) of 3,5-dinitro-4-cholorbenzotrifluoride (3.48) gm, 12.6 mmol). This mixture was allowed to react for 20 hrs at room temperature with vigorous stirring. The ethanol was removed under reduced pressure, the pH was raised to 10.5 to dissolve the DNTP-GABA produced, the solution was washed with 3 x 25 ml of ether, and the product was precipitated by acidification with HCl. This filtered and dried product weighed 2.0 gm, 61% yield. A portion of product was further purified by recrystallization in benzene, m.p. 139-140°C. Infrared spectra of DNTP-GABA (KBr pellet) had absorptions at 3300 cm^{-1} (N-H), 1700 cm^{-1} (C=O), and 1630 cm^{-1} (C=C); NMR spectra (d_6 acetone) had a singlet at δ8.52 ppm (2H), a quartet δ3.5 ppm (2H), two overlapping multiplets centered at δ2.1 (2H) and δ2.5 ppm (2H) and a broad N-H signal under the phenyl peak; ^{19}F NMR showed a single

peak 13.75 ppm downfield from an external standard of trifluoroacetic acid (2.5 mmol TFA in a D_2O, H_2O mixture); visible spectra λ_{max} 428 nm with a molar absorptivity of 6.36×10^3 cm^{-1} M^{-1}. Anal. Calcd for $C_{11}H_{10}F_3N_3O_6$: C, 39.18; H, 2.99; F, 16.90; N, 12.46. Found: C, 39.21; H, 3.04; F, 16.87; N, 12.44.

2-Nitro-4-trifluoromethylchlorobenzene, NTCB. NTCB was prepared from 4-amino-3-nitrobenzotrifluoride (PCR inc.) using a modification of the procedure outlined by Gunstone and Tucker (1963). The yield was 75% after petroleum extraction. This product was used in the synthesis of 2NTP-GABA without further purification.

γ-N-(2-Nitro-4-trifluoromethylphenyl) aminobutyric acid, 2NTP-GABA. NTCB[2] (2.9 gm, 13 mmol) was dissolved in 54 ml of ethanol and added to a stirred solution of 1.0 gm (9.7 mmol) γ-aminobutyric acid and 2.2 gm $NaHCO_3$ in 28 ml of water. This mixture was refluxed for 20 hrs and the product isolated by the procedure used for DNTP-GABA. The yield was 2.1 gm (74%). Part of the product was purified by recrystallization in benzene to give yellow crystals m.p. 102-103°C. Structure of 2NTP-GABA was verified by ir spectroscopy (KBr pellet) which had absorptions at 3300 cm^{-1} (N-H), 1700 cm^{-1} (C=O), and

[2] 4-Fluoro-3-nitrobenzotrifluoride can be used in place of NTCB and is now commercially available from Columbia Organics.

peak 13.75 ppm downfield from an external standard of trifluoroacetic acid (2.5 mmol TFA in a D_2O, H_2O mixture); visible spectra λ_{max} 428 nm with a molar absorptivity of 6.36×10^3 cm^{-1} M^{-1}. Anal. Calcd for $C_{11}H_{10}F_3N_3O_6$: C, 39.18; H, 2.99; F, 16.90; N, 12.46. Found: C, 39.21; H, 3.04; F, 16.87; N, 12.44.

2-Nitro-4-trifluoromethylchlorobenzene, NTCB. NTCB was prepared from 4-amino-3-nitrobenzotrifluoride (PCR inc.) using a modification of the procedure outlined by Gunstone and Tucker (1963). The yield was 75% after petroleum extraction. This product was used in the synthesis of 2NTP-GABA without further purification.

γ-N-(2-Nitro-4-trifluoromethylphenyl) aminobutyric acid, 2NTP-GABA. NTCB[2] (2.9 gm, 13 mmol) was dissolved in 54 ml of ethanol and added to a stirred solution of 1.0 gm (9.7 mmol) γ-aminobutyric acid and 2.2 gm $NaHCO_3$ in 28 ml of water. This mixture was refluxed for 20 hrs and the product isolated by the procedure used for DNTP-GABA. The yield was 2.1 gm (74%). Part of the product was purified by recrystallization in benzene to give yellow crystals m.p. 102-103°C. Structure of 2NTP-GABA was verified by ir spectroscopy (KBr pellet) which had absorptions at 3300 cm^{-1} (N-H), 1700 cm^{-1} (C=O), and

[2]4-Fluoro-3-nitrobenzotrifluoride can be used in place of NTCB and is now commercially available from Columbia Organics.

1620 cm^{-1} (C$\underline{\underline{\ }}$C); the NMR spectrum ($d_6$ acetone) had a split singlet at δ8.40 ppm (1H), a doublet of doublets at δ7.75 ppm (1H), doublet centered at δ7.27 ppm (1H), a quartet centered at δ3.57 ppm (2H); two overlapping multiplets at δ2.5 (2H) and δ2.1 ppm (2H), and the N-H proton giving a broad peak at δ8.5 ppm; the ^{19}F NMR spectrum had a single peak 13.97 ppm downfield from an external standard trifluoroacetic acid solution; visible spectrum λ_{max} 429 nm with a molar absorptivity of 6.06 x 10^3 cm^{-1} M^{-1}. Anal. Calcd for $C_{11}H_{11}F_3N_2O_4$: C, 45.21; H, 3.79; F, 19.50; N, 9.59. Found. C, 45.12; H, 3.83; F, 19.55; N, 9.58.

γ-N-(4-Nitro-2-trifluoromethylphenyl) aminobutyric acid, NTP-GABA. 5-Nitro-2-fluorobenzotrifluoride (3.6 gm, 17.2 mmol) from Pierce Chemical, was dissolved in 54 ml of ethanol; and added to a stirred solution of 1.0 gm (9.7 mmol) γ-aminobutyric acid and 2,2 gm $NaHCO_3$ in 28 ml of water adjusted to pH 9.0. After reacting for 60 hrs at ambient temperature, NTP-GABA was isolated as described for DNTP-GABA. Crude yield of product was 0.94 gm, 36% (increased yields and faster reaction times could probably be obtained by heating the reaction mixture to reflux). Some NTP-GABA was recrystallized in benzene and had a m.p. of 181-182°, and its structure was verified by: ir spectroscopy (KBr pellet) which had peaks at

ppm (1H); ^{19}F NMR spectra (showed a single absorption) 13.71 ppm downfield from an external trifluoroacetic acid standard; and had a visible abosption λ_{max} 426 nm with a molar absorptivity of 6.42×10^3 cm^{-1} M^{-1}. Annal: Calcd. for $C_9H_6F_3N_3O_6$: C, 34.63; H, 1.94; N, 13.46. Found: C, 35.17; H, 2.05; N, 13.19.

Buffered solutions of DNTP-Gly formed a precipitate on standing for long periods of time.

ε-N-(4-Nitro-2-trifluoromethylphenyl)-L-lysine, NTP-Lys. NTP-Lys was prepared by reacting 2-fluoro-5-nitrobenzotrifluoride with α-N-carbobenzoxy-L-lysine (Sigma) by a slight modification of the procedure used by Goetzl and Metzger (1970a) to make ε-N-p-nitrophenyl lysine. Yield of yellow solid was 70%. NTP-lysine was purified by multiple precipitations at its isoelectric point. A final attempt was made to crystallize NTP-Lys by adding just enough HCl to cause it to dissovle when heated on a steam bath, but it precipitated out of solution without forming crystals. NTP-Lys decomposed at 198-200°C. Structure was verified by: ir spectroscopy (KBr pellet) showed peaks at 3500 cm^{-1} (N-H), 1625 cm^{-1} (C=O), and 1600 cm^{-1} (C--C); NMR spectra (1:1 TFA, D_2O) has an overlapping singlet and doublet centered at δ8.2 ppm (2H), a doublet at δ6.8 (1H), two unresolved triplets at δ4.3 ppm (1H) and δ3.4 ppm (2H), and a multiplet centered at δ2.0

ppm (6H); and a single fluorine absorption was observed at 11.96 ppm downfield from an external trifluoroacetic acid standard. Anal: Calcd. for $C_{13}H_{16}F_3N_3O_4$: C, 46.57; H, 4.81, N, 12.53. Found: C, 45.44; H, 4.86; N, 11.79; and 0.7 % Cl. No further attempt was made to purify NTP-Lys.

ε-N-(2,6-Dinitro-4-trifluoromethylphenyl)-L-lysine, DNTP-Lys. DNTP-Lys was made by reacting 2,6-dinitro-4-trifluoromethylchlorobenzene with α-N-CBZ-L-lysine by the procedure of Goetzl and Metzger (1970a). The product was crystallized in water by adding just enough HCl to cause DNTP-Lys to dissolve when heated on a steam bath. Yield was 33% of yellow crystals that decomposed at 204-205°C. An ir spectrum (KBr pellet) had absorptions at 3400 cm^{-1} (N-H), 1650 cm^{-1} (C=O) and 1590 cm^{-1} (C--C); NMR spectra (1:1 TFA, D_2O) had a single phenyl absorption at δ8.5 ppm (2H), two unresolved triplets at δ4.1 ppm (1H) and δ3.1 ppm (2H), and a broad multiplet centered at δ1.9 ppm (6H); and ^{19}F NMR spectrum showed a single absorption 13.75 ppm downfield from trifluoroacetic acid. Anal: Calcd. for $C_{13}H_{15}F_3N_4O_6$: C, 41.06; H, 3.98; N, 14.78. Found: C, 39.14; H, 3.80; N. 12.72; Cl, 3.1. No further efforts were made to purify DNTP-Lys. DNTP-Lys was very difficult to work with, because its solubility in buffer at pH 7.4 was only about 2 x 10^{-4} M and

it decomposed when stored in higher pH solutions.

ε-N-(2-Nitro-4-trifluoromethylphenyl)-L-lysine, 2NTP-Lys. 2NTP-Lys was prepared by reacting NTCB with ε-N-CBZ-L-lysine. The product was crystallized by adding just enough HCl to dissolve 2NTP-Lys in hot water giving a 14% yield of yellow crystals which decomposed at 201-203°C. An ir spectrum (KBr pellet) had peaks at 3350 cm^{-1} (N-H), 1640 cm^{-1} (C=O) and 1570 cm^{-1} (C--C); NMR spectra (1:1 TFA, D_2O) singlet δ8.3 ppm (1H), doublet δ7.6 ppm (1H), doublet δ7.0 ppm (1H), and broad multiplets at δ4.3 ppm (1H), δ3.5 ppm (2H), and δ2.0 ppm (6H); and a ^{19}F NMR absorption at 13.99 ppm with a small impurity (<5%) at 13.83 ppm downfield from an external trifluoroacetic acid standard. Anal: Calcd. for $C_{13}H_{16}F_3N_3O_4$: C, 46.57; H, H, 4.81; N, 12.53. Found: C, 46.07; H, 4.84; N, 11.93; Cl, 2.42. No further attempts were made to purify 2NTP-Lys.

Determination of Binding Affinities. Binding affinities of the fluorinated nitrophenyls were determined by NMR spectroscopy and fluorescence quenching.

Fluorescence Quenching. Initial determinations of the binding affinity of DNTP-GABA and 2NTP-GABA to MOPC-315 7S monomer were hampered by high affinity, nonspecific quenching. This nonspecific quenching was minimized by using protein further purified on a DE-52 column. The re-

Figure 1

Structure and abbreviations of fluorinated nitrophenyl haptens.

FIGURE 1.

STRUCTURE AND ABBREVIATIONS

OF FLUORINATED NITROPHENYL HAPTENS

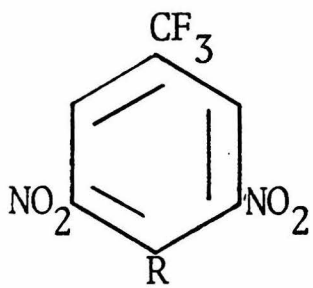

DNTP-GABA

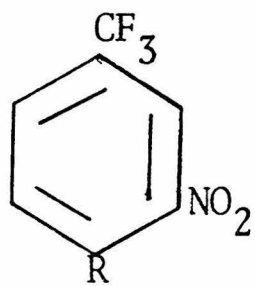

2NTP-GABA

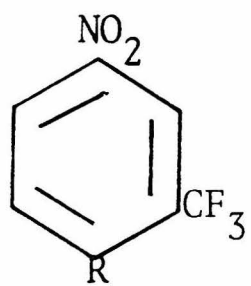

NTP-GABA

R = $-NH(CH_2)_3CO_2^-$

R = $-NH(CH_2)_4CH(CO_2^-)(NH_3^+)$

DNTP-Lys 2NTP-Lys NTP-Lys

R = $-NHCH_2CO_2^-$

DNTP-Gly

maining nonspecific quenching and machine fluctuations were corrected by using a solution of Fc peptides (material not absorbed by the affinity column after pepsin digest to make Fab' fragments).

Protein samples in buffer were adjusted to a concentration of 0.05-0.5 mg/ml and centrifuged to remove any dust or precipitate[3] and the concentration rechecked by absorption at 278 nm. The fluorescence spectra were run on 3 ml of this protein solution using a Perkin Elmer Fluorescence Spectrophotometer MPF-4. The excitation wavelength was 290 nm and the fluorescence was observed at 332 nm. The protein was titrated with 10 µl aliquots of hapten solution and the blank fluorescence was obtained by a simultaneous titration of a sample containing only the buffer. Nonspecific binding and machine fluctuations were determined by a concurrent titration of the Fc peptides of equal absorption at 278 nm. The fluorescence data were analyzed and the dissociation constant determined from the slope and intercept of the Sips plot (Eisen, 1964). In the actual analysis of the fluorescence data the value of Q_{max} was treated as an unknown. The value of Q_{max} was varied until the best fit to a straight line

[3]Originally solutions were filtered through a 0.45 micron millipore filter, but the coatings on the filter added to protein and buffer absorption at 278 nm.

was achieved from the data when plotted according to the Sip equation.

NMR binding determinations. The binding affinity of the fluorinated haptens were also determined by NMR spectroscopy. The ^{19}F NMR spectra of NTP-GABA are in fast exchange on the NMR time scale. The observed chemical shift, δ, of this fluorinated label is dependent on the ratio of the concentration of the label bound, [AbHap], to the total hapten concentration [Hap_o], and on the total chemical shift, Δ, eq. 1.

$$\delta = \frac{[AbHap]}{[Hap_o]} \Delta \qquad (1)$$

From the ^{19}F NMR spectra of a number of different antibody hapten ratios it is possible to determine the dissociation constant as described by Gammon et al. (1972). Using this method the dissociation constant and total chemical shift, Δ, for NTP-GABA and NTP-Lys were determined.

Once the dissociation constant and Δ are determined for NTP-GABA the binding affinity of the other labels can be determined by inhibition of NTP-GABA binding. The procedure for determination of the binding of a competitive substrate by NMR spectroscopy is outlined by Smallcombe et al. (1972a) for chymotrypsin. The procedure used by them is slightly more complicated than

needed here because they included enzyme dimerization. Their equations can be rewritten without dimerization in terms of antibody, [Ab], hapten [Hap] and competitive hapten [Hap'] concentration to give:

$$[Ab_o] = [Ab] + [AbHap] + [AbHap'] \tag{2}$$

$$[Hap_o] = [Hap] + [AbHap] \tag{3}$$

$$[Hap'_o] = [Hap'] + [AbHap'] \tag{4}$$

$$K_d = \frac{[Ab][Hap]}{[AbHap]} \tag{5}$$

$$K'_d = \frac{[Ab][Hap']}{[AbHap']} \tag{6}$$

$$K'_d = \frac{([Ab_o] - [AbHap] - [AbHap'])([Hap'_o] - [AbHap'])}{[AbHap']} \tag{7}$$

$$[AbHap'] = \frac{K_d[AbHap]-[Ab_o][Hap_o]+[AbHap][Hap_o]+[Ab_o][AbHap]-[AbHap]^2}{[AbHap] - [Hap_o]} \tag{8}$$

from equation 1

$$[AbHap] = \frac{\delta[Hap_o]}{\Delta} \tag{9}$$

RESULTS

Binding Affinities. Table I lists the binding affinities for various fluorinated haptens as determined both by magnetic resonance and by fluorescence quenching technique. In the case for protein concentrations of less than 0.5 mg/ml the binding constants were calculated from the slope and intercept of Sips plots using fluorescence quenching data. In the case of magnetic resonance techniques, protein concentration was about 40 mg/ml. Early work seemed to substantiate the claim (Johnston et al., 1974) that binding affinities for MOPC-315 proteins are dependent on protein concentrations. However, studies using DE-52 purified protein and Fc peptides to correct for nonspecific quenching gave binding affinities which were essentially in agreement with those determined by the magnetic resonance techniques, which gave values only to one significant figure. This inaccuracy is not inherent in the NMR method, but in these cases, to obtain good signal to noise sensitivity in a reasonable observation time, one must use protein concentrations considerably greater than the hapten-antibody dissociation constant. The fact that $[Ab_o] >> K_d$ leads to the inaccuracy.

The binding affinities of DNTP-Lys and 2NTP-Lys were not determined because of difficulties of obtaining pure samples and the low solubility at pH 7.4 of DNTP-

Table I

BINDING AFFINITY[a] OF FLUORINATED HAPTENS FOR MOPC-315 IMMUNOGLOBULIN DETERMINED BY FLUORESCENCE QUENCHING AND NMR SPEC.

	K_a by Fluorescence Quenching	Q_{Max}[b]	Sips Coeff.[c]	K_a by NMR Spectroscopy
DNTP-GABA	3.4×10^6	67	.99	1×10^6
2NTP-GABA	7.8×10^5	66	1.01	$>3 \times 10^5$
NTP-GABA	1.3×10^5	67	1.06	2×10^5
DNTP-Gly	2.4×10^4	69	1.02	3×10^4
NTP-Lys				1×10^5

[a]Binding affinities measured at 25.0 ± .1°C for fluorescence quenching and 25.5 ± 1°C for NMR spectroscopy.

[b]Fraction of protein fluorescence quenched when saturated by hapten.

[c]Sips index of heterogeneity from fluorescence measurements.

Lys; however, the binding affinities of these two ligands are probably roughly similar to those for their γ-amino-butyric acid analogues. For example, Haimovich et al., (1971) found the binding affinity of MOPC-315 for DNP-GABA (7.0×10^7 M^{-1}) to be higher by a factor of 3.5 than for DNP-Lys (2.0×10^7 M^{-1}) at 4°C. Johnston et al., (1974) measured the binding of DNP-Lys at both 4°C and 25°C; binding was stronger by an order of magnitude at 4°C relative to 25°C. Though the affinities of MOPC-315 for DNP-GABA and TNP-GABA (the analogues of the haptens we have studied in which a nitro group replaces a trifluoromethyl group) were not determined, we can estimate the effect of exchanging a trifluoromethyl group for nitro group if we assume that the DNP-GABA analogue still binds more strongly at 25°C than the DNP-Lys analogue by a factor of about 3.5. Using this type of comparison together with the experimental results in Table I, we estimate that substitution of a p-nitro substituent by a p-trifluoromethyl group causes ΔG for binding to increase by about 1 kcal/mole (i.e. p-CF_3 binds less strongly). Substitution of an o-nitro group by an o-trifluoromethyl group causes ΔG for binding to increase by about 2 kcal/mole. Various published determinations of the affinity for DNP-Lys differ by about 0.5 kcal/mole (Johnston et al., 1974, measured the binding affinities by both

fluorescence quenching and equilibrium dialysis and also list several other literature values). While such comparisons are not likely to be quantitatively precise, they suggest two general conclusions: (i) substitution of a nitro group by a trifluoromethyl group does not cause a major change in binding energy (ii) binding is somewhat more sensitive to such substitutions at the ortho compared to the para position of the phenyl ring.

Though we have not determined the affinities for binding of the various fluorinated haptens to the Fab' and Fv fragments of MOPC-315, they are probably similar to those for binding to the intact immunoglobulin molecule. Hochman et al., (1973) found the affinity for binding of DNP-Lys to the intact MOPC-315 7S protein and to the Fab' fragment to be equal (2.4×10^6 M^{-1}).

Chemical Shift. The fluorine nuclei of all the haptens studied in this work show a downfield shift when the haptens bind to MOPC-315. Table II tabulates these shifts and shows that their magnitudes depend primarily on the structural relationship between the side chain of the hapten and the trifluoromethyl group and are essentially independent of the other substituents on the aromatic ring. In contrast to these observations for binding to MOPC-315, these same haptens show strikingly different behavior when they interact with other anti-

Table II

TOTAL CHEMICAL SHIFT, Δ, OF FLUORINATED HAPTENS BOUND TO MOPC-315 IMMUNOGLOBULIN AND ITS PROTEOLYTIC FRAGMENTS

	7S Immunoglobulin	Fab' Fragment	Fv Fragment
DNTP-GABA	1.79 ± .05	1.79 ± .05	1.81 ± .05
DNTP-Lys	1.79 ± .05	1.79 ± .05	1.77 ± .05
DNTP-Gly		>1.53	>1.51
NTP-GABA	.62	.60 ± .05	.66 ± .05
NTP-Lys	.72 ± .05	.62 ± .05	
2NTP-GABA	1.85 ± .05	1.83 ± .05	1.79 ± .05
2NTP-Lys			1.76 ± .05

NOTE: All shifts are downfield and measured in ppm.

DNP myeloma proteins. For example, in this work we have found that DNP-GABA when bound to MOPC-315 shows a downfield shift of 1.8 ppm whereas, in other work, binding to XRPC-25 causes an upfield shift of 1.0 ppm. Thus both the direction and magnitude of the shifts observed are crucially dependent on the protein to which a given hapten binds.

DISCUSSION

Binding Affinities. The data of Table I show that neither the nature of the substituents nor their relative position about the phenyl ring greatly affect the binding constants. Thus 2NTP-GABA, NTP-GABA and DNTP-GABA have K_{ass} values within about an order of magnitude of each other. In contrast the side chain has a larger effect (DNTP-GABA binds 140 times more strongly to MOPC-315 than does DNTP-Gly). Previous work (Hochman et al., 1973) indicates that the Fv fragment of MOPC-315 has a slightly stronger affinity for DNP-Lys than does either the Fab' fragment or the 7S monomer.

Our results for the binding affinities of various haptens can be compared with structural models proposed by Padlan et al., (1976) and Dwek et al., (1977) which place the DNP ring into a hydrophobic aromatic box. In this location, the major interactions between the hapten

and the protein can be viewed as ring stacking or charge transfer involving the nitrophenyl ring of the hapten and trp 93 of the light chain of the immunoglobulin together with hydrogen bonding between the p-nitro group and tyr-34 (L) and between an o-nitro group and asn-36 (L). As both a nitro and trifluoromethyl group are strongly electron withdrawing, substitution of one for the other might not significantly alter charge transfer interactions between hapten and protein.

Inter- and intra-molecular hydrogen bonds have been reported involving nitro groups (Baitinger et al., 1964). In contrast only weak intra-molecular hydrogen bonding in dilute solutions are usually observed for trifluoromethyl groups (Doddrell et al., 1969; Kiehlmann et al., 1973; and Baker and Shulgin, 1965). Thus, substitution of a nitro group by a trifluoromethyl group should weaken somewhat that part of the binding affinity which results from hydrogen bonding interactions.

Other characteristics of a nitro group and trifluoromethyl group are somewhat similar. For example, the dipole moments of both should be in the same direction so that both should participate similarly in dipole-dipole and ion-dipole interactions, which as in the case of hydrogen bonding, will probably not be of the same strength. The van der Waals radii of a trifluoromethyl group

(2.7 Å) and a nitro group (2.6 Å) are essentially the same. (These values are calculated from bond distances determined by x-ray diffraction of a trifluoromethylphenyl compound (Cohen-Addad, 1973) and of nitrobenzene (Trotter, 1959) together with van der Waals radii listed by Pauling (1960)). Of course, the trifluoromethyl group, being spherical, will occupy more space than the planar nitro groups.

Thus, qualitatively, one might observe as we do, that a trifluoromethyl and a nitro group interact similarly with MOPC-315. The weaker binding of NTP-GABA (with the CF_3 group in the ortho position) relative to 2NTP-GABA (with the $-CF_3$ group in the para position) suggests a stronger hydrogen bond to the ortho than to the para substituent (which should favor a nitro over a trifluoromethyl group). Alternately, this subsite in the protein for the o-nitro group may be narrow and oblong which could force the phenyl ring to be rotated 180° so that the o-CF_3 group in fact occupies the subsite normally occupied by a third nitro group at C-6 of TNP-haptens.

The binding data for 2,6-dinitro; 4-nitro; 2,4-dinitro; and 2,4,6-trinitro compounds (Haselkorn et al., 1974) indicate strong binding interactions between the protein and nitro groups in the 2 and 4 position; a nitro group in the 6-position interacts much more weakly. The

binding affinities of the NTP compounds when compared to 4-nitrophenyl compounds show a strong interaction between the o-CF_3 group and the protein which causes us to favor a binding mode in which this o-CF_3 group does, in fact, occupy the position normally occupied by a 2-NO_2 substituent.

Environment of Bound Ligand. The environment of the bound hapten can be probed by observing the chemical shift of the ^{19}F nucleus of the trifluoromethyl group of the hapten (Table II). Though very sensitive to environmental effects, the total chemical shift Δ (for the hapten in the hapten-antibody complex relative to the hapten free in solution) should be independent of such other factors as binding affinity and dynamics (Gammon et al., 1972). (This shift, Δ, should be distinguished from the chemical shift, δ, actually observed under a given set of experimental conditions; in the case of fast exchange, δ depends crucially on such factors as binding affinity).

Downfield shifts of ^{19}F nuclei on binding to protein have previously been observed, for example in chymotrypsin-inhibitor complexes (Gammon et al., 1972). Many factors can be responsible for such shifts but one which is likely to be particularly germane to antibodies, such as MOPC-315 with specificity for aromatic haptens, is the downfield shift experienced by nuclei brought near the plane

of an aromatic ring in the protein. These shifts arise from the effects of the diamagnetic ring currents in the delocalized π electron systems of aromatic rings. Since the magnetic currents resulting from these fields do not distort the electronic wave functions of the probe nucleus, the magnitude of the shift observed for a given ring current will be independent of the kind of nucleus (Millet and Raftery, 1972). The shifts to be expected for nuclei at various distances and directions from benzene rings have been calculated (Emsley et al., 1967; Johnson and Bovey, 1958). For a 1.7 ppm downfield shift to be caused entirely by diamagnetic ring current, deshielding would require that the fluorine nuclei be held very close to an aromatic system. The likely importance of such ring current contributions to the observed chemical shift finds support in the observation that nitrophenyl diazonium affinity labels react specifically with tyrozine-34 of the light chain of MOPC-315; this amino acid is in the first hypervariable region (Goetzl and Metzger, 1970b). Further evidence comes from circular dichroism studies of the binding of ε-N-2,4,6-trinitrophenylaminocaporate of MOPC-315; the circular dichroism spectrum of the complex showed strong interactions between this hapten and a nearby tryptophan residue(s) of the antibody (Freed et al., 1976; Orin et al., 1976). They calculated that an interaction of the hapten with

only one tryptophan residue (with parallel or tilted orientations) would require a separation of 3.5 Å. Interaction with four tryptophans increased their calculated distance to 7 Å. More precise deductions about such interactions have recently been drawn (Dwek et al., 1977; Padlan et al., 1976) which place the nitrophenyl ring of the hapten in a pocket lined by aromatic residues and in intimate contact with trp-93 (L).

Other effects which can contribute to a change in chemical shift for a nucleus on a hapten free in solution compared to one bound to antibody include van der Waals interactions, electric fields, and specific bonding with neighboring groups, such as hydrogen bonding (Millet and Raftery, 1972). These are more difficult to evaluate quantitatively, but moving a ^{19}F nucleus into an environment with a higher polarizability (Evans, 1960) or the formation of a new hydrogen bond (Doddrell et al., 1969; Kiehlmann et al., 1973) both usually cause downfield shifts. Given the specificity of MOPC-315 for nitrophenyl haptens, the possibility of hydrogen bond donating residues in the binding pocket seems high. For example such hydrogen bonds have been suggested between tyr-34 (L) and a para substituent and between asn-36 (L) and an ortho substituent of the hapten (Dwek et al., 1977; Padlan et al., 1976).

Two further points about the observed chemical shift deserve emphasis: (i) the shift depends only on the location of the ^{19}F nucleus on the phenyl ring of the hapten; it does not depend on the nature or location of other substituent about the phenyl ring and is, in this sense, relatively insensitive to the changes in affinity caused by such alterations in the structure of the hapten; (ii) the chemical shift is not influenced by the amount of the constant region of the antibody which is present (Fv~Fab~7S immunoglobulin, Fig. 3).

The essential invariance of the chemical shift of a p-CF_3 group in DNTP-GABA, DTNP-Lys, DNTP-Gly, 2NTP-GABA, and 2NTP-Lys suggests that the binding pocket of MOPC-315 for the phenyl ring is a relatively rigid, preformed pocket (lock and key model), that provides the main specific attractive interactions between antibody and hapten. Thus changing the number of nitro groups from two to one, or changing the side chains from GABA to Lys or Gly does not appreciably alter the orientation of the hapten phenyl group relative to the binding pocket of the antibody. These changes can nevertheless alter the total attraction between hapten and antibody with resulting variations in the binding affinities.

The independence of chemical shift on the size of the immunoglobulin fragment (Fv, Fab;, 7S, IgA) suggests that the structure of the binding site when filled with hapten is essentially the same regardless of how much of the rest of the immunoglobulin molecule is attached. Further, these results do not indicate any observable differences between the two binding sites of a single immunoglobulin molecule. Thus, there are not two classes of binding sites. Our best evidence for this contention is the finding that in those cases where the hapten is in slow exchange, the spectra show only two species of hapten, one bound and the other free in solution (Fig. 2). The fact that we observe no differences between the two binding sites by NMR spectroscopy is consistent with binding data we determined by fluoroescence quenching. Table I lists the Sips coefficient, for the binding of MOPC-315 to the fluorinated haptens. The Sips coefficient measures heterogeneity in the observed binding affinities. A value of one indicates that all binding sites have equal binding affinity and do not interact. Thus, antigen binding can be accurately described by a simple mass action equation such as (5), which assumes equivalent and noninteracting binding sites on the antibody molecule (Nisonoff and Pressman, 1958).

Figure 2

^{19}F NMR spectra of DNTP-GABA

(a) 4.4×10^{-4} M with 3.3×10^{-4} M Fv MOPC-315.

(b) 7.6×10^{-4} M with 3.6×10^{-4} M Fab' MOPC-315.

(c) 5.8×10^{-4} M with 3.0×10^{-4} M (in binding site) 7S MOPC-315.

(d) 10^{-3} M in buffer with no protein. 0.5 KHz of 2.5-3.0 KHz spectra width, 0.3 sec acquisition time, 1.8-2.1 sec pulse delay, 9-23 K transients, 0.1 sec sensitivity enhancement, 4 or 8K Fourier transform, 90° r.f. pulse, D_2O lock. Probe temperatures 25°C. Chemical shifts are in ppm downfield relative to an external trifluoroacetic acid standard (2.5 mmol in D_2O, H_2O).

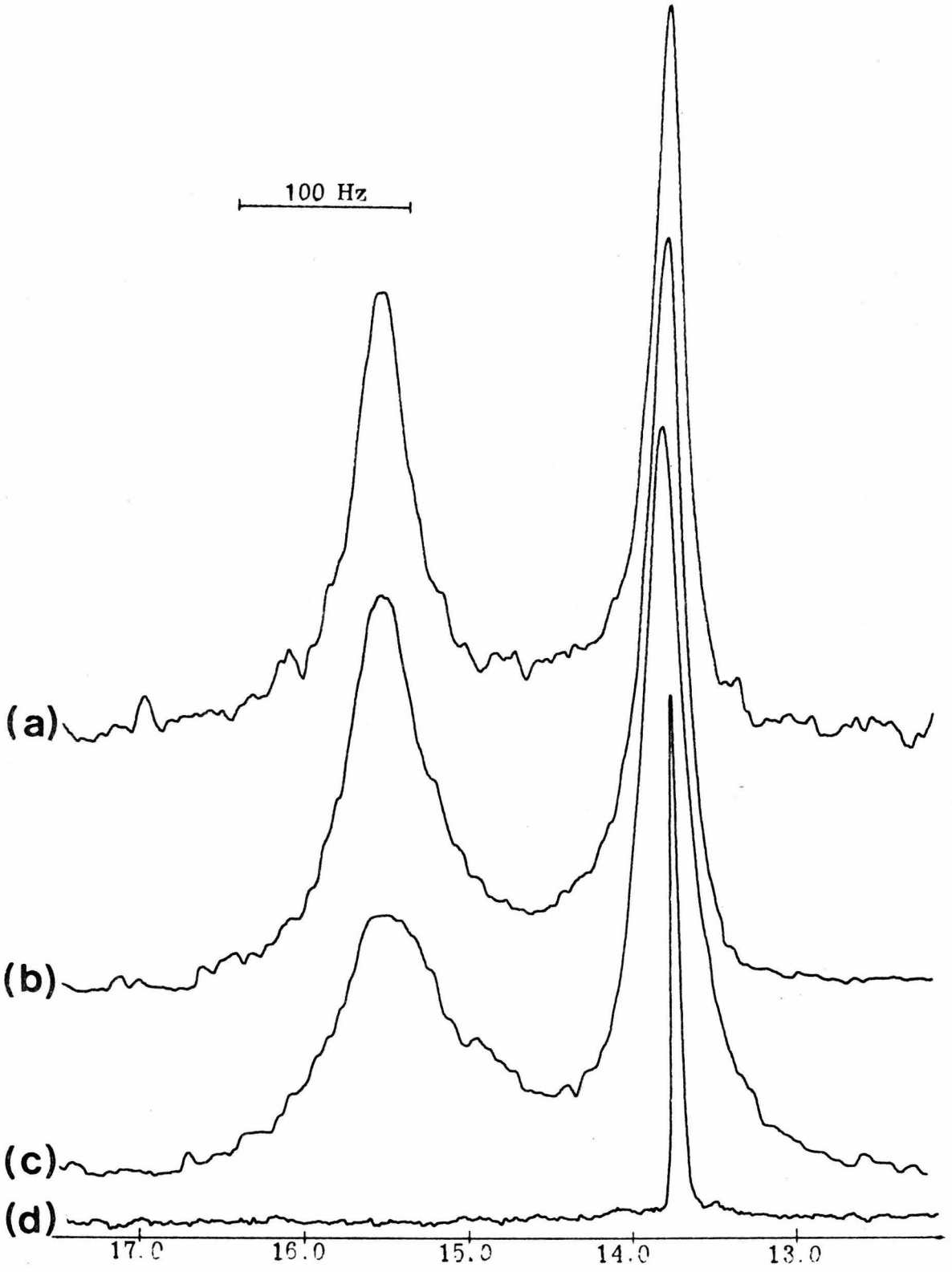
100 Hz
(a)
(b)
(c)
(d)
17.0
16.0
15.0
14.0
13.0
ppm downfield from TFA

REFERENCES

Baker, A.W. and Shulgin, A.T. (1965), Nature 206, 712.

Baitinger, W.F., Schleyer, P., Von R., Murty, T.S.S.R., and Robinson, L. (1964), Tetrahedron 20, 1635.

Cohen-Addad, P.C. (1973), Acta Cryst. B, 29, 157.

Doddrell, D., Wenkert, E., and Demaro, P.V. (1969), J. of Mol. Spect. 32, 162.

Dugan, E.S., Bradshaw, R.A., Simms, E.S., and Eisen, H.N. (1973), Biochemistry 12, 5400.

Dwek, R.A., Wain-Hobson, S., Dower, S., Gettens, P., Sutton, B., Perkins, S.J., and Givol, D. (1977), Nature 206, 31.

Eisen, H.N., Simms, E.S., and Potter, M. (1968), Biochemistry, 7, 4126

Eisen, H.N. (1964), Methods of Med. Res. 10, 94, 106, 115.

Emsley, J.W., Feeney, J., and Sutcliffe, L.H. (1965), High Resol. Nucl. Mag. Res. Spec. 1, 595.

Evans, D.F. (1960), J. Chem. Soc., 877.

Francis, S.H., Leslie, R.G.Q., Hood, L., and Eisen, H.N. (1974), Proc. Nat. Acad. Sci. USA, 71, 1123.

Freed, R.M., Rockey, J.H., and Davies, R.C. (1976), Immunochemistry 13, 509.

Gammon, K.L., Smallcombe, S.H., and Richards, J.H. (1972), J. Amer. Chem. Soc. 94, 4573.

Goetze, A.M. and Richards, J.H. (1977), Biochemistry 16, 228.

Goetzl, E.J. and Metzger, H. (1970a), Biochemistry 9, 1267.

Goetzl, E.J. and Metzger, H. (1970b), Biochemistry 9, 3862.

Gunstone, F.D. and Tucker, S.H. (1963), Org. Syn., Coll. Vol. IV, 160.

Haimovich, J., Eisen, H.N., and Givol, D. (1971), Ann. N.Y. Acad. Sci. 180, 352.

Haselkorn, D., Friedman, S., Givol, D., and Pecht, I. (1974), Biochemistry 13, 2210.

Hinderman, D.K. and Cornwell, C.D. (1968), J. Chem. Phys. 48, 2017.

Hochman, J., Inbar, D., and Givol, D. (1973), Biochemistry 12, 1130.

Huestis, W.H. and Raftery, M.A. (1972), Biochemistry 11, 1648.

Inbar, D., Rotman, M., and Givol, D. (1971), J. Biological Chem. 246, 6272.

Inbar, D., Hochman, J., and Givol, D. (1972), Proc. Nat. Acad. Sci. USA 69, 2659.

Johnson, C.E. and Bovey, F.A. (1958), J. Chem. Phys. 29, 1012.

Johnston, M.F.M., Barisas, B.G., and Sturtevant, J.M. (1974), Biochemistry 13, 390.

Kiehlmann, E., Menon, B.C., and McGillivray, N. (1973), Can. J. Chem. 51, 3177.

Maddox, M.L., Rose, D.C., and Gerig, J.T. (1975), J. Chem. Soc. (Chem. Comm.) 902.

Millet, F. and Raftery, M.A. (1972), Biochem. Biophys. Res. Comm. 47, 625.

Nisonoff, A. and Pressman, D. (1958), J. Immunol. 80, 417.

Orin, G.B., Davies, R.D., Freed, R.M., and Rockey, J.M. (1976), Immunochemistry 13, 517.

Padlan, E.A., Davies, D.R., Pecht, I., Givol, D., and Wright, D. (1976), Cold Spring Harbor Symp. Quant. Bio. 41, 627.

Pauling, L. (1960), "The Nature of the Chemical Bond", 3rd ed., Ithaca, N.Y., Cornell University Press, p. 260.

Porter, R.R. (1950), Methods in Med. Res. 3, 256.

Potter, M. (1972), Physiological Reviews 52, 631.

Smallcombe, S.H., Gammon, K.L., and Richards, J.H. (1972a) J. Amer. Chem. Soc. 94, 4581.

Smallcombe, S.H., Ault, B., and Richards, J.H. (1972b), J. Amer. Chem. Soc. 94, 4585.

Trotter, J. (1959), Acta Cryst. 12, 884.

Underdown, E.J., Simms, E.S., and Eisen, H.N. (1971), Biochemistry 10, 4359.

PART III

Perturbation Mixing as a Technique for Studying Binding Dynamics in Biological Systems. Interaction of MOPC-315 with ^{19}F Labelled Nitrophenyl Haptens

INTRODUCTION

Recognition and binding of antigen by antibody occurs as a first step in the response of the immune system to a foreign invader. This interaction between antibody and antigen (or hapten) has been studied by a variety of methods; most recently NMR techniques have proved useful in obtaining information about binding affinities and the environments experienced by bound ligands in the case of several antibodies specific for haptens related to phosphorylcholine (Goetze and Richards, 1977a, 1977b) and of MOPC-315 (both the intact 7S immunoglobulin and Fab' and Fv fragments) which specifically binds nitrophenyl haptens (Dwek et al., 1977; Kooistra and Richards, 1977). With MOPC-315, these studies demonstrated that the binding pocket of the 7S, Fv and Fab' proteins provided the same environment to bound hapten and also that different nitrophenyl haptens with very different thermodynamic binding affinities are bound in the same way in the same site. Thus, the environment experienced by a trifluoromethyl group (as the ^{19}F NMR probe) attached to a phenyl ring depended only on the structural relationship between the CF_3 group and the side chain of the hapten and not on the nature of other phenyl substituents or the structure of the side chain (Kooistra and Richards, 1977).

In this paper, we explore the relative dynamics of binding of nitrophenyl haptens by 7S, Fab' and Fv proteins. In brief, we find that the rates (k_{off})[1] are the same for dissociation of hapten from the 7S, Fab', or Fv protein as determined by NMR techniques. The association rates (k_{on}), calculated from these k_{off} values and equilibrium binding affinities, agree with k_{on} values determined by other techniques (Pecht et al., 1972a, b; Haselkorn et al., 1974; and Hochman et al., 1972) though, in our studies, the measurements were made at considerably higher protein concentrations (10-30 mg/ml) than were used previously ($\leq$ 1 mg/ml).

The similarities in results for the intact immunoglobulin and its various fragments suggest that, apart from possible influences on the mobility of the binding site as a whole, there is little interaction between the

---

[1] Abbreviations used are: k_{off}, off rate; k_{on}, on rate; Δ, total chemical shift (separation of NMR absorption of the bound and free hapten) measured in Hz; δ, observed chemical shift, actual position of the NMR signal dependent on the mole fraction of the ligand bound; B, subscript used to represent hapten bound; F, subscript used to represent free unbound hapten; P, mole fraction; τ, average life time equal to the weighted average of the life time in the bound (τ_B) and free (τ_F) state $\tau_B\tau_F/\tau_B+\tau_F$ or $\tau_B P_F$ or $\tau_F P_B$; $\delta_{\nu_{\frac{1}{2}}}$, line width of NMR peak at half height; T_1, spin lattice or longitudinal relaxation time; T_2, transverse or spin-spin relaxation time equal to $1/\pi^2\delta_{\nu_{\frac{1}{2}}}$; M, net magnetization of nuclei aligned with the magnetic field, proportional to the peak area; DNTP-GABA, γ-N-(2,6-dinitro-4-trifluoromethylphenyl) aminobutyric acid; NTP-GABA, γ-N-(4-nitro-2-trifluoromethylphenyl) aminobutyric acid; 2NTP-GABA, γ-N-(2-nitro-4-trifluoromethylphenyl aminobutyric acid.

variable and the constant regions of the protein. Moreover, the independence of binding dynamics on concentration over a thirty-fold, or more, range indicates that no important interactions occur between individual immunoglobulin molecules, such as aggregation.

In measuring the dissociation dynamics we have used a novel method for the study of rate processes in biological systems (perturbation mixing). This method is independent both of line widths and chemical shifts but requires that the exchange lifetime, τ, should be faster than the spin-lattice relaxation time (T_1) averaged for the two sites and that the chemical shift separation between the peaks for the nuclei in the two environments should be sufficiently large to allow selective perturbation of only one of the two peaks. This technique also, of course, requires that the exchange process be slow relative to the chemical shift separation, Δ, for the nuclei in the two environments, $\tau > \frac{\sqrt{2}}{2\pi\Delta}$, ($\tau$ is the weighted average lifetime in the two environments). When used in conjunction with line width and chemical shift data, this technique has revealed the existence of low affinity binding site(s) in the variable region of the antibody.

Transverse relaxation times, T_2, were also determined for haptens bound to 7S, Fab', and Fv proteins. The observed values show that the motional freedom of the

binding site region is less in the 7S immunoglobulin than it is in the Fab' fragment which in turn is less than the motional freedom in the Fv fragment. Thus, attachment of constant regions of the immunoglobulin to the binding site does restrict the freedom of that site.

General Theory

Two complementary methods were used to study the rate of exchange of different nitrophenyl haptens between solution and the binding site of MOPC-315 proteins (7S, Fab', Fv): the chemical shift-line width technique and a technique we have called perturbation mixing.

Chemical Shift-Line Width

Three general behaviors characterize the exchange process and its effect on the NMR spectra for nuclei which are exchanging between two magnetically nonequivalent environments; the important characteristic separating these three behaviors is the relationship between the average lifetime in one of the environments and the chemical shift difference between the two environments.

(i) For slow exchange, when

$$\tau = \tau_F P_B = \tau_B P_F > \sqrt{2}/(2\pi\Delta) \qquad 1$$

τ_F and τ_B are the life times of the unbound or free hapten and the bound hapten respectively and P_F and P_B are the mole fraction of the free and bound hapten respectively.

The two absorptions can be considered separately and the observed line width of each peak is the sum of the intrinsic line width (in the absence of exchange) and the reciprocal of the lifetime in that state:

$$1/T_{2F} = 1/T'_{2F} + 1/\tau_F \qquad 2$$

$$1/T_{2B} = 1/T'_{2B} + 1/\tau_B \qquad 3$$

$$1/\tau_B = P_F/\tau_F P_B = k_{off} \qquad 4$$

T_{2F} and T_{2B} are the observed transverse relaxation times of the free and bound ligand respectively.

T'_{2F} and T'_{2B} are the intrinsic (in the absence of exchange) transverse relaxation times of the free and bound hapten.

(ii) As one moves from the region of slow exchange to the region of intermediate exchange, the two peaks come closer together and coalesce at

$$k_{off} = 1/\tau_B = (\sqrt{2}\ \pi\Delta/2) \qquad 5$$

under conditions of equal populations of bound and free hapten, $P_F = P_B$ and $\tau_F = \tau_B$

(iii) As the exchange rate further increases, a single absorption is observed at a chemical shift which is the weighted average of the two environments.

$$\delta = \Delta \frac{[Ab \cdot Hap]}{[Hap_o]} = \Delta P_B \qquad 6$$

$[Hap_o]$ and [Ab·Hap] are the concentrations of total hapten in solutions and of hapten bound to antibody respectively. The observed line width of this absorption is the weighted average of the intrinsic line widths for the bound and free hapten plus further broadening caused by the exchange process itself.

$$\frac{1}{T_2} = \frac{P_B}{T'_{2B}} + \frac{P_F}{T'_{2F}} + \frac{4\pi^2 P_B P_F{}^2 \Delta^2}{k_{off}} \qquad 7$$

Under appropriate conditions, each of the nitrophenyl hapten MOPC-315 systems falls into a different one of these three regions.

Perturbation Mixing

This technique is the Fourier transform, pulse analogue of the continuous wave, double resonance technique previously used to study exchange rates slower than T_1 (Forsén and Hoffman, 1963a and b; Anet and Bourn, 1967). This technique is a modification of that used to measure conformational flipping of [2.2]2,5-pyrolloparacyclophane (Dahlquist et al., 1975).

Perturbation mixing, like other non-NMR techniques used for determining reaction rates (for example, temperature jump and stop flow), perturbs the system and then measures the return of the system to its equilibrium condition. In this case, the perturbation does not alter the chemical equilibrium of the system, but alters only

the alignment of the nuclear spin states from their equilibrium position in the magnetic field. This technique requires that (i) the nuclei in question undergo exchange at a rate which is slow relative to $\sqrt{2}\pi\Delta$, and in other words, that the chemical shift separation and line widths of the two resonances should be such that overlap between them is sufficiently small to allow selective inversion of the spins of the nuclei in one of the two environments. (ii) the exchange rate is preferably faster than, or at least not slower than, $1/T_1$. (An accurate knowledge of neither the chemical shift nor the line width of either resonance is, however, required.)

One perturbs the spins of the nuclei in one environment and then follows the return to equilibrium as a function of time. Though any magnitude of perturbing pulse can be used, a pulse near 180° is most effective for it causes the largest initial change. Return of the system to equilibrium occurs through spin lattice relaxation (T_1) and, most importantly for measuring exchange rates, by the physical transfer of those nuclei with their magnetization opposed to the applied field (those spins which have been inverted by the 180° pulse) and nuclei with their spins aligned with the applied field. This exchange process causes the net magnetization of nuclei in both sites to decrease. The equation describing the magnetization of

such a perturbed system to equilibrium is first order in the exchange rate and T_1 (Dahlquist et al., 1975).

$$\frac{dMz_B}{dt} = \frac{Mo_B - Mz_B}{T_1} - k_{off}\, Mz_B + k_F\, Mz_F$$

$$\frac{dMz_F}{dt} = \frac{Mo_F - Mz_F}{T_1} - k_F\, Mz_F + k_{off}\, Mz_B$$

where Mz_B and Mz_F are the net magnetization (peak areas) as time, t, for the bound and free peaks respectively; Mo_B, Mo_F are the net magnetizations at equilibrium; $k_{off} = 1/\tau_B$ and $k_F = 1/\tau_F$; T_{1B} and T_{1F} are the spin-lattice relaxation times of the bound and free haptens, respectively.

The complete solution of these equations is not, in general, determined by a single time constant (Forsen and Hoffman, 1963a) unless a simple relationship exists between Mz_B and Mz_F. One such relationship occurs when $T_{1B} = T_{1F}$ and $Mo_B = Mo_F$ (equal populations of nuclei in the two exchanging sites). Equal populations in the two sites can usually be achieved by prior knowledge of the equilibrium constant or by mixing protein and ligand to achieve equal integrated areas for the two absorptions. One has less control over T_1 values; if the nuclei in both sites have similar correlation times, their T_1 values should be comparable. But even when the two sites are characterized by very different correlation times (as in the interactions between a protein and a small molecule) the effective T_1

relaxations can be very similar if exchange is sufficiently fast that relaxation in one site provides the primary relaxation pathway for nuclei in both environments. (For example, the T_1 for the ^{19}F signal for DNTP-GABA, in the absence of protein, is about 1.5 sec. When an equivalent is bound to antibody, the observed T_1 is 0.5-0.65 sec which is essentially the same as the T_1 for the ^{19}F nuclei in the DNTP-GABA/MOPC-315 complex, Table III.) In our case, the rate of exchange is much faster than $1/T_1$ so that this difference between T_1 of the bound and free hapten is even less significant.

If $Mo_B = Mo_F$ and $T_{1F} = T_{1B}$, the decay can be described by a simple exponential, if one considers the difference in the decay rate of the peaks for the bound and free hapten:

$$\frac{dMz_B}{dt} - \frac{dMz_F}{dt} = \frac{d(Mz_B - Mz_F)}{dt}$$

$$= \frac{Mo_B - Mz_B}{T_{1B}} - k_{off}\, Mz_B + k_{on}\, Mz_F - \frac{Mo_F - Mz_B}{T_{1F}} + k_F\, Mz_F - k_{off}\, Mz_B$$

for $Mo_B = Mo_F$ $(k_{off} = k_F)$

and for $T_{1B} = T_{1F}$

$$\frac{d(Mz_B - Mz_F)}{dt} = \frac{-(Mz_B - Mz_F)}{T_1} - 2k_{off}(Mz_B - Mz_F)$$

$$= -\left(\frac{1}{T} + 2k_{off}\right)(Mz_B - Mz_F)$$

This equation can be integrated to give

$$\ln(Mz_B - Mz_F) = -\left(\frac{1}{T_1} + 2k_{off}\right)t + C$$

where

Under conditions when the inverting pulse is 180° and is short compared to $1/k_{off}$ so that no significant exchange occurs during the period of the inverting pulse itself, $C = \ln 2Mz_B = \ln 2Mz_F$.

Thus plots of $\ln(Mz_B - Mz_F)$ should be linear and their slopes will give $-\left(\frac{1}{T_1} + 2k_{off}\right)$. Independent determination of T_1, as by progessive saturation techniques (Freeman and Hill, 1971), then leads to a determination of k_{off}. When k_{off} is much larger than $1/T_1$ as in our case T_1 makes only a small correction on the rate measurement.

If the rate equations for Mz_B and Mz_F are added (rather than subtracted), the exchange term cancels and one has only terms for T_1 relaxation.

$$\frac{dMz_B}{dt} + \frac{dMz_F}{dt} = \frac{d(Mz_B + Mz_F)}{dt}$$

$$= \frac{Mo_F - Mz_F}{T_1} + \frac{Mo_B - Mz_B}{T_1}$$

$$\text{if} \quad T_{1B} = T_{1F}$$

$$\text{and} \quad Mo_B = Mo_F$$

$$\frac{d(Mz_B + Mz_F)}{dt} = \frac{2Mo - (Mz_F + Mz_B)}{T_1}$$

whence $\ln[2Mo - (Mz_F + Mz_B)] = - t/T_1 + C$

Thus slopes of $\ln[2Mo - (Mz_F + Mz_B)]$ plotted against time should be linear with a slope of $-1/T_1$. Though a modification of this relationship was used in determining the values of T_1 for [2.2]2,5-pyrolloparacylophane, we did not determine T_1 values used in this work by this method as we used only very short pulse delays.

Materials and Methods

Preparation of trifluoromethyl labelled nitrophenyl haptens, purification of MOPC-315 IgA immunoglobulin and its fragments, and preparation of NMR samples have been described previously (Kooistra and Richards, 1977).

Binding Affinities

The affinity constants for the association of several fluorinated nitrophenyl haptens with the Fv fragment of MOPC-315 were measured by fluorescence quenching techniques

as described previously (Kooistra and Richards, 1977); the Fv fragments were purified as described by Inbar et al. (1972) and not lyophilized as they were for the NMR experiments. The data are collected in Table I; the reason for the lower Sips coefficients observed for 2NTP-GABA and especially for DNTP-GABA binding to the Fv fragment probably arises from the relationship between affinity and concentrations used. To achieve optimum fluorescence signal and ratio of bound to free ligand, binding studies are best carried out under conditions where the molar concentration of protein is near the protein-hapten dissociation constant. Because of the high affinity of the protein for these haptens (hence a small dissociation constant), protein concentrations in the range 0.03-0.05 mg/ml were appropriate. At such low concentrations, any impurity with absorbence at 278 nm will cause a significant error in determining the protein concentration. We could partially correct this problem by preparing samples by addition of small aliquots of a more concentrated protein solution to a solution in a cuvette which had previously been zeroed. Another source of error may be the absorption of some protein on the walls of the quartz cuvette diminishing thereby the number of binding sites actually available. (Such an effect has been observed previously (Underdown et al., (1971).) Nevertheless, in different experiments,

Table I

Binding Affinities of Various Fluorinated Haptens for MOPC 315, 7S, and Fv Fragment Measured by Fluorescence Quenching[a]

	Fv			7S[d]		
Hapten	Ka	Qmax[b]	Sips[c] Coeff.	Ka	Qmax[b]	Sips[c] Coeff.
DNTP-GABA	5.4×10^6	88	.63	3.4×10^6	67	.99
2NTP-GABA[e]	7.0×10^5	88	.88	7.8×10^5	66	1.01
NTP-GABA	1.9×10^5	85	.99	1.3×10^5	67	1.06

[a]Binding affinities measured at 25.0 ± .1°C.

[b]Fraction of protein fluorescence quenched when saturated by hapten.

[c]Sips index of heterogeneity.

[d]Binding data for 7S monomer from (Kooistra and Richards, 1977).

[e]Binding affinity of this hapten for the Fab' fragment is 5.5×10^5 M^{-1}; Q_{max} = 83, Sips Coeff. = .99.

that had different heterogeneity indices and even different values of Qmax, we obtained comparable binding constants.

Perturbation Mixing

As shown in Figure 1, the ^{19}F NMR spectra for mixtures of the hapten, DNTP-GABA, and the 7S, Fab', and Fv proteins show two absorptions separated by 168 Hz, one for the hapten bound to protein and the other for the hapten free in solution (Kooistra and Richards, 1977). The spin of the upfield signal (free hapten) was selectively inverted with a 0.01 sec 180° pulse (a 0.01 sec pulse has an effective band width of about 50 Hz and has little effect beyond 90 Hz) with approximately 1 watt of power from the decoupler into the lower sideband.[2] Both signals are then sampled with a 75 μsec 90° pulse at various delay intervals after the 180° inversion pulse (Figure 2).

Rates for hapten exchanging between solution and antibody were measured on samples which contained equal populations of free and bound DNTP-GABA. (The relative populations were determined by integration using a line fitting technique described in Results, see Figure 1).

---

[2]We shall be pleased to provide upon request details of the program modifications to obtain computer controlled decoupler pulsing.

Figure 1

Comparison of observed ^{19}F NMR spectra for DNTP-GABA bound to MOPC-315 (7S, Fab', Fv) with the calculated line shapes used to determine intrinsic line widths of bound and free hapten.

a) 4.4×10^{-4} M DNTP-GABA with 3.3×10^{-4} M Fv MOPC-315 calc: Δ = 168 Hz, k_{off} = 36 sec^{-1}, P_B = .51, $\delta_{\nu\frac{1}{2}B}$ = 24 Hz, $\delta_{\nu\frac{1}{2}F}$ = 8 Hz.

b) 7.6×10^{-4} M DNTP-GABA with 3.6×10^{-4} M Fab' MOPC-315. calc: Δ = 168 Hz, k_{off} = 39 sec^{-1}, P_B = .52, $\delta_{\nu\frac{1}{2}B}$ = 37 Hz, $\delta_{\nu\frac{1}{2}F}$ = 9 Hz.

c) 5.8×10^{-4} M DNTP-GABA with 3.0×10^{-4} (in binding sites) 7S MOPC-315, calc: Δ = 168 Hz, k_{off} = 40 sec^{-} , P_B = .52, $\delta_{\nu\frac{1}{2}B}$ = 62 Hz, $\delta_{\nu\frac{1}{2}F}$ = 11 Hz.

All spectra represent .45 KHz of 2.5-3.0 KHz spectra width, 0.3 sec acquisition time, 1.8-2.1 pulse delay, 9-23 K transients, 0.1 sec sensitivity enhancement, 4-8 K Fourier transform, 90° r.f. pulse, D_2O lock. Probe temperature 25 C. Chemical shifts are in ppm downfield relative to an external trifluoroacetic acid standard (2.5 mmol in D_2O, H_2O). $\delta_{\nu\frac{1}{2}B}$ and $\delta_{\nu\frac{1}{2}F}$ values reported are corrected for sensitivity enhancement.

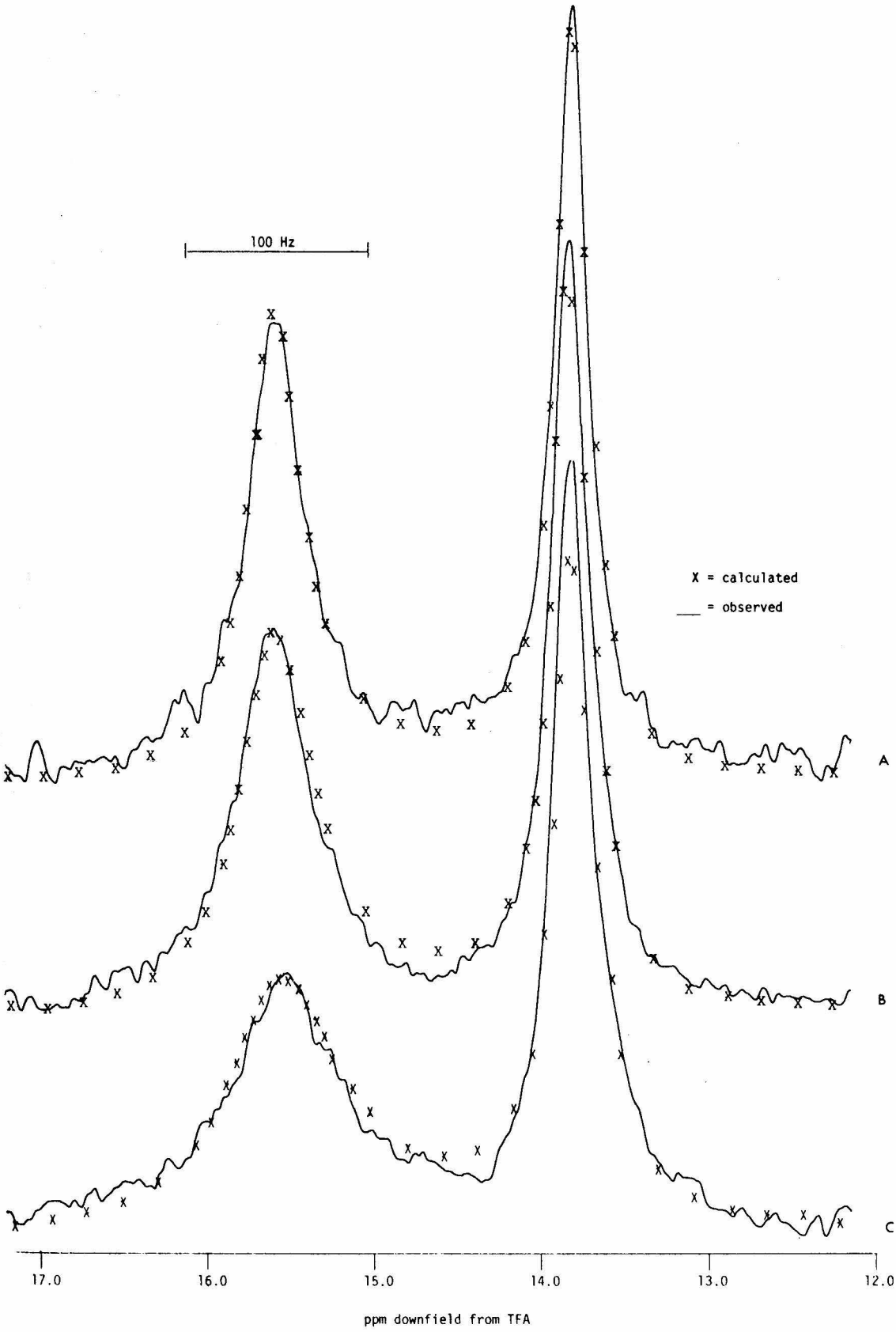
100 Hz
X = calculated
___ = observed
A
B
C
17.0
16.0
15.0
14.0
13.0
12.0
ppm downfield from TFA

Figure 2

^{19}F nmr spectra for DNTP-GABA binding to MOPC 315 Fv fragment from the perturbation mixing experiment. These spectra were taken at the delay time listed following a selective 180° pulse to the unbound hapten peak.

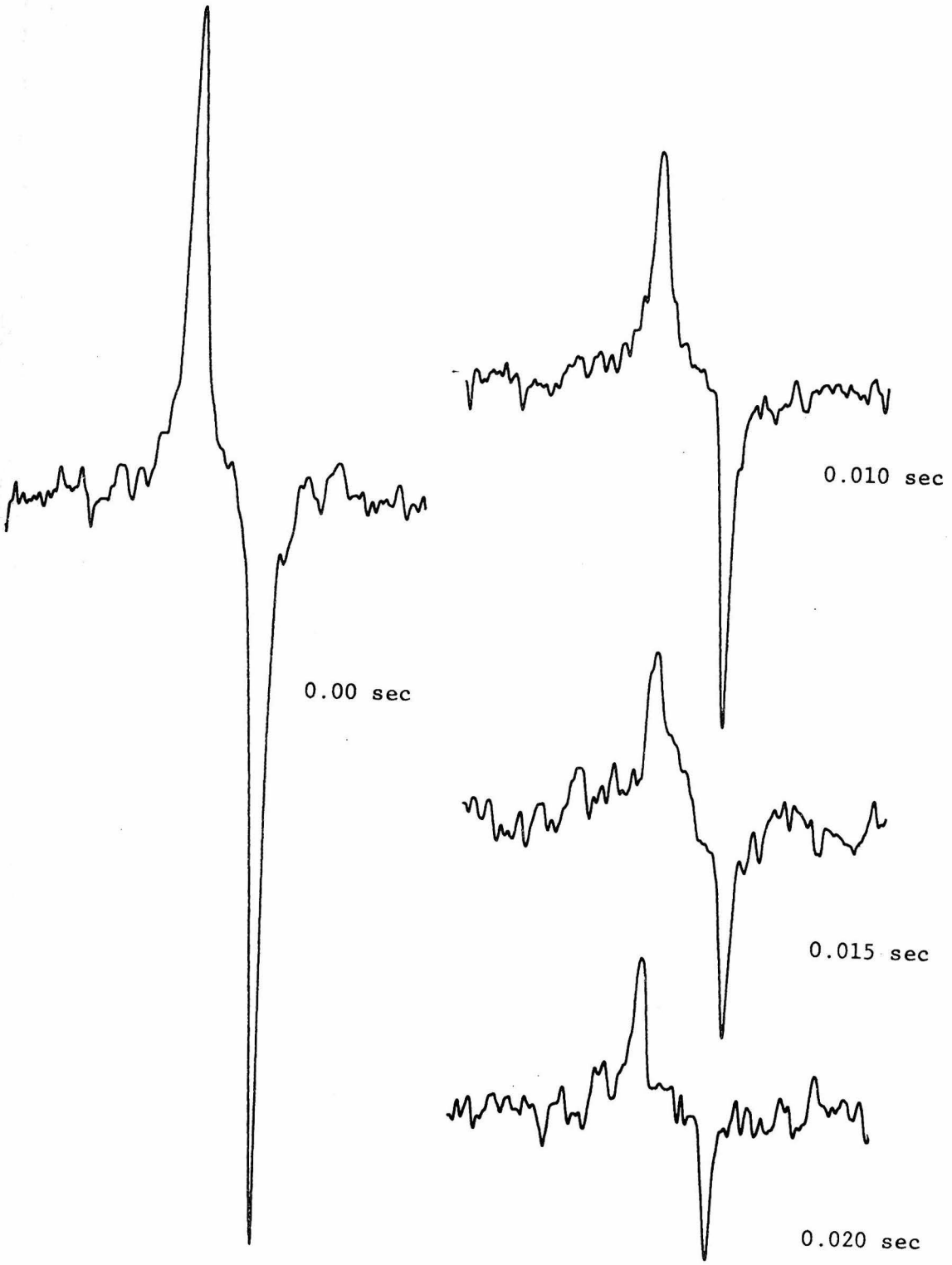
0.00 sec
0.010 sec
0.015 sec
0.020 sec

A plot of the natural log of the difference in peak areas versus the delay time is linear and has a slope equal to $-(1/T_1 + 2k_{off})$. In actual practice peak areas were more readily determined, and with quite adequate accuracy, from peak heights which had been corrected for the difference in line widths for bound and free hapten. The observations after 0.02 sec delay time gave poor signal to noise and usually gave peak differences slightly larger than anticipated from the other observations; these values were therefore not incorporated in determining the final results. The off rates determined in this way have an estimated uncertainty of ± 10%.

The spin-lattice relaxation time was determined by progressive saturation (Freeman and Hill, 1971) without concomitant proton decoupling because this causes a negative NOE enhancement. The T_1 values measured under these conditions may be perturbed by cross-relaxation; these values will, nevertheless, be the appropriate ones to use in correcting the results of perturbation mixing for spin-lattice relaxation (Hull and Sykes, 1975). T_1 values for haptens in buffer were determined by inversion-recovery.

Spin-spin relaxation times, T_2, were determined from measurements of line widths which had been corrected for the effects of sensitivity enhancement ($1/T_2 = \pi\delta_{\nu\frac{1}{2}}$).

The intrinsic line width values for the bound and free hapten were determined by manually fitting the observed spectra to the theoretical line shape equation for exchanging nuclei (Rogers and Woodbrey, 1962) and using the off rates determined by perturbation mixing (Fig. 2). Errors in measuring line widths are probably about 10% and are similar to the errors due to magnetic field inhomogeneity (less than 2 Hz).

Results

Table II collects the values of k_{off} as determined by perturbation mixing and chemical shifts and line widths for the interaction of MOPC-315 7S, Fab', and Fv proteins with DNTP-GABA, 2NTP-GABA and NTP-GABA.

Any given hapten gave the same chemical shift when bound to the 7S, Fab', or Fv protein. In contrast, the line width of the peaks varied inversely with the size of the binding protein(7S > Fab' > Fv). Determination of the intrinsic line width and of the exchange rate for the various haptens will be discussed separately.

DNTP-GABA

The hapten DNTP-GABA is in slow exchange between solution and MOPC-315. The line width for hapten bound to protein increases with the size of the protein fragment (Fv < Fab' < 7S); there is also a small difference in the

Table II

Relaxation Data and Rate Constants for Several CF_3 Labelled Nitrophenyl Haptens Binding to MOPC 315 Proteins (7S, Fab' and Fv)

	Hapten	DNTP-GABA	2NTP-GABA	NTP-GABA
	$\delta_{\nu\frac{1}{2}B}$(Hz)	62		59
	$\delta_{\nu\frac{1}{2}F}$(Hz)	11		3-10
7S	$k_{off}(sec^{-1})$	40[a]	370[c]	980-2000[c]
	$k_{on}(sec^{-1}M^{-1})$	$1.4x10^{8}$[b]	$2.9x10^{8}$[b]	$1.3\text{-}2.6x10^{8}$[b]
	T_1(sec)	.45		
	$\delta_{\nu\frac{1}{2}B}$(Hz)	37		30
	$\delta_{\nu\frac{1}{2}F}$(Hz)	9		
Fab'	$k_{off}(sec^{-1})$	39[a]	370[c]	
	$k_{on}(sec^{-1}M^{-1})$		$2.0x10^{8}$[b]	
	T_1(sec)	.39		
	$\delta_{\nu\frac{1}{2}B}$(Hz)	24		24
	$\delta_{\nu\frac{1}{2}F}$(Hz)	8		
Fv	$k_{off}(sec^{-1})$	36[a]	370[c]	
	$k_{on}(sec^{-1}M^{-1})$	$1.9x10^{8}$[b]	$2.6x10^{8}$[b]	
	T_1(sec)	.34		

[a] k_{off} rates determined by perturbation mixing,

[b] k_{on} rates determined from the off rates and the binding constants in Table I $Ka = k_{on}/k_{off}$,

[c] k_{off} rates determined by line width chemical shift method described in the text.

line width of the free peaks in the presence of proteins of various sizes (Fig. 1). In order to achieve similar molar concentrations of binding sites, the amount of protein present in solution for the 7S monomer was about three times higher than in a solution of the Fv fragment.

To assess the role of viscosity on line widths, spectra were observed at various concentrations of protein. Between 10-40 mg/ml of protein, little difference in line widths of bound and free hapten were observed but some increase was noted at very high protein concentrations (> 100 mg/ml). Spectra of samples containing a 20-fold excess of hapten gave an absorption for the free hapten with a line width of 6 Hz for the Fv fragment and 7 Hz for the 7S monomer.

2NTP-GABA

Two equivalents of 2NTP-GABA with 7S, Fab', and Fv proteins give spectra with two, very broad overlapping peaks at 24-25°C; these peaks coalesce into a single broad peak ($\delta\nu_{\frac{1}{2}} \sim 200$ Hz) at 27-30°C. In these observations, the spectra of hapten with Fv fragment showed a slightly higher coalescence temperature but this difference is more likely due to differences in intrinsic line widths than to differences in rates.

NTP-GABA

Spectra of NTP-GABA interacting with 7S, Fab', and Fv proteins consist of a single peak which shifts linearly as a function of the mole fraction of hapten bound (eq. 6). A plot of line width versus mole fraction of hapten bound was essentially linear over the range from 10% to 98% of hapten bound.

Discussion

Dynamic behavior of molecules exchanging between two environments can, in principle, be determined from the line width and chemical shift parameters inherent in the NMR spectra observed for such systems. (See the discussion in the section on General Theory). In order to calculate exchange rates from such information alone, one must have independent knowledge of the intrinsic line width of bound and free haptens. However, if the exchange rates have been previously determined by some other method (as, for example, perturbation mixing) these exchange rates can then be used as a basis for the calculation of what the line widths should be in the absence of exchange.

Such intrinsic line widths reflect molecular motions. In the present case, line widths reflect (i) viscosity (an increase in solution viscosity slows molecular tumbling) (ii) correlation time of the protein/hapten complex (tumbling rate of the complex) (iii) internal rotation

of the trifluoromethyl group about the carbon carbon bond between it and the phenyl ring (iv) inhomogeneities in the magnetic field. (In this work the line broadening due to such inhomogeneities was always less than 2 Hz and so, except for a small influence of the Y^3 component on the shape of the absorption peaks near their base, does not play a significant role relative to other effects.)

In these studies, the three haptens typify three types of exchange behavior on the NMR time scale. DNTP-GABA is in slow exchange; 2NTP-GABA exchanges between solution and protein at an intermediate rate; NTP-GABA is in fast exchange. They will be discussed as separate cases.

DNTP-GABA

The exchange rates for the binding of DNTP-GABA to MOPC-315 proteins (7S, Fab', Fv) were determined directly by perturbation mixing; Table II lists the off rates. These off rates can now be used to calculate the line widths (in the absence of exchange), $\delta_{\nu\frac{1}{2}}$, for both the bound and free hapten (Table II). In practice this determination of line widths involved manually fitting the observed spectra to a sequence of theoretical spectra calculated for exchanging nuclei using of the total line shape equation (Rogers and Woodbrey, 1962). Calculated spectra were generated by using the off rates determined by per-

turbation mixing and by varying the mole fraction of bound hapten and the intrinsic line widths of both bound and free hapten. Figure 1 shows representative fits between the observed spectra and their best-fit, theoretical counterparts. Errors between calculated and observed spectra arise from the coarseness of manual fitting techniques and other effects which include: inhomogeneity in the Y^3 component of the magnetic field which affects the shape at the base of the peaks, phasing errors and low affinities binding.

The primary factors influencing the intrinsic line widths of free hapten are the solution viscosity and low affinity binding. The effect of viscosity itself can account for no more than 6-7 Hz of the line width of free hapten; this assertion is supported by the following observations. Variation in concentration of protein from 10-40 mg/ml does not lead to significant differences in line widths. Also when hapten is in a 20-fold excess relative to either 7S monomer (at 30 mg/ml of protein) or to Fv fragment (at 10 mg/ml of protein), the peak width of unbound hapten is 6-7 Hz. Under these conditions, exchange broadening should contribute at most 1 Hz to the observed line width (exchange broadening = $P_B k_{off}/\pi P_F$ and $P_B/P_F \ll 1$). These line widths (6-7 Hz) for unbound hapten are considerably smaller than those calculated from the observed spectra after correcting for the contribution of

exchange broadening determined independently by perturbation mixing (Table II). Thus the observed line widths for free hapten considerably exceed those anticipated from the estimated effects of solution viscosity and exchange broadening. A possible source for this additional line broadening could be low affinity binding of hapten to antibody at some site(s) other than the specific combining site; hapten bound in this way would interact with the antibody molecule in such a fashion that its trifluoromethyl group would experience an environment sufficiently like that in solution so that the ^{19}F chemical shift was unchanged. However, the line width of hapten bound to such a low affinity site(s) would be broadened by virture of its association with the large, relatively immobile protein molecule. Since this low affinity binding site(s) has (have) the same chemical shift as the free hapten in solution there will be no exchange related broadening.

If one assumes that the line width of truly "free" hapten is relatively unaffected by protein ($\sim$ 3 Hz) and that the line width of hapten bound in the low affinity site(s) is the same as that specifically associated with the combining site of the antibody, then one can estimate the amount of low affinity binding necessary to account for the observed intrinsic line widths. This estimate is 13% low affinity binding to the 7S monomer, 16% to the

Fab' fragment and 21% to the Fv fragment. Such binding requires an affinity constant of about 10^3 M^{-1} for this hapten/antibody interaction.

As the amount of low affinity binding necessary to account for the observed line widths of the free DNTP-GABA remains nearly constant for all MOPC-315 proteins (7S, Fab', Fv) we conclude that the site(s) for such binding is (are) localized in the Fv region of the immunoglobulin. Moreover, if this binding can occur only at one or a very few site(s), then its contribution to the line width of free hapten should diminish as the amount of hapten relative to protein increases. This is, in fact, the observed behavior. Thus, we conclude that, at most, a very limited number of sites exist in the Fv region of the antibody molecule which have a relative low affinity (10^3 M^{-1}) for hapten and provide an essentially solution-like environment to hapten bound in such sites.

For bound hapten, the line widths increase appreciably with increasing size of the protein fragment in the complex (Fv < Fab' < 7S). We have previously shown (Kooistra and Richards, 1977) that the trifluoromethyl group of bound hapten experiences the same environment whether associated with Fv, Fab', or 7S protein, and in this paper we show that the binding affinities of these different proteins are the

same (Table I). Thus, the rotational freedom of the trifluoromethyl group of bound hapten should not change as increasing amounts of constant region are attached to the Fv fragment of the antibody, and no changes in line width by virtue of restricted rotation of the trifluoromethyl group of bound hapten are anticipated. To account for the increasing line width as hapten binds to increasingly larger fragments of immunglobulin, we conclude that, though not changing the environment of bound hapten, attachment of increasing amounts of constant regions of immunoglobulin to the Fv fragment does increasingly restrict the motional freedom of the combining site and the hapten bound to it.

2NTP-GABA

The MOPC-315/2NTP-GABA system is in intermediate exchange. The differences in the observed spectra of 2NTP-GABA bound to different proteins probably reflects more the differences in intrinsic line widths than it does significant differences in dynamics. Because of the large sensitivity enhancement used to obtain reasonable signal to noise and because of the uncertainties in the ratio of bound to free hapten, a detailed curve fitting was not attempted in this case. The coalescence observed at 27-31°C could, however, be used to calculate the off rates listed in Table II.

NTP-GABA

The interaction of NTP-GABA with MOPC-315 proteins leads to a single NMR absorption which shifts linearly with mole fraction of hapten bound (eq. 6). This behavior is characteristic of the fast exchange limit where the observed line width is the weighted average of that for the bound and for the free hapten plus an exchange broadening term that depends on the chemical shift difference between free and bound hapten, Δ, on the ratio of bound to free hapten, and on the off rate (eq. 7). If exchange broadening contributes significantly to the observed line width, there should be a non-linear relationship between line width and mole fraction bound (Smallcombe et al., 1972). However, in this case such a plot was close to linear over the range of bound hapten from 10-98%; thus line broadening due to exchange must be small.

At a high mole fraction of hapten bound ($P_B > 0.95$) the observed line width becomes very close to that of the intrinsic line width for bound hapten, since the contribution to the line width due to free hapten ($0.05 \times \delta_{\nu_{\frac{1}{2}F}} << 1$ Hz) and due to exchange (a term which goes to zero because $P_F^2 << 1$) becomes insignificant in this limit. Use of this value (59 Hz) for the intrinsic line width of bound hapten and a range of 3 to 10 Hz for the intrinsic line width of unbound hapten at $P_B = 0.5$ led

to the range of off rates listed in Table II.

General

The off rates either from perturbation mixing or from line width measurements are essentially the same for dissociation of hapten from a complex with either the 7S, Fab', or Fv protein. This result extends earlier work (Kooistra and Richards, 1977) which showed that the binding affinity and the micro-environment that each of these proteins provided the trifluoromethyl group are essentially similar. Thus, at least in this case, both the dynamical and environmental aspects of immunoglobulin-hapten interaction are not signficantly influenced by the amount of constant region of the antibody molecule attached to the Fv fragment.

As NMR observations do not affect the position of a chemical equilibrium, the on rates can be calculated from the off rates and the thermodynamic affinity constant. Table II lists on rates calculated in this way using binding affinities determined by fluorescence quenching. Although these binding constants were measured at protein concentrations appreciably lower than those used in the NMR experiments, we have previously shown that the measured binding affinities are essentially independent of protein concentration for the 7S monomer (Kooistra and Richards, 1977); we have assumed similar behavior for the Fab' and Fv fragments. Moreover, these on rates agree with those

measured by techniques dependent upon electronic spectroscopy (Pecht et al., 1972a, b; Haselkorn et al., 1974; and Hochman et al., 1972) even though these other rates were measured at protein concentrations $\leq$ 1 mg/ml. Thus techniques dependent on the electronic properties either of protein or hapten in the complex or dependent on the magnetic environment of bound hapten yield similar results for the dynamics of protein hapten interaction; these similarities suggest that both types of techniques are measuring essentially the same behavior. Moreover, the similarity of the results, over a wide range of protein concentrations, and for the various fragments, suggests that protein aggregation, even if it exists, does not affect binding of hapten by antibody.

The o_n rates from these various techniques are close to those anticipated for association between antibody and hapten which is controlled by diffusion (Froese and Schon, 1975). The accurate estimation of a diffusion controlled on rate is complicated by the difficulty in knowing just what fraction of the antibody surface is available to hapten: is the combining site accessible only through a narrow orifice or is it a broad, shallow basin which can be entered from several directions? Thus one cannot unambiguously eliminate the presence of an energy barrier

for binding of hapten to antibody, but if one does exist its height cannot exceed 5 kcal/mole.

Lastly, rotation of the trifluoromethyl group of bound hapten about the single bond between it and the aromatic ring provides one mechanism for dipolar relaxation and does not change appreciably with increasing antibody size.' Moreover, the observed intrinsic line width of bound hapten increases with increasing molecular weight of the hapten/protein complex. We take this to indicate that there is increasing restriction of the motion of the region of the antibody combining site as larger sections of constant chain are attached.

REFERENCES

Anet, F.A.L. and Bourn, A.J.R. (1967), J. Amer. Chem. Soc. 89, 760.

Dahlquist, F.W., Longmuir, K.J., and Du Vernet, R.B. (1975), J. Mag. Res. 17, 406.

Dwek, R.A., Wain-Hobson, S., Dower, S., Gettins, P., Sutton, B., Perkins, S.J., and Givol, D. (1977), Nature 266, 31.

Forsén, S. and Hoffman, R.A. (1963a), J. Chem. Phys. 39, 2892.

Forsén, S. and Hoffman, R.A. (1963b), Acta Chem. Scand. 17, 1787.

Freeman, R. and Hill, H.D.W. (1971), J. Chem. Phys. 54, 3367.

Froese, A. and Schon, A.H. (1975), Cont. Topics in Mol. Immunol. 4, 23.

Goetze, A.M. and Richards, J.H. (1977a), Biochemistry 16, 228.

Goetze, A.M. and Richards, J.H. (1977b), Proc. Natl. Acad. Sci. USA 74, 2109.

Haselkorn, D., Friedman, S., Givol, D., and Pecht, I. (1974), Biochemistry 13, 2210.

Hochman, J., Inbar, D., Wilchek, M., Pecht, I., and Givol, D. (1972), Israel J. Med. Sci. 8, 635.

Hull, W.W. and Sykes, B.D. (1975), J. Chem. Phys. 63, 867.

Inbar, D., Hochman, J. and Givol, D. (1972), Proc. Nat. Acad. Sci. USA 69, 2659.

Kooistra, D.A. and Richards, J.H. (1977), Biochemistry, in press.

Padlan, E.A., Davies, R.D., Pecht, I., Givol, D. and Wright, C. (1976), Cold Spring Harbor Symp. Quant. Biol. 41, 627.

Pecht, I., Givol, D. and Sela, M. (1972a), J. Mol. Biol. 68, 241.

Pecht, I., Haselkorn, D. and Friedman, S. (1972b), FEBS Letters 24, 331.

Rogers, M.T. and Woodbrey, J.C. (1962), J. Phys. Chem. 66, 540.

Smallcombe, S.H., Ault, B. and Richards, J.H. (1972), J. Amer. Chem. Soc. 94, 4585.

Underdown, B.J., Simms, E.S. and Eisen, H.N. (1971), Biochemistry 10, 4359.

PART IV

pH and Double Resonance Studies of ^{19}F Labelled Nitrophenyl Haptens Binding to Mouse Myeloma Immunoglobulin MOPC-315

INTRODUCTION

In previous studies we have used fluorine nuclear magnetic resonance (NMR) to explore the binding site of MOPC-315. The chemical shift of bound trifluoromethyl labelled nitrophenyl haptens has shown the identity of the binding site of the different MOPC-315 binding proteins (7S, Fab', Fv) (Kooistra and Richards, 1977). In this study we look at the pH dependence of the ^{19}F NMR shift of several of these fluorinated haptens bound to MOPC-315 protein. Moreover, by using various double resonance techniques fluorine NMR has been used to determine the chemical shift of several hapten protons when they are bound to MOPC-315.

The binding of DNTP-GABA[1] and NTP-GABA to the 7S monomer of MOPC-315 shows no change between pH 5 and 9. At pH values less than five the hapten precipitates, then at pH values lower than three the NMR signal of the bound hapten is lost irreversibly, probably due to protein precipitation. At pH values higher than nine binding is

---

[1]Abbreviations used are: DNTP-GABA, γ-N-(2,6-dinitro-4-trifluoromethylphenyl) aminobutyric acid; NTP-GABA, γ-N-(4-nitro-2-trifluormethylphenyl) aminobutyric acid; Δ, total chemical shift (separation between the NMR absorption of the bound and unbound free hapten) measured in Hz; δ, observed chemical shift, actual position of the NMR signal dependent on the mole fraction of the ligand bound; τ_c, molecular correlation time; γ, gyromagnetic ratio; H_2, effective field of the decoupler; NOE, Nuclear Overhäuser Effect, the ratio of the NMR signal with decoupler on to the NMR signal with the decoupler off.

lost initially in a reversible manner by the ionization of one or two groups thought to be in the binding site, and then irreversibly when the pH is araised above 11.

Comparison of the total chemical shift change on binding, Δ, of the benzyl proton and fluorine nuclei of CHF_2-GABA shows that the fluorine chemical shift is not caused entirely by ring currents from nearby aromatic amino acid residues. In fact, it appears by analogy to the proton shift that ring currents cause an upfield shift, which is offset by other molecular interactions to produce an overall downfield shift of the fluorine nuclei.

Studies of the Nuclear Overhauser Effect (NOE) of NTP-GABA and DNTP-GABA were used to explore the proton environment of the binding site surrounding the trifluoromethyl group of these haptens when bound to the Fv fragment of MOPC-315. The NOE results for DNTP-GABA bound to MOPC-315 Fv fragment when used in conjunction with spin lattice, T_1, and transverse, T_2, relaxation times of the fluorines indicate that the correlation time, τ_c, of the protein-hapten complex is 1.8×10^{-8} sec with no internal rotation, and that the major source of dipolar relaxation is probably between the fluorine nuclei and the aromatic protons on the hapten. The NOE data indicate that these hapten protons are shifted 2.0 ppm upfield upon binding to the Fv fragment.

The T_2 relaxation time of NTP-GABA bound to the Fv fragment of MOPC-315 is similar to that of bound DNTP-GABA indicating that both hapten-protein complexes have similar rates of isotropic rotation. However, the shorter T_1 and smaller NOE[2] indicates the presence of internal rotation of approximately 10^{-8} sec. The single aromatic proton of NTP-GABA next to the trifluoromethyl group is thought to be responsible for the observed NOE in the aromatic region, and appears to be shifted 1.5 ppm upfield upon binding.

The upfield shift of the aromatic protons of DNTP-GABA and NTP-GABA upon binding are in agreement with the proton shifts seen by Dwek et al. (1977) for DNP-asp bound to MOPC-315 Fv fragment.

Studies in deuterium oxide buffer indicate that there are no hydrogen bonds between the fluorines of DNTP-GABA and the protein binding site.

Materials and Methods

Preparation of DNTP-GABA, NTP-GABA, NMR samples, and isolation and purification of MOPC-315 proteins (7S, Fab', and Fv) have been described previously (Kooistra and Richards, 1977) and the same procedures are used here with only minor modifications. In some experiments Fv fragments

[2] An NOE of one means no cross relaxation. The larger the deviation from one the larger the amount of cross relaxation whether or not the NOE is greater than or less than one. In this paper we shall use larger and smaller to refer to the magnitude of the deviation in the NOE value from one.

that were concentrated by pressure dialysis were used instead of reconstituting lyophilized protein.

pH Studies. The pH of NMR samples were measured using a Radiometer pH meter equipped with a 7 mm electrode that could be inserted directly into the NMR tube, so that, the pH could be measured without removing the sample. These samples were titrated by adding 5-20 μℓ aliquots of approximately one normal hydrochloric acid or sodium hydroxide.

Calibration of the Decoupler

The frequency offset and power of the decoupler were determined by its ability to collapse the fluorine triplet of a 15% solution of 2,2,2-trifluoroethanol deuterium oxide (^{1}H NMR quartet centered at δ3.9 ppm downfield from TMS), and the fluorine doublet of CHF_2-GABA in buffer using a slight modification of the technique outlined by Pachler (1972). $\gamma H_2/2\pi$ was 28 Hz at 95 dB, 52 Hz at 101, 236 Hz at 113 dB (a change in the decoupler power of 6 dB changes $\gamma H_2/2\pi$ by a factor of about 2) and 17 Hz (calc.) at 90 dB.

The effective bandwidth of radiation from the decoupler depends not only on the $\gamma H_2/2\pi$ but also on the spin lattice, T_1, and transverse, T_2, relaxation times. Assuming proton line widths of 10-30 Hz and T_1 values of 0.1 sec on the protein the bandwidth for 50% saturation (Gerig, 1977) is about 0.5-1 ppm at 90 dB and about 1.2-

1.7 ppm at 95 dB.

Since the spacing between decoupler offsets in NOE experiments was about 0.5 ppm those experiments run at 90 dB probably do not represent full NOE values, whereas, the experiments run at 95 dB probably represent greater than 85% saturation.

Experiments used to measure the total NOE were done at 119 dB using square wave noise decoupling (Ernst, 1966). The NMR was adjusted so that enough decoupling power was spread throughout the entire proton spectra to collapse the triplet of 2,2,2-trifluoroethanol 5 ppm away from the center band.

NOE Studies. NOE measurements were made by taking the ratio of peak height of NMR spectra taken with the decoupler on to the peak height of spectra taken with decoupler off. Peak heights were used instead of peak areas because they were easier to measure, more reproducible than the machine integrator, and since all the peaks were fairly broad[3] (> 20 Hz) they should be relatively insensitive to small changes affecting peak widths.

[3] NMR spectra of DNTP-GABA and NTP-GABA in buffer (no protein) used for NOE measurements were broadened using a 0.02 sec exponential sensitivity enhancement. The decoupler was off during the acquisition time so that no changes in proton fluorine coupling ($J_{HF} \sim 0.5$ Hz) would affect the peak height.

NMR spectra used to measure the cross relaxation between fluorine and protons were run using a total pulse delay of greater than three times T_1 between the 90° r.f. pulses (spin lattice relaxation times were determined by progressive saturation (Freeman and Hill, 1971) with no proton developing).

Since the length of the 90° r.f. pulse changed when the decoupler was turned on, the "non-decoupled" references were determined by decoupling about 100 ppm upfield or downfield from the center of the proton spectra.

In some experiments the decoupler remained on constantly but in most of the experiments the decoupler was pulsed at a time approximately equal to T_1, just before the 90° r.f pulse, which is then immediately followed by acquisition of data. Since NOE results from a change in the equilibrium distribution of the fluorine nuclei upon saturation of the proton nuclei that are coupled to the fluorines by a dipolar mechanism the rate of change in the equilibrium distribution of the fluorine will be exponential with a time constant of T_1. Therefore, when the decoupler output is pulsed at a time equal to T_1 only about 67% of the NOE will be seen. NMR spectra used to measure the NOE of NTP-GABA and DNTP-GABA in the absence of protein were observed with the decoupler on during the pulse delay but off during the acquisition time so that no changes in proton fluorine coupling ($J_{HF} \sim 0.5$ Hz) would

affect the peak height.

Some spectra were run in deuterium oxide instead of water. These samples were prepared by lyophilizing the hapten in 2.5 ml of buffer (0.15 M NaCl, 0.01 M sodium phosphate, 10^{-3} M EDTA, and 0.02% sodium azide at pH 7.4; this buffer was used for all protein solutions except those used for proton NMR spectra) and adding approximately 30 mg of lyophilized MOPC-315 Fv fragment, and reconstituting with 2.5 ml of deuterium oxide (Merck 99.8%, that was doubly distilled). These samples were equilibrated for at least six hrs at room temperature before NMR spectra were taken.

Proton NMR Spectra. Samples were prepared from buffer,[4] hapten and MOPC-315 Fv fragments which were all twice lyophilized separately from doubly distilled deuterium oxide. (The Fv fragments were equilibrated for about 24 hrs in deuterium oxide before each lyophilization.) The NMR samples were reconstituted under an argon atmosphere using 100% deuterium oxide (Aldrich). Proton spectra were run either on a Varian XL-100-15 NMR at 100.1 MHz in a 12 mm sample tube (2.5 ml) or a Varian HR-220 NMR at 220 MHz in a 5 mm tube (0.75 ml). Protein

[4]The buffer used to make samples for proton NMR spectra contained no EDTA but otherwise was the same as the buffer used for other protein experiments. The EDTA was removed to prevent interference from its protons with those of the protein plus hapten.

concentrations ranged from 0.5-1 x 10^{-3} M (10-25 mg/ml).

CHF_2-GABA. NMR spectra of CHF_2-GABA bound to MOPC-315 7S and Fv fragment were run using varying amounts of decoupling power at different offsets. To prevent loss of signal due to "negative" Overhauser enhancement the decoupler was on only during the acquisition time.

Fluorescence Quenching. Binding affinity of MOPC-315 7S monomer for NTP-GABA at pH 9.3 and 10.0 was determined by fluorescence quenching using a slight modification of the procedure described before (Kooistra and Richards, 1977). Protein solutions (1.0 mg/ml) MOPC-315 immunoglobulin, "Fc peptides" (0.8 mg/ml) (from pepsin digest used to correct for non-specific quenching), and buffer blank were titrated to the proper pH with approximately 2 M sodium hydroxide. A standard hapten solution was titrated to pH 8.7. Because the pH of the hapten solution was lower than the protein solutions the pH dropped about 0.1 pH units during the experiment.

The amount of non-specific quenching observed in the "Fc" fragment was about two-thirds the total amount of quenching observed for the 7S immunoglobulin. This is thought to be due to the fact that the high concentration of protein and hapten needed to observe specific binding is also high enough to cause some non-specific binding and is not due to the high pH values.

γ-N-(2,6-dinitro-4-methylphenyl) aminobutyric acid, DNMP-GABA. 3,5-Dinitro-4-chlorotoluene (4.0 gm, 18 mmol.) from ICN·K and K Laboratories, Inc. was dissolved in 54 ml of ethanol; and added to a stirred solution of 2.1 gm (20 mmol) γ-aminobutyric acid and 2.2 gm sodium bicarbonate in 28 ml of water at pH 7.0. After refluxing for 16 hrs, DNMP-GABA was isolated as described for DNTP-GABA (Kooistra and Richards, 1977). The crude yield was 4.0 gm, 78%. Recrystallization in benzene gave an orange product m.p. 14.55-14.65°C. Proton NMR spectra (d_6 acetone) showed an overlapping sharp and broad singlet at δ8.0 ppm (3H), a quartet at δ3.1 ppm (2H), a multiplet centered at δ2.4 ppm (5H), (the methyl group is in the center of this multiplet), and a misshapen quartet at δ2.1 ppm (2H); visible spectra in buffer had a λ_{max} at 455 nm and a molar absorptivity of 5.91×10^3 cm^{-1} M^{-1}. Anal. Calculated for $C_{11}H_{13}N_3O_6$: C, 46.65; H, 4.62; N, 14.84. Found: C, 46.75; H, 4.60; N, 14.80.

Several attempts were made to synthesize γ-N-(4-fluoromethyl-2,6-dinitrophenyl) aminobutyric acid, but problems of hydrolysis of the fluorine during the preparation indicated that the mono fluorinated compound would probably not be stable in neutral buffer solution.

4-Chloro-3,5-dinitrobenzyl alcohol. This alcohol was made by reducing 4-chloro-3,5-dinitrobenzoic acid (Aldrich) with diborane using two similar methods, that are modifications of the techniques used by Harrison et al. (1970) to reduce carboxylic aicds.

The first procedure used a borane tetrahydrofuran (THF) solution purchased from Ventron. This borane THF solution (1.3 to 2.2 equivalents gave similar yields) was added, slowly at first but faster as gas evolution ceased, to a stirred solution of 25 gm (100 mmol) 4-chloro-3,5-dinitrobenzoic acid (Aldrich) dissolved in 150 ml of dry THF. The reaction proceeded for about 12-16 hrs at room temperature before being quenched with 200 ml of water. The alcohol product was extracted with 3 x 75 ml of dichloromethane. The combined organic extracts were washed with 3 x 75 ml of water, then 3 x 100 ml saturated sodium bicarbonate, then water again, and dried with magnesium sulfate. The dichloromethane solvent was removed under reduced pressure and the solid alcohol recrystallized in ethanol water to give 19.8 gm, 85%.

In the second procedure the diborane was generated by adding freshly distilled boron trifluoride etherate to a reaction flask containing a mixture of sodium borohyrdide (Zweifel and Brown, 1963) in diglyme.

The diborane generated in this manner was carried by a stream of argon into a reaction flask containing the acid dissolved in dry THF. The reaction was followed by watching the disappearance of starting acid by TLC (dicholoromethane solvent). The alcohol product was isolated as described above giving a 75% yield after recrystallization in ethanol water. The white crystals melted at 89-90°C, NMR (d_6 acetone) a singlet at δ8.1 ppm (2H) and at δ4.7 ppm (2H). Anal. calculated for $C_7H_5ClN_2O_5$: C, 36.15; H, 2.17; Cl, 15.24; N, 12.05. Found. C, 36.20; H, 2.15; Cl, 15.33; N, 11.88.

4-Chloro-3,5-dinitrobenzaldehyde. This aldehyde was made by oxidizing 4-chloro-3,4-dinitrobenzyl alchol with pyridinium chlorochromate (Aldrich) by using a slight modification of the procedure outlined by Corey and Suggs (1975). 4-Chloro-3,5-dinitrobenzyl alcohol (7.5 gm 32 mmol) dissolved in 150 ml of dichloromethane (with gentle heating) was added to a stirred suspension of 10.4 gm (48 mmol) pyridinium chlorochromate in 75 ml of dichloromethane. This mixture turned black within a minute and the reaction was complete in 2-2½ hrs at room temperature. The black solution was filtered through a half inch of silica gel on a sintered glass filter, and the black residue was washed three times with 25 ml of warm dichloromethane. This filtered dichloromethane,aldehyde solution

was washed three times with 50 ml of water, then dried with magnesium sulfate, and the dichloromethane removed under reduced pressure. The yellow aldehyde was redissolved in 100 ml of dichloromethane and passed down 1½ inches of silica gel on a sintered glas filter and washed with dichloromethane until the yellow color started to come through. Removal of solvent produced 3.8 gm of aldehyde, 15% yield, NMR spectra showed two singlets, one at δ8.7 ppm (2H) and one at δ9.6 ppm (1H). This aldehyde was used without further purification.

4-Difluoromethyl-2,6-dinitrochlorobenzene. 4-Chloro-3,5-dinitrobenzaldehyde was fluorinated with Fluoreze-M (0.8 M molybdenum hexafluoride in dichloromethane from PCR) by a modification of the procedure supplied by PCR in their technical bulletin.

In a 50 ml round bottom flask equipped with a magnetic stirrer, drying tube, and cooling bath (-10 to -15°C), was placed 12 ml of 0.8 M (9.6 mmol) Fluoreze-M. To this cooled solution was added 2.2 gm (9.6 mmol) 4-chloro-3,5-dinitrobenzaldehyde in 20-30 ml of dichloromethane. This solution was allowed to slowly warm to room temperature as the dry ice in the cooling bath evaporated (2-3 hrs). The reaction was followed by TLC (dichloromethane, r.f. of aldehyde and difluoride are 0.51 and 0.83, respectively) by watching the disappearance of aldehyde and appearance

of difluoride. The reaction was quenched with water when the TLC plates showed the formation of side products about 3-4 hrs. Another 25 ml of dichloromethane was added and the dichloromethane, difluoride solution was washed with 2 x 30 ml of water, dried with magnesium sulfate, charcoal was added, and filtered through silica gel on a sintered glass filter. After removing the solvent, the remaining aldehyde was removed by adding 20 ml of 40% sodium metabisufite and heating on a steam bath for approximately 30 minutes with shaking and then allowed to sit for at least five hrs with occasional shaking. The solid bisufite was filtered and washed with 75 ml of ether. The ether layer was separated, washed with 3 x 25 ml of water, dried with magnesium sulfate, and removed under reduced pressure leaving the solid difluoride. The difluoride was recrystallized in ethanol water with some difficulty (after removal of early "precipitating" oils) to give 0.5 gm of white crystals 23%. NMR (d_6 acetone) singlet δ8.6 ppm (2H) and a triplet δ6.9 ppm (1H) J_{HF} 55 Hz.

γ-N-(4-difluoromethyl-2,6-dinitrophenyl) aminobutyric acid, CHF_2-GABA. To a solution containing 0.69 gm (6.7 mmol) of γ-aminobutyric acid and 2.2 gm sodium bicarbonate in 28 ml of water at pH 7.5 was added to an ethanolic solution (54 ml) containing 1.55 gm (6.1 mmol) 4-difluoromethyl-2,6-dinitrochlorobenzene. This stirred mixture was heated sporadically on a steam bath (about two hrs

total) over a 12 hr period. The solvent was removed under reduced pressure and the acid product dissolved in about 90 ml of basic water and washed with 3 x 25 ml of ether. This ether washed water layer was acidified with hydrochloric acid to pH 1-2 and the product extracted with 3 x 25 ml of ether. The combined ether extracts were collected dried with magnesium sulfate and removed under vacuum.

This yellow product contained 20-30% of an aldehyde impurity (probably from hydroysis of the difluoride). The aldehyde was removed by adding a 100 ml of 10% sodium metabisulfite and 100 ml of ether and stirred until everything dissolved. The pH was lowered between 1-1.5 and the difluoride extracted into 3 x 25 ml of ether. The ether solution was dried and the solvent removed under reduced pressure. The solid difluoride was recrystallized in benzene, yield about 0.5 gm, 26%, Mp = 125-126°C, NMR (d_6 acetone) singlet δ8.4 ppm (2H), a triplet centered at 6.9 ppm (1H), J_{HF} = 55 Hz; ^{19}F NMR showed a doublet at 34.9 ppm upfield from TFA J_{HF} = 56 Hz. Anal. Calculated for $C_{11}H_{11}F_2N_3O_6$: C, 41.39; H, 3.47; N, 13.16. Found: C, 41.43; H, 3.33; N, 12.49. ^{19}F NMR showed a small impurity (< 5%) 9.0 ppm (singlet) further upfield in standard samples of CHF_2-GABA in buffer, these samples were stored at 4°C.

Theory

NOE. To help those unfamiliar with the Nuclear Overhauser Effect (NOE) to understand some of the basic principles and terminology, a brief qualitative introduction will be given. For simplicity, this discussion will start with a simple system of two loosely coupled spins (½) (no spin-spin coupling) and then extrapolate these results to the more complicated system of a trifluoromethyl group bound to a large protein. A more thorough derivation can be found (for example, Noggle and Schirmer, 1971; Hull and Sykes; 1975a and b; Gerig, 1977; and Doddrell et al., 1971).

For two dipolar coupled spins (say, F and H for a fluorine coupled to a proton) there will be four energy levels and four different transition probabilities (Figure 1).

Level 1: spin F is α, spin H is α- $\alpha\alpha$

Level 2: spin F is β, spin H is α- $\beta\alpha$

Level 3: spin F is α, spin H is β- $\alpha\beta$

Level 4: spin F is β, spin H is β- $\beta\beta$

W_1^F; the single quantum transition probability that spin F will go from α to β (or β to α) while H remains unchanged.

Figure 1

Energy level diagram for two spin 1/2 nuclei that are coupled by a dipolar mechanism. The W's are spin-lattice transition probabilities. The spin state of the F nuclei are listed first.

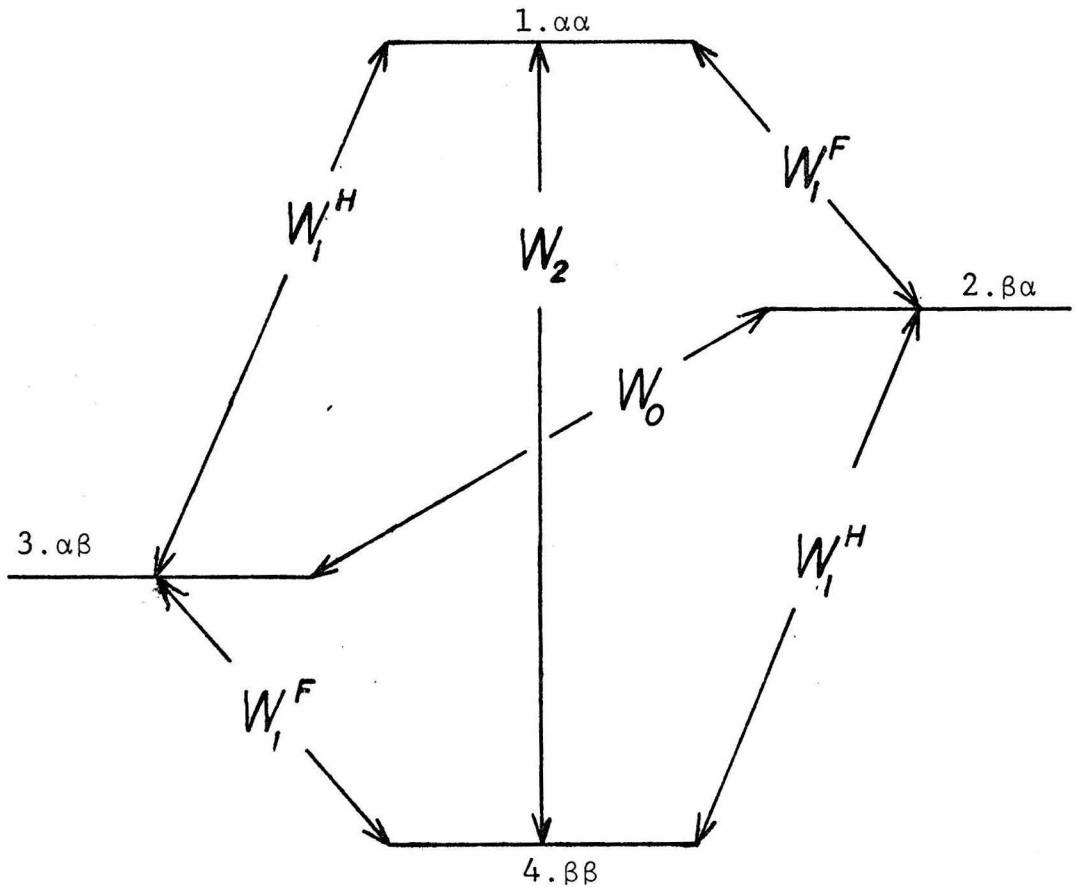
1.αα
2.βα
3.αβ
4.ββ
W_1^H
W_2
W_1^F
W_0
W_1^H
W_1^F

W_1^H; the single quantum transition probability for spin H to go from α to β (or β to α) while F remains unchanged.

W_2; the two quantum transition probability for both spins to relax simultaneously in the same direction $\alpha\alpha$ to $\beta\beta$ (or $\beta\beta$ to $\alpha\alpha$)

W_0; the zero quantum transition probility for both spins to relax simultaneously in the opposite direction $\alpha\beta$ to $\beta\alpha$ (or $\beta\alpha$ to $\alpha\beta$).

These transition probabilities can be related to the change in the observed magnetization by the following two equations:

$$\frac{dF_z}{dt} = - \rho^{FH}[F_z - F_o] - \sigma^{FH}[H_z - H_o] \qquad 1$$

$$\frac{dH_z}{dt} = - \rho^{HF}[H_z - H_o] - \sigma^{FH}[F_z - F_o] \qquad 2$$

$$\rho^{HF} = 2W_1^F + W_o + W_2$$

$$\rho^{HF} = 2W_1^H + W_o + W_2$$

$$\sigma^{HF} = W_2 - W_o \ .$$

F_z and H_z are the observed magnetization of spins F and H at time t; F_o and H_o are the equilibrium magnetization of F and H; σ is the cross relaxation terms and will only be present when some type of relaxation mechanism connects F and H, such as dipole-dipole relaxation; ρ is the relaxation rate in the absence of cross relaxation or when the unobserved spin is decoupled.

These equations illustrate two important points about a coupled system: (1) changes in the equilibrium value of spin H can affect the magnitude of spin F and vice versa. (2) the decay of F and H are not in general a simple exponential. (There are two important times when a coupled system relaxes by a single exponential; when F and H are equivalent or "like spins" and when H is decoupled during the relaxation measurement of F, or vice versa. When H is decoupled the relaxation rate, $1/T_1$, of F is equal to ρ^{FH}.) In multi spin systems with slow correlation times the fluorine nuclei may again have exponential relaxation rates (Hull and Sykes, 1975a).

As mentioned above changes in the equilibrium distribution of H can affect the equilibrium value of F. It is this interaction that is responsible for NOE. The NOE of F is the ratio of F_o when spin H is saturated to F_o when the decoupler off. The nuclear Overhauser enhancement of F when H is saturated, $f_F(H)$, is the NOE minus one and is equal to:

$$f_F(H) = \frac{\gamma_H \sigma^{FH}}{\gamma_F \rho^{FH}} = \frac{\gamma_H}{\gamma_F} \cdot \frac{W_2 - W_o}{2W_1^F + W_o + W_2} \qquad 3$$

γ_F and γ_H are the gyromagnetic ratio of spin F and H, and are nearly equal for ^{19}F and ^{1}H ($\gamma_F = 94\% \gamma_H$).

Random translational and rotational motion of molecules in liquid can cause fluctuating magnetic fields. If these fluctuating fields have frequency components at the Larmor frequency they can induce nuclear transitions that lead to relaxation. In the same way dipolar coupling between nuclei can also affect relaxation. The effectiveness of different dipolar interactions to cause relaxation is dependent on the sixth power of the inverse of the distance separating the nuclei and a spectral density function, $J(\omega_o)$, given by,

$$J(\omega_o) = \frac{\tau_c}{1 + \omega_o^2 \tau_c^2}, \text{ where}$$

τ_c, is the molecular correlation molecular time, a large value of τ_c is characterized by slow molecular motion and a smaller value of τ_c results from faster molecular motion.

$$W_1^F = \frac{3}{20} \frac{\gamma_F^2 \gamma_H^2 \hbar^2}{r^6} J(\omega_F) \qquad 4$$

$$W_o = \frac{1}{10} \frac{\gamma_F^2 \gamma_H^2 \hbar^2}{r^6} J(\omega_H - \omega_F) \qquad 5$$

$$W_2 = \frac{3}{5} \frac{\gamma_F^2 \gamma_H^2 \hbar^2}{r^6} J(\omega_H + \omega_F) \qquad 6$$

For our ^{19}F - ^{1}H system $\omega_F = 2\pi$ x 94 MHz, $|\omega_H - \omega_F| = 2\pi$ x 6 MHz, and $\omega_H + \omega_F = 2\pi$ x 194 MHz it can be seen that the $J(\omega_o)$ terms will be approximately equal at short correlation time ($< 10^{-10}$) and σ^{HF} will be equal to 1/2 ρ^{HF} and the Overhauser effect will be approximately 1/2 that is $\gamma H/\gamma F \sim 1/2$. At longer correlation times ($> 10^{-8}$ sec) as for a nuclei bound to a large protein, the ω_o cross relaxation term will dominate ($\rho^{HF} = - \sigma^{HF}$) and the enhancement $f_F(H)$ will become -1 (in other words, the signal disappears when the decoupler is turned on). These are the maximum enhancement possible, if other relaxation pathways exist they will tend to decrease the magnitude of the observed NOE in proportion to their importance.

In macromolecular systems the NOE can be much more complicated then this simple two spin system, especially, for systems that have fairly large correlation times ($> 10^{-9}$ and show a NOE less than one). In these slow tumbling systems the cross relaxation term, W_o, becomes the dominate mode of relaxation. Not only will the cross relaxation between fluorines coupled with protons increase at slow correlation times, but the cross relaxation between coupled protons will also become very efficient. Therefore, fluorine relaxation will be influenced not only by the proton it interacts with directly, but also by neighboring protons that do not interact directly with the fluorine nuclei protons (Hull and Sykes, 1975a; and Gerig,

1977). These secondary relaxation mechanism can lead to a complete loss of resolution in ^{19}F-^{1}H NOE experiments, and a NOE is seen regardless of the proton region being decoupled.

This secondary relaxation effect can not only cause a loss of NOE selectivity, but it can lead to exponential spin lattice relaxation times, T_1, (Hull and Sykes, 1975a) in the absence of proton decoupling.

The correlation time(s) that is (are) important in dipolar interactions is not just the correlation time due to the isotropic motion of the protein-hapten complex but also that due to internal motion in the microenvironment of the trifluoromethyl group. The effect of internal motion can be qualitatively viewed as adding other components to the correlation time for relaxation. For example, a rapidly rotating group connected to a slower rotating macromolecule will be able to relax efficiently by relaxation mechanisms that occur best at the slower correlation times (i.e. W_o) and also with mechanisms that occur better with more rapid correlation times (i.e. W_1 and W_2).

The capability of internal motion to cause relaxation by a dipolar mechanism is also dependent on the angle between the interacting nuclei and the axes of rotation. In general internal rotation will increase both the spin lattice and transverse relaxation times (Hull and Sykes, (1974).

The use of trifluoromethyl labels on our nitrophenyl haptens adds another important relaxation pathway for fluorine relaxation not available to a single fluorine nuclei. The fluorines can now relax not only to surrounding protons, but the fluorines can also relax to each other through a dipolar mechanism. The rate of dipolar relaxation between the "like spins" of the fluorines on the trifluoromethyl group is η^{FF}, where

$$\eta^{FF} = \rho^{FF} + \sigma^{FF} = 2W_1^{FF} + 2W_2^{FF}. \qquad 8$$

This adds two important considerations to our NOE system: (1) only those protons that can compete with fluorine-fluorine relaxation will cause a NOE. Therefore, proton-fluorine distances must be comparable to the fluorine-fluorine internuclear distance. (2) Since η^{FF} contains no W_o term, proton-fluorine relaxation will become more efficient than fluorine-fluorine relaxation at larger correlation times ($> 10^{-9}$) for an equivalent internuclear distance.

The size of the NOE seen by a given dipolar pathway is dependent on the efficiency of that pathway relative to all other relaxation mechanisms. The size of the NOE seen in nuclei F when nuclei H are saturated is proportional to the percentage of the total relaxation that takes place by the dipolar mechanism linking F and H, and the maximum NOE possible at the correlation time of the molecule. The

rate of relaxation by a dipolar mechanism is dependent on the inverse sixth power of the distance and the spectral density function.

In these discussions of the nuclear Overhauser effects observed for DNTP-GABA and NTP-GABA bound to Fv fragments of MOPC-315, we shall ignore possible contributions to the NOE which might arise from the rapid exchange of these haptens between solution and the binding site of the immunoglobulin. Such neglect of the influence of the exchange process itself on the NOE is warranted by the fact that virtually all spin-lattice relaxation of a given molecule of hapten occurs when that molecule is bound to the antibody, and not when it is free in solution. This follows from the smaller value of T_1 for the free hapten in presence of protein than for free hapten, in buffer, the fact that each molecular of hapten spends an appreciable fraction of its life bound to antibody during the time required for spin lattice relaxation, which is due to the fact that the rate of exchange is fast relative to relaxation (Kooistra et al., 1977). The validity of this assumption is supported by the data of Figure 7 in which the NOE of the ^{19}F nuclei of both bound and free hapten respond in an almost identical manner to the irradiation of the ^{1}H nuclei.

RESULTS

pH Studies

DNTP-GABA. The fluorine NMR spectra of DNTP-GABA plus MOPC-315 7S monomer or Fv fragment shows very little change between pH 5 and 10 (Figures 2-5).

At pH values higher than 10 the downfield peak due to bound hapten begins to decrease until at pH 10.9 it has almost totally disappeared. When the pH is lowered from pH 10.6 to neutral pH greater than 90% of the original area due to the bound hapten is regained. However, when the pH is lowered from 11.9 no signal due to bound hapten is seen (bottom of Figure 3). Not only is binding lost at these high pH values but the viscosity of the solutions also increases until it becomes almost gel like. This viscosity change does not decrease when the pH is again lowered back to neutral.

As the pH drops below 5 the peak due to unbound hapten (the upfield peak) disappears, but the bound peak remains essentially constant until pH 3. Below pH 4 the bound peak also begins to slowly disappear.

The amount of binding regained when the pH is raised back to neutral is approximately equal to the amount bounding at the lower pH value and the area of the unbound hapten peak while broader has an area very close to the original pH 7.5 spectra (Figure 3).

Figure 2

^{19}F NMR spectra of 1.2×10^{-3} M DNTP-GABA plus 6.3×10^{-4} M (binding site) MOPC-315 7S monomer at different pH values. All spectra, except, pH 11.90 were plotted with the same spectral amplitude and represent 500 Hz of a 2.5 KHz sweep width, 0.3 sec acquisition time, 0.1 sec exponential sensitivity enhancement, 52 μsec 90° r.f. pulse, 23 K transients, 8 K Fourier transform, D_2O lock, temperature 24.5°C. Spectra taken at pH 11.9 and 6.9 R were very viscous. Spectra 6.9 R was taken after neutralizing the pH 11.9 spectra.

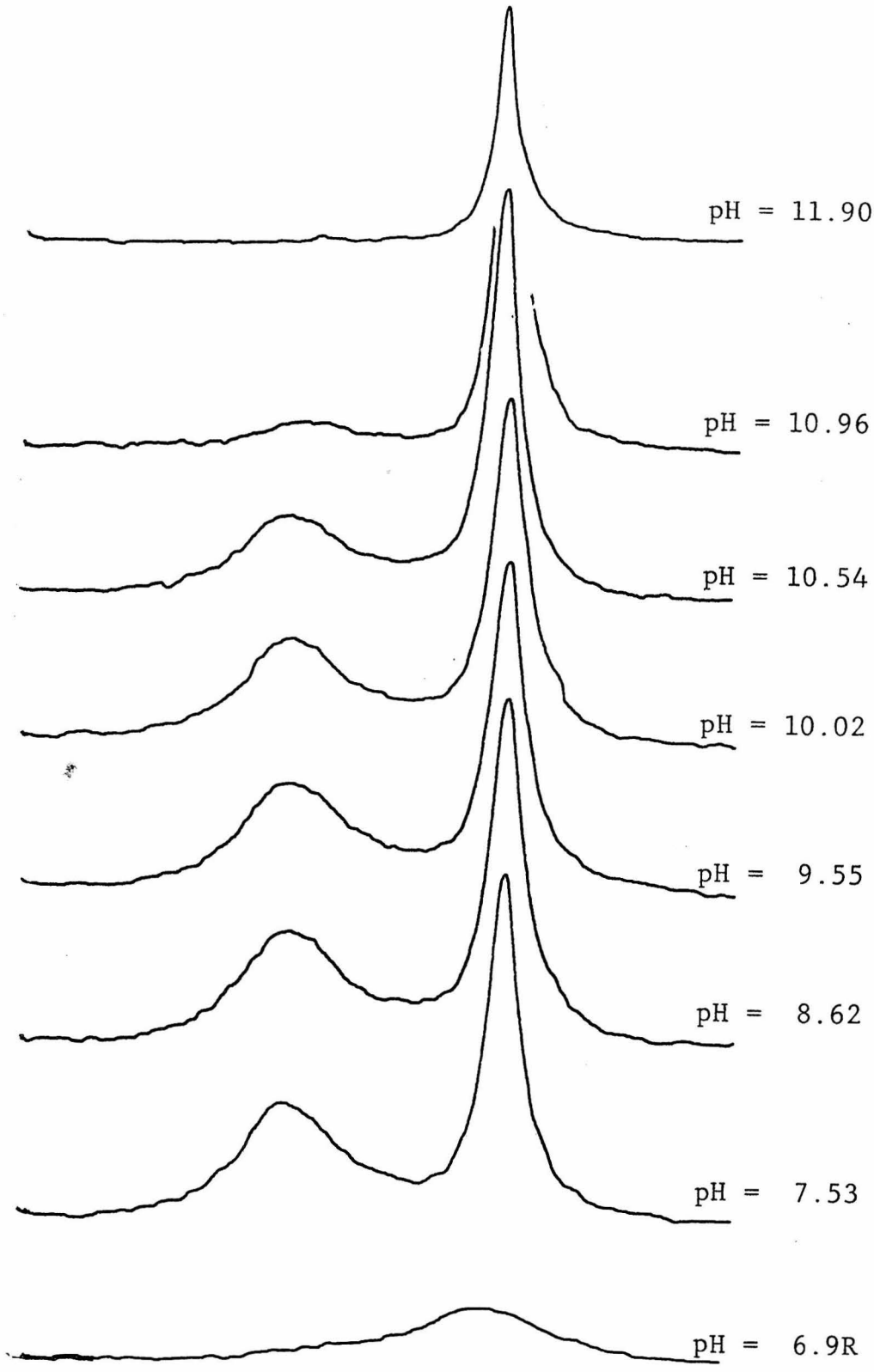
pH = 11.90
pH = 10.96
pH = 10.54
pH = 10.02
pH = 9.55
pH = 8.62
pH = 7.53
pH = 6.9R

Figure 3

^{19}F NMR spectra of 1.2×10^{-3} M DNTP-GABA plus 6.3×10^{-4} M MOPC-315 7S monomer at different pH values. All spectra were taken under the same conditions as given in Figure 2. Spectra at pH 7.5 R was taken after neutralizing the spectra taken at pH 1.6.

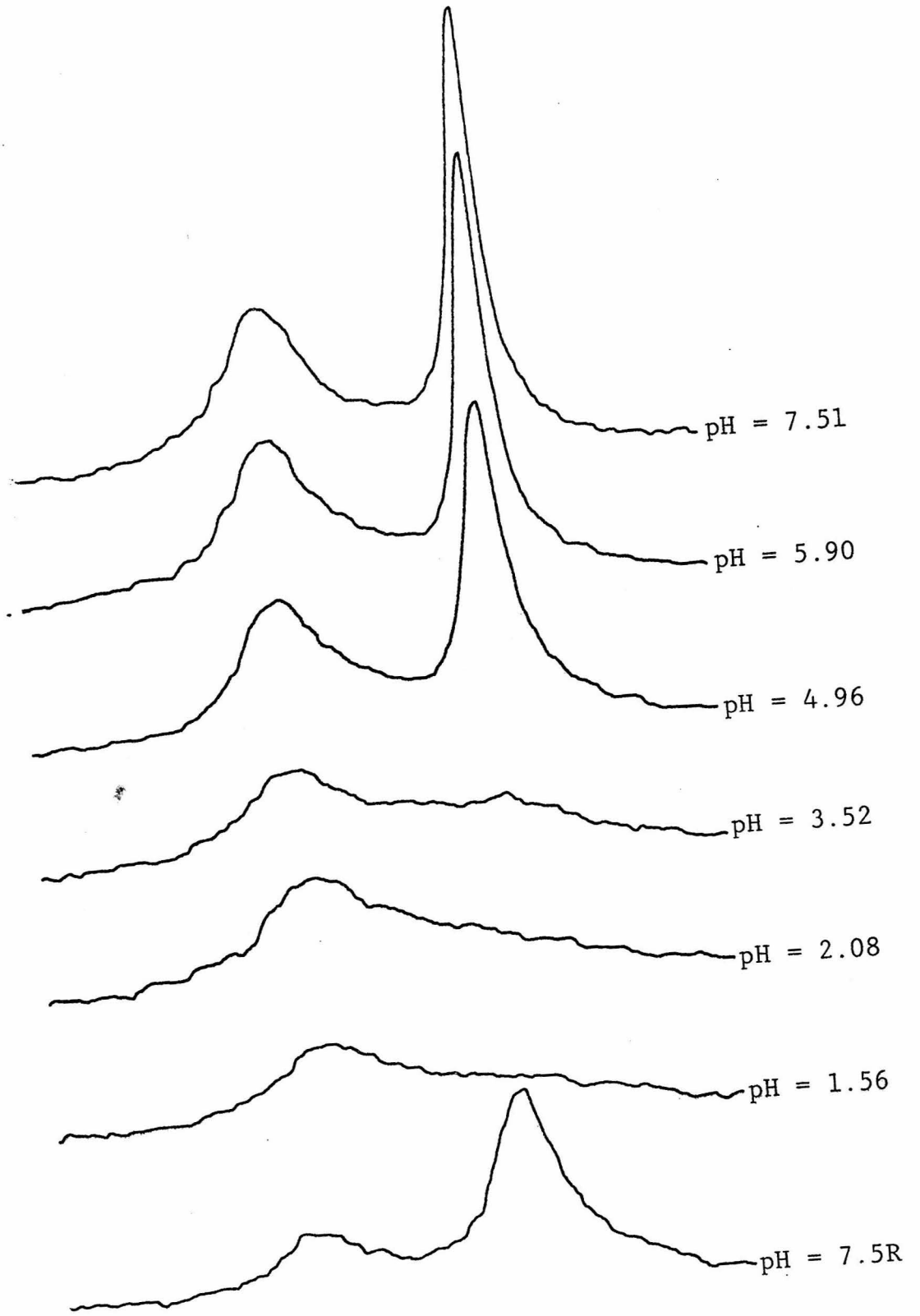
pH = 7.51
pH = 5.90
pH = 4.96
pH = 3.52
pH = 2.08
pH = 1.56
pH = 7.5R

Figure 4

^{19}F NMR spectra of 6.7×10^{-4} M DNTP-GABA plus 3.6×10^{-4} M MOPC-315 Fv fragment at different pH values. All spectra, except, the pH 11.1 were run at the same spectral amplitude and represent 500 Hz of a 2.5 KHz sweep width, 21 K transients, 80 μsec 90° r.f. pulse, 0.3 sec acquisition time, 0.1 sec exponential sensitivity enhancement, 8 K Fourier transfer, D_2O lock, temperature 24.5°C.

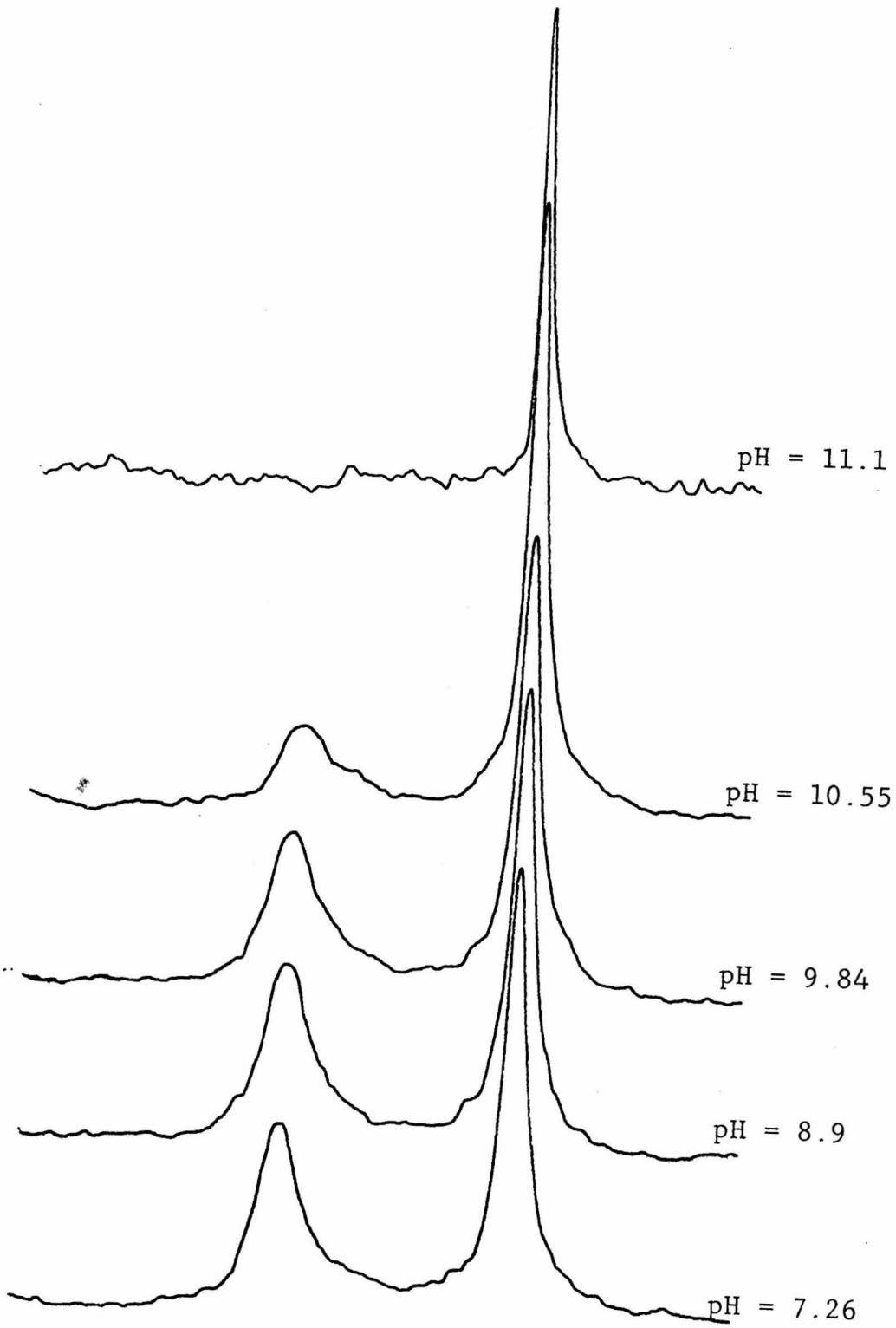
pH = 11.1
pH = 10.55
pH = 9.84
pH = 8.9
pH = 7.26

Figure 5

^{19}F NMR spectra of 6.7×10^{-4} M DNTP-GABA plus 3.3×10^{-4} M MOPC-315 Fv fragment at different pH values. Spectral conditions were identical to those in Figure 4.

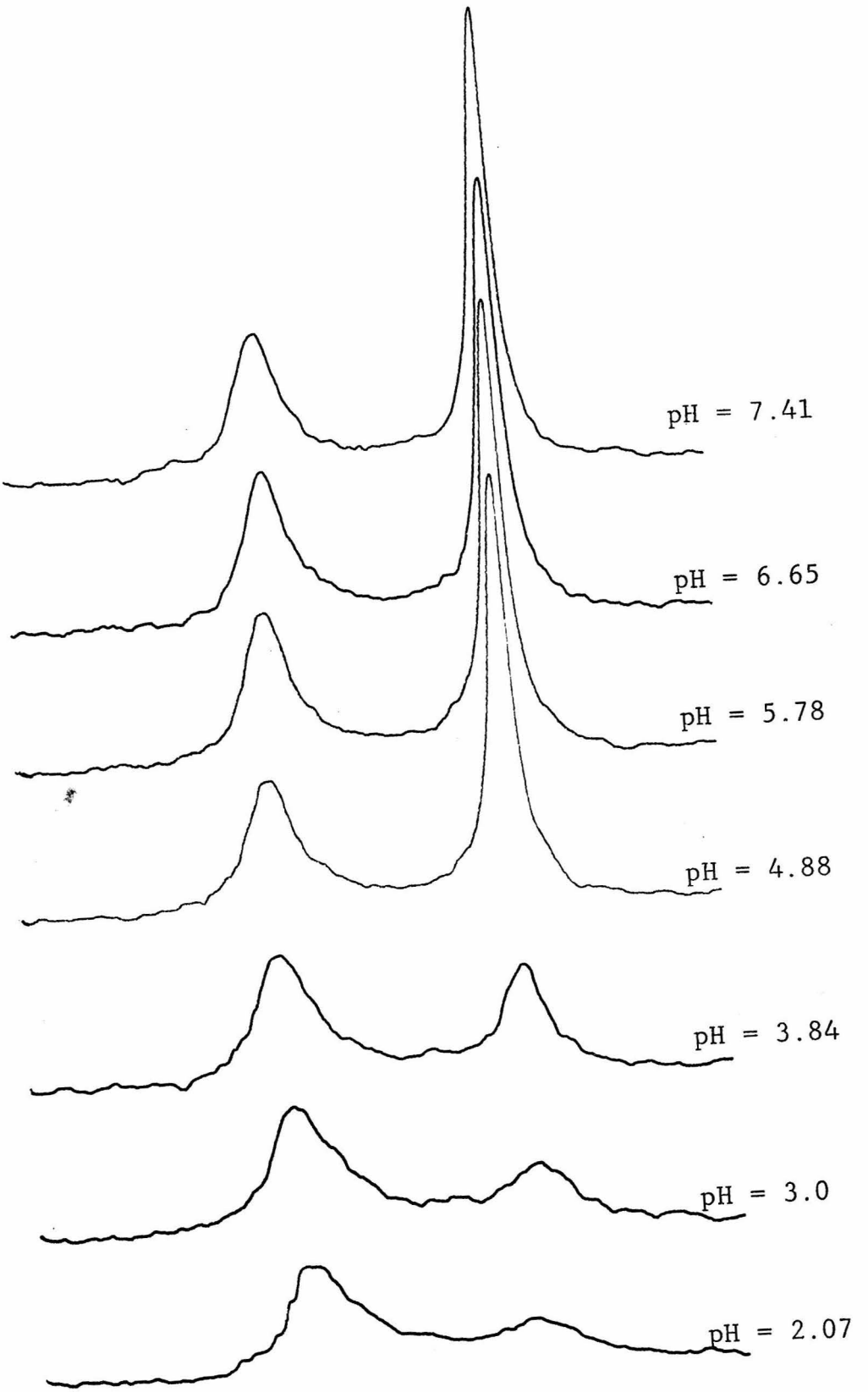
pH = 7.41
pH = 6.65
pH = 5.78
pH = 4.88
pH = 3.84
pH = 3.0
pH = 2.07

As the pH was lowered past five some precipitate began to appear in the NMR tube. This initial precipitate is thought to be due to free hapten; at still lower pH values the protein is thought to precipitate also. Because of the precipitation due to the hapten it was difficult to tell when and to what extent the protein precipitated. However, some precipitate remained even when the pH was raised back to 7 or 9, this precipitate is thought to be due to the protein. The actual amount of precipitate was never very great and while the solution did become fairly cloudy it was usually possible to see through the NMR tube, the amount of precipitate, of course, was proportional to the protein concentration.

Fluorine NMR spectra taken of the hapten in buffer with no protein showed no shift between pH 5.9 and 11.3. Below pH 5 the hapten precipitated. No spectra were taken above pH 11.3.

NTP-GABA. Unlike DNTP-GABA the fluorine NMR spectra of NTP-GABA binding to MOPC-315 is in the fast exchange limit, such that, the observed chemical shift, δ, is proportional to the mole fraction of the hapten bound times the total chemical shift, Δ. Thus, the position of the single NMR absorption for NTP-GABA binding to MOPC-315 is dependent on the amount of hapten bound times a factor, Λ which is dependent on the difference in the microenviron-

ment of the fluorine nuclei of the hapten bound to the protein and free in solution (Gammon et al, 1972). Therefore, a change in chemical shift, δ, indicates a difference in the amount of hapten bound and/or a change in the binding site surrounding the trifluormethyl group of the bound hapten.

As the pH value of NMR samples containing NTP-GABA bound to MOPC-315 7S monomer is raised above 9 the chemical shift, δ, moves upfield until at pH 10.5, it is essentially equal to that of the free ligand[5] (Figure 6). When titrated back to neutrality from pH 10.6 the fluorine NMR spectrum of NTP-GABA bound to the 7S monomer of MOPC-315 gave a spectrum almost identical (similar chemical shift, peak size, and peak shape) as a fresh sample at neutral pH.

As the pH is lowered the chemical shift, δ, initially moves further upfield in the pH 4-5 range and then downfield at still lower pH values (Figure 6). When the pH was raised back to neutral from pH 1.5 the chemical shift, δ, was the same as it was at the lower pH.

---

[5]Some of this small difference between the NMR spectra of protein ligand solution at high pH and the hapten in buffer solution with no protein can be due to a small change in the bulk magnetic susceptibility caused by the protein (Gammon et al., 1972) and pH.

Figure 6

This figure shows the effect of changing pH on the chemical shift, δ, of the fluorine nuclei of NTP-GABA (2.9×10^{-4} M) plus (2.9×10^{-4} M binding sites) MOPC-315 7S monomer. Each point represents a spectrum taken with a 3.0 KHz sweep width, 0.2 sec acquisition time, 0.03 sec exponential sensitivity enhancement, 45 μsec 90° r.f. pulse, 18 K transients, an 8 K Fourier transform, with a D_2O lock, probe temperature 24.5°C. The chemical shifts are given in ppm downfield from the position ^{19}F NMR absorption of NTP-GABA in buffer with no protein.

○ and Δ are used to show that different samples were used for the acid and base titration.

Observed Chemical Shift δ in ppm Downfield from Unbound NTP-GABA
0.0
0.1
0.2
0.3
0.4
0.5
0.6
0.7
pH
2.0
3.0
4.0
5.0
6.0
7.0
8.0
9.0
10.0
11.0

The peak height and width of this bound hapten also changed as the pH was varied. At higher pH values the peak height increased while the peak width and the chemical shift decreased. As the pH was lowered past neutral the peak height decreased while the peak width and the chemical shift, δ, increased. However, at pH values below 3.5 the peak width narrows and grows taller and the chemical shift decreased. The peak area decreased as the pH drops below 5 to about 80-85% of its value above pH 5, but remained fairly constant as the pH was lowered further. The peak area, chemical shift, and width of the sample neutralized from pH 1.5 stays about the same as they were at pH 1.5.

The NMR samples become cloudy due to precipitation as the pH is lowered past 5 and some precipitate remains when the pH is raised back to about 7 from pH 1.5, similar to the observations mentioned previously for DNTP-GABA binding to MOPC-315.

The fluorine NMR spectra of NTP-GABA in buffer showed no shift as the pH was varied between 5.2 and 11.5. Below 5 it precipitated. No spectra were taken at higher pH values.

The binding affinity of MOPC-315 7S monomer for NTP-GABA determined by fluorescence quenching was $1.5 \times 10^4\ M^{-1}$

at pH 9.3 and less than 10^3 M^{-1} at pH 10.0.

NOE Studies

DNTP-GABA. The variation of the NOE of DNTP-GABA bound to MOPC-315 Fv fragment as a function of the proton frequency irradiated is shown in Figures 7-9.

Figure 7 shows the NOE of an excess of DNTP-GABA plus the Fv fragment of MOPC-315 when different regions of the proton spectra are saturated. This figure illustrates that the NOE of the bound and free hapten are similar. This figure also shows three positions of greatest cross relaxation when protons at δ6.7 ppm, δ4.7 ppm and δ2.5 ppm are saturated. However, the background NOE is also fairly large indicating the possible presence of non-specific NOE due to a cascading effect of decoupling energy from nearby but not directly interacting protons (Hull and Sykes, 1975a, and b; and Gerig, 1977). In an effort to minimize this cascading effect the decoupler was pulsed for a time approximately equal to T_1 just before the 90° r.f. pulse and the acquisition time.

When the decoupler was pulsed in this manner the fluorine NOE observed when different regions of the proton spectra was irradiated had less background NOE but still showed the same areas of maximum cross relaxation (Figures 8 and 9).

Figure 7

NOE of DNTP-GABA (4.4×10^{-4} M) plus the Fv fragment of MOPC-315 (3.3×10^{-4} M) as various regions of the proton NMR spectra are saturated with a second radio frequency. The decoupler was on continuously at 90 dB of power ($\gamma H_2/2\pi$ = 17 Hz). Each point represents a spectrum taken at a 3.0 KHz sweep width, 0.3 sec acquisition time, 1.8 sec pulse delay, 63 μsec 90° r.f. pulse, 5.0 K transients, a 0.05 sec exponential sensitivity enhancement, an 8 K Fourier transform, temperature 24.5°C. Decoupler offsets are in ppm downfield from TMS.

○ bound hapten, estimated error 5%.

□ excess unbound ligand, estimated error about 12%.

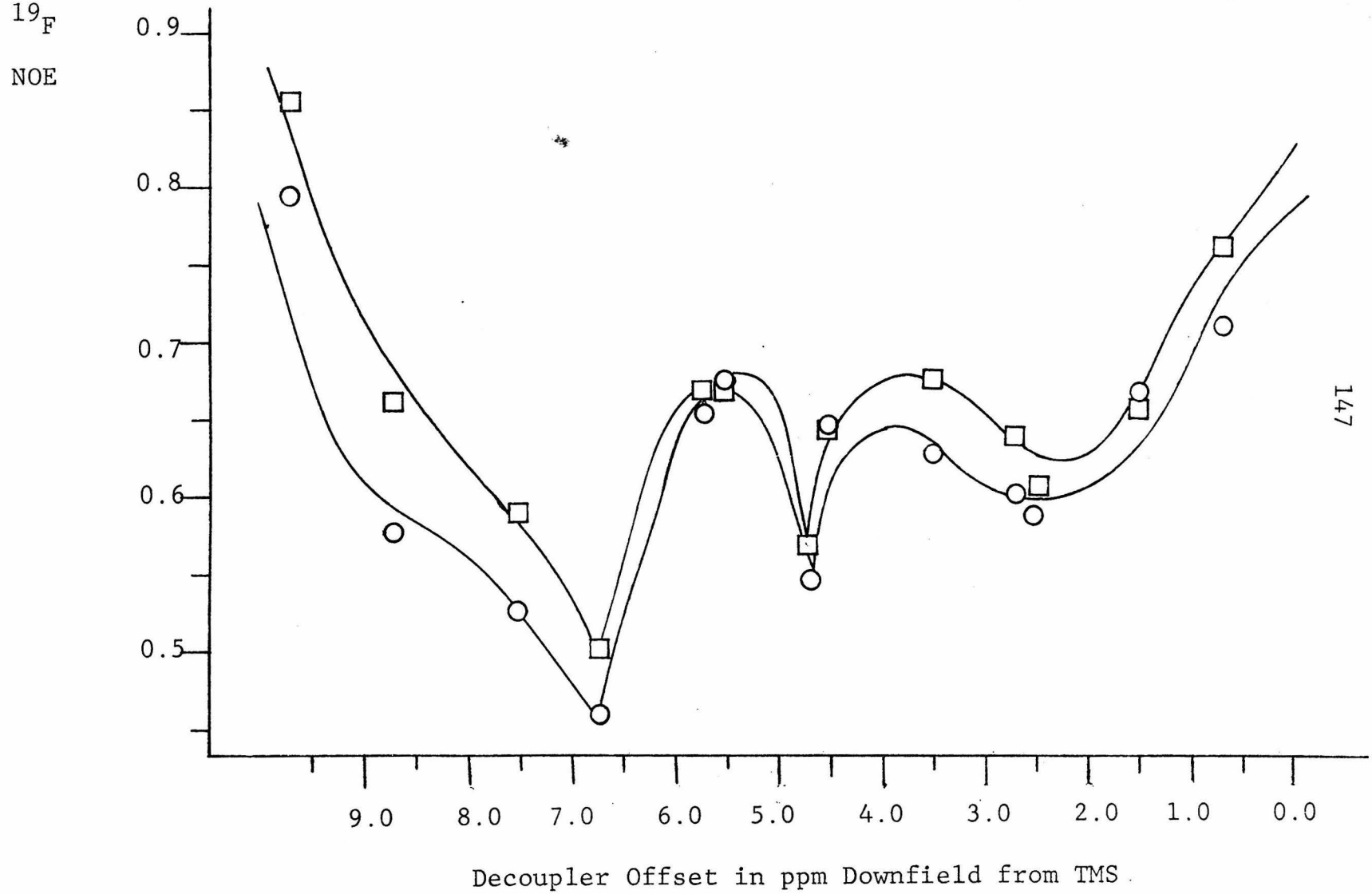
^{19}F
NOE
0.9
0.8
0.7
0.6
0.5
9.0
8.0
7.0
6.0
5.0
4.0
3.0
2.0
1.0
0.0
Decoupler Offset in ppm Downfield from TMS

Figure 8

○ NOE of DNTP-GABA (2.8×10^{-4} M) plus the Fv fragment of MOPC-315 (4.0×10^{-4} M) when various regions of the proton NMR spectra are saturated by a second radio frequency from the decoupler. The decoupler was pulsed for 0.25 sec immediately prior to the 90° r.f. pulse (61 μsec). The decoupling power was 95 dB ($\gamma H_2/2\pi$ = 28 Hz). Each point represents a spectrum taken with a 3.0 KHz sweep width, 0.2 sec acquisition time, pulse delay of 0.65 sec, exponential sensitivity enhancement of 0.05 sec, 4 K transients, 4 or 8 K Fourier transform. All hapten is bound estimated error 5%.

□ Approximately 5×10^{-3} M DNTP-GABA in buffer, 3.0 KHz sweep width, 1.0 sec acquisition time, 6.0 sec, pulse delay, 0.02 exponential sensitivity enhancement. 54 μsec 90° pulse width, 60 transients, 8 K Fourier transform, decoupler off during acquisition time. Estimated error 1%.

Decoupler offsets are in ppm downfield from TMS, probe temperature 24.5°C.

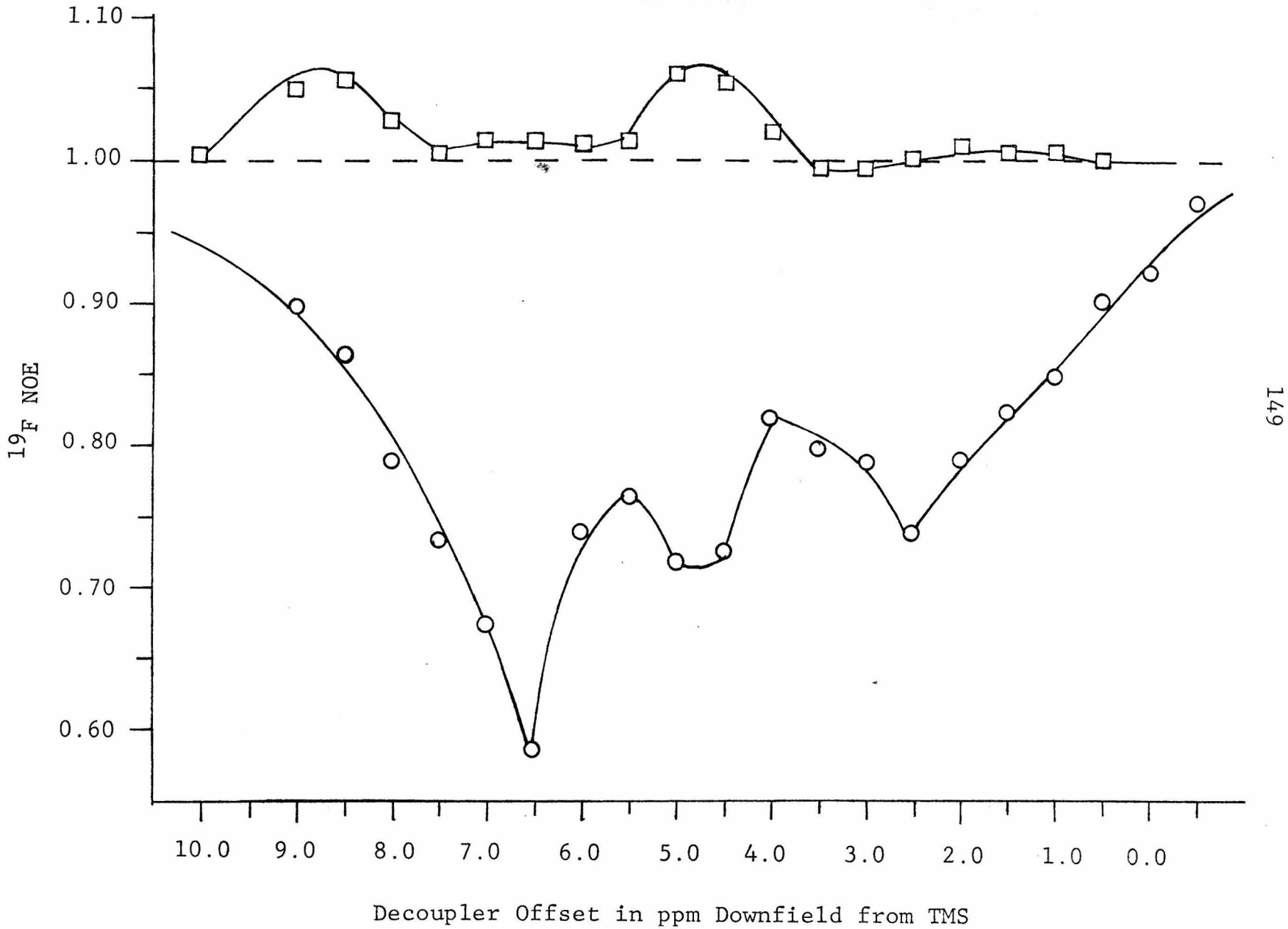
1.10
1.00
0.90
0.80
0.70
0.60
$^{19}_{F}$ NOE
10.0
9.0
8.0
7.0
6.0
5.0
4.0
3.0
2.0
1.0
0.0
Decoupler Offset in ppm Downfield from TMS

Figure 9

○ NOE of DNTP-GABA (2.8×10^{-4} M) plus 31 mg of lyophilized Fv fragment of MOPC-315 (5.0×10^{-4} M) in 2.5 ml of D_2O buffer when various regions of the proton NMR spectra are saturated by a second radio frequency from the decoupler. The decoupler was pulsed for 0.24 sec immediately before the 90° r.f. pulse (54 μsec). The decoupling power was 95 dB ($\gamma H_2/2\pi$ = 28 Hz). Each point represents a spectrum taken with a 3.0 KHz sweep width, 0.3 sec acquisition time, 0.5 sec pulse delay, 0.03 sec exponential sensitivity enhancement, 6 K transients, 8 K Fourier transform. All hapten is bound, estimated error 5%.

□ Approximately 5×10^{-3} M DNTP-GABA in D_2O buffer, 3.0 KHz sweep width, 0.6 sec acquisition time, 72 μsec 90° r.f. pulse width, 0.02 sec exponential sensitivity enhancement, 6.0 sec pulse delay, 75 transients, 8 K Fourier transform, decoupler power at 95dB, decoupler off during the acquisition time, estimated error 1%.

Decoupler offsets are in ppm downfield from TMS, probe temperature 24.5°C.

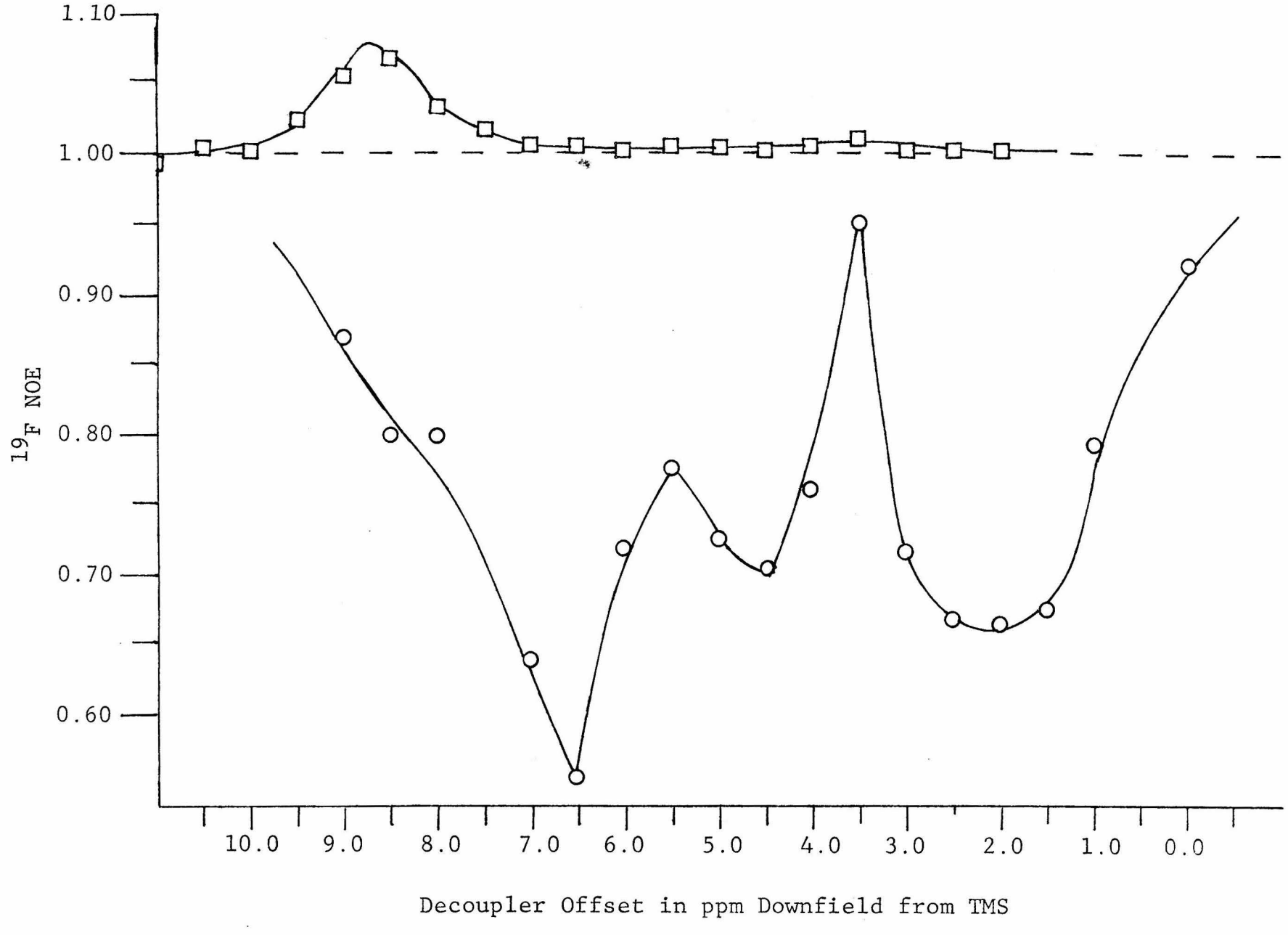
1.10
1.00
0.90
0.80
0.70
0.60
$^{19}_{F}$ NOE
10.0
9.0
8.0
7.0
6.0
5.0
4.0
3.0
2.0
1.0
0.0
Decoupler Offset in ppm Downfield from TMS

However, to get similar NOE enhancements in pulse experiments about four times as much decoupling power (5 more dB) or about twice the effective field strength was needed. This indicates that the power level used in the continuous decoupling experiments was probably not causing full saturation, however, more power caused a loss in selectivity. These pulsed experiments seemed to be somewhat less sensitive to slight increases in decoupler power.

NOE experiments run with and without an excess of hapten over protein were essentially the same.[6] The error in reproducibility of the NOE for a given sample was larger for the free unbound hapten then for the bound hapten. Differences as large as 12% were seen in the free peak, but the NOE of the bound peak was reproducible to better than 5%. The reason for the larger error in measuring the NOE of the free peak is not known.

Figure 8 shows the variation in fluorine NOE with decoupler offset of DNTP-GABA bound to the Fv fragment of MOPC-315, and the NOE of DNTP-GABA in buffer with no pro-

---

[6]Some spectra determined with an excess hapten showed a minor downward peak between δ7.5-δ8.5 ppm, this may be due to the aromatic proteins of the free hapten, but this second aromatic peak was not very reproducible and may be due to fluctuations in signal to noise.

tein present. The decoupler was only on for 0.25 sec ($\sim T_1$) before the 90° r.f. pulse followed by data accumulation. Figure 9 shows a similar experiment that had deuterium oxide instead of water as the solvent.

The maximum NOE seen using broad band noise decoupling is 0.13 in water buffer and 0.09 in deuterium oxide buffer (decoupler on continuously).

NTP-GABA. The NOE of NTP-GABA (both bound to MOPC-315 Fv and in buffer with no protein) at different decoupler offsets is shown in Figure 10 and in deuterium oxide buffer in Figure 11. An experiment run at different ratios of bound and free hapten showed essentially the same variation in NOE when different regions of the proton spectra were saturated.

The maximum NOE of NTP-GABA bound to the Fv fragment of MOPC-315 was 0.50 in water buffer and 0.49 in deuterium oxide buffer when higher power broad band noise decoupling was used (decoupler on continuously).

DNMP-GABA. The proton NMR spectra of MOPC-315 Fv fragment with and without DNMP-GABA is shown in Figure 12 (100.1 MHz) and Figure 13 (220 MHz). A comparison of spectra taken with and without hapten shows very little difference until a large excess of hapten is added. Then two new "aliphatic" peaks appear at δ3.1 ppm and δ2.2 ppm.

Figure 10

△ NOE of NTP-GABA (3.8×10^{-4} M) plus the Fv fragment of MOPC-315 (2.1×10^{-4} M) when various regions of the proton NMR spectra are saturated with a second radio frequency from the decoupler. Decoupler was pulsed for 0.2 sec immediately before the 90° r.f. pulse (59 μsec). The decoupling power was 95 dB ($\gamma H_2/2\pi$ = 28 Hz). Each point represents a spectrum taken with a sweep width of 3.0 KHz, 0.8 sec pulse delay, 0.30 sec acquisition time, 3.0 K transients, 0.05 sec exponential sensitivity enhancement, 4 or 8 K Fourier transform. Ratio of bound to total hapten concentration about 70%. Estimated error 5%.

□ Approximately 5×10^{-3} M NTP-GABA in buffer, 3.0 KHz sweep width, 0.6 sec acquisition time, 6.0 sec pulse delay, 0.02 sec exponential sensitivity enhancement, 61 μsec 90° r.f. pulse width, 75 transients, 8 K Fourier transform, decoupler power 95 dB, decoupler off during acquisition time. Estimated error 1%.

Decoupler offsets are in ppm downfield from TMS. Probe temperature 24.5°C.

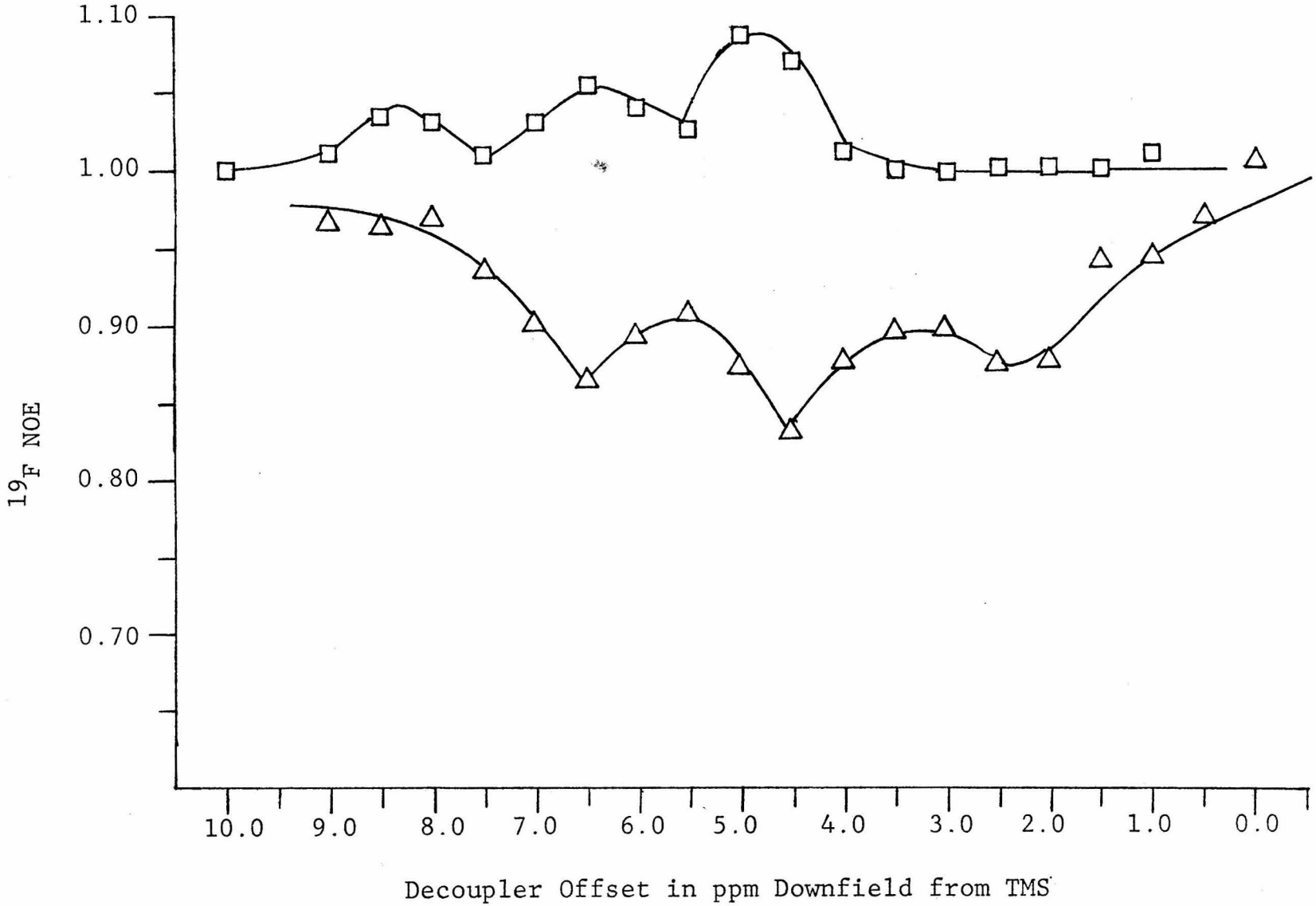
1.10
1.00
0.90
0.80
0.70
^{19}F NOE
10.0
9.0
8.0
7.0
6.0
5.0
4.0
3.0
2.0
1.0
0.0
Decoupler Offset in ppm Downfield from TMS

Figure 11

△ NOE of NTP-GABA (2.0×10^{-4} M) plus 32 mg of lyophilized MOPC-315 Fv fragment (5.1×10^{-4} M) in 2.5 ml of D_2O buffer when various regions of the proton NMR spectra are saturated by a second radio frequency from the decoupler. The decoupler was pulsed for 0.16 sec immediately before the 90° r.f. pulse (61 μsec). The decoupling power was 95 dB ($\gamma H_2/2\pi$ = 28 Hz). Each point represents a spectrum taken with a sweep width of 3.0 KHz, 0.3 sec acquisition time, 0.2 sec pulse delay, 6 K transients, 0.05 sec exponential sensitivity enhancement, 4 or 8 K Fourier transform. Ratio of bound to total hapten concentration about 80%, estimated error 5%.

□ Approximately 5×10^{-3} M NTP-GABA in D_2O buffer. 3.0 KHz sweep width, 0.6 sec acquisition time, 6.0 sec pulse delay, 0.02 sec exponential sensitivity enhancement, 61 μsec 90° r.f. pulse, 75 transients, decoupler power 95 dB, decoupler off during acquisition time. Estimated error 1%.

Decoupler offsets are in ppm downfield from TMS. Probe temperature 24.5°C.

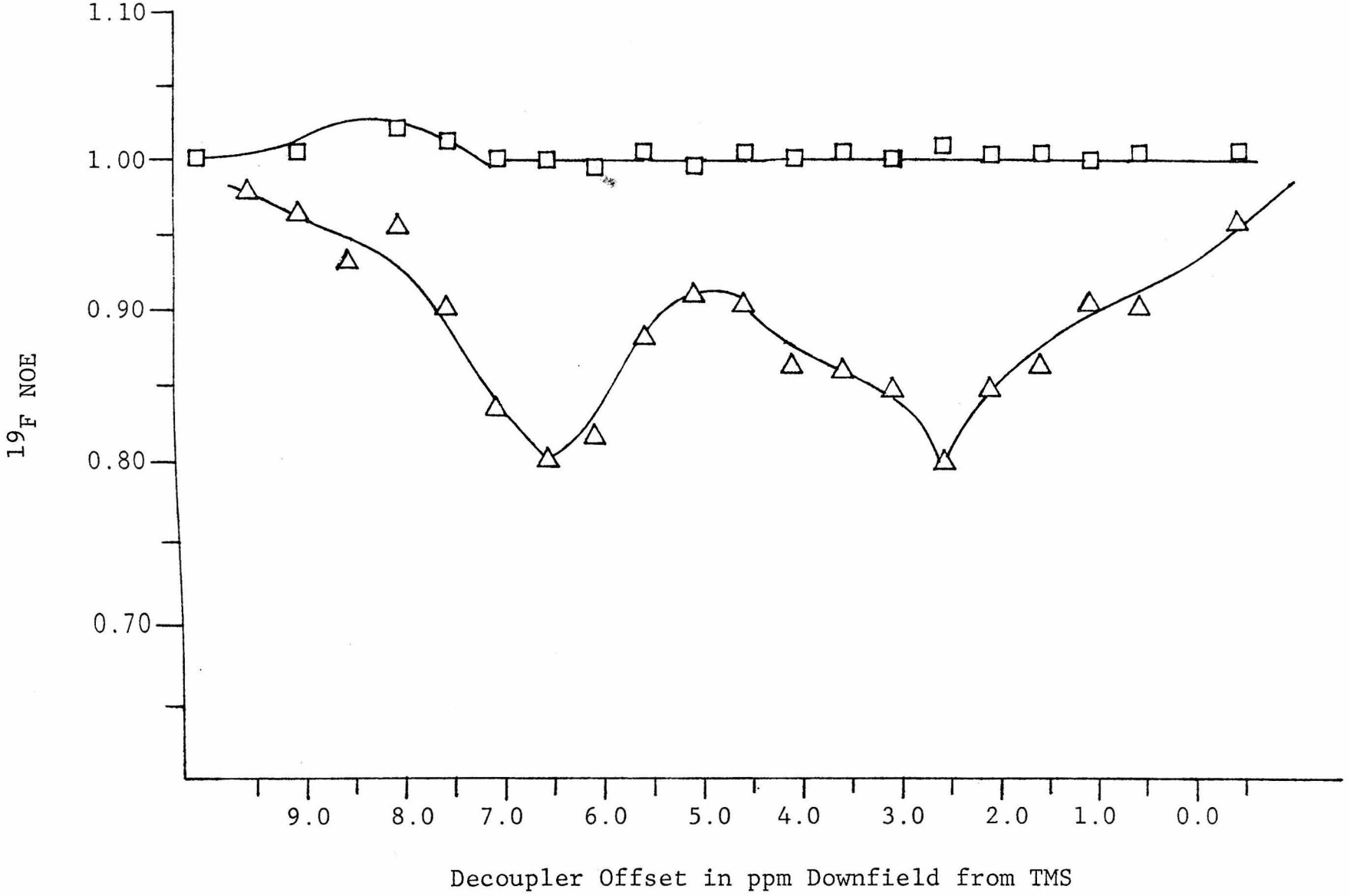
1.10
1.00
0.90
0.80
0.70
$^{19}_{F}$ NOE
9.0
8.0
7.0
6.0
5.0
4.0
3.0
2.0
1.0
0.0
Decoupler Offset in ppm Downfield from TMS

Figure 12

^{1}H NMR spectra at 100.1 MHz of MOPC-315 Fv fragment plus increasing amounts of DNMP-GABA.

A. 5.5×10^{-4} M MOPC-315 Fv fragment

B. 5.5×10^{-4} M MOPC-315 Fv fragment plus 1.0×10^{-3} M DNMP-GABA.

C. 5.5×10^{-4} M MOPC-315 Fv fragment plus 3.0×10^{-3} M DNMP-GABA

Spectra were taken under similar conditions as listed in Figure 14.

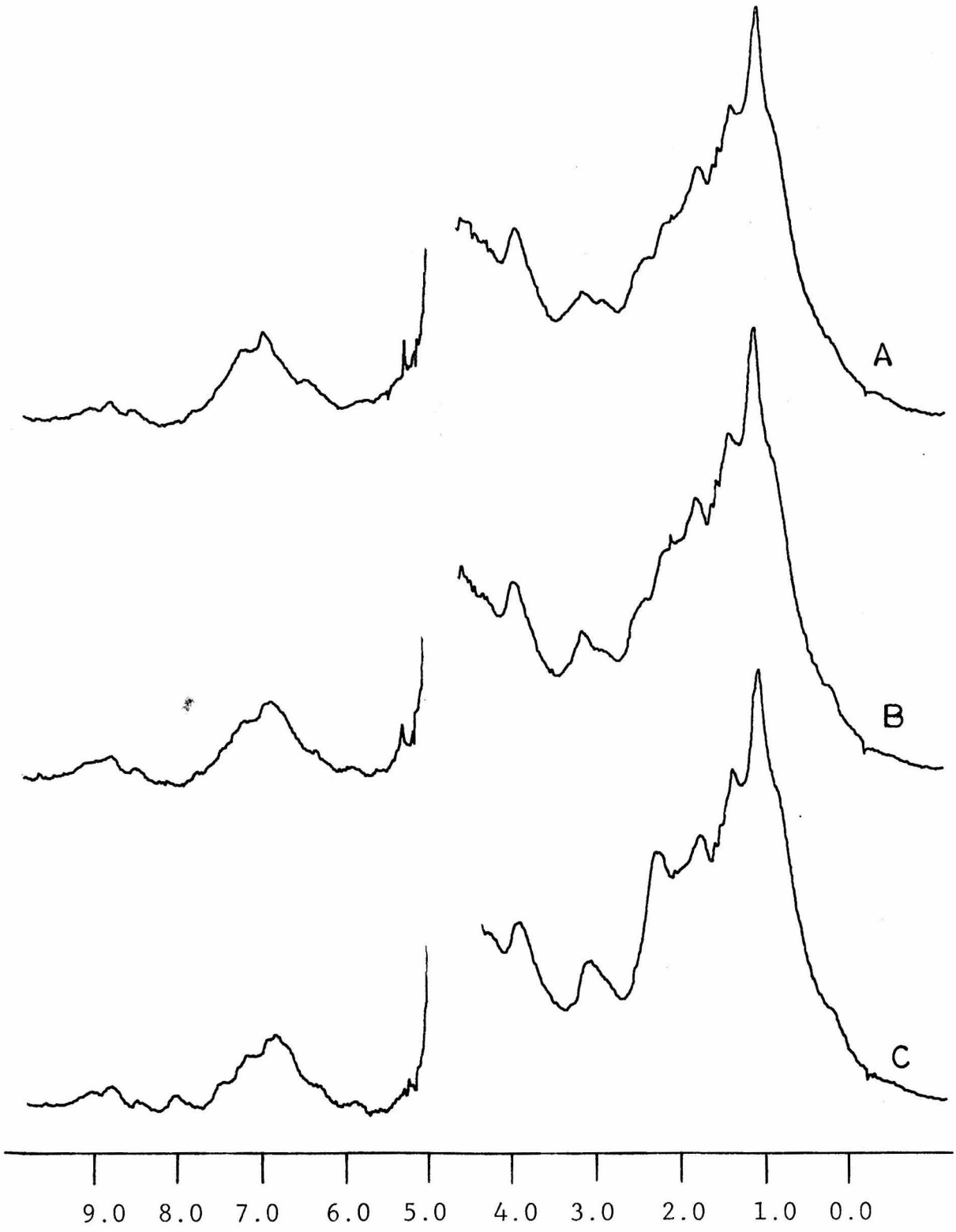
A
B
C
9.0
8.0
7.0
6.0
5.0
4.0
3.0
2.0
1.0
0.0

Figure 13

^{1}H NMR spectra at 220 MHz of MOPC-315 Fv fragment plus increasing amounts of DNMP-GABA

A. 9.6×10^{-4} M MOPC-315 Fv

B. 9.6×10^{-4} M MOPC-315 Fv plus 1.0×10^{-3} M DNMP-GABA

C. 9.6×10^{-4} M MOPC-315 Fv plus 2.0×10^{-3} M DNMP-GABA

All spectra were taken in 100% D_2O buffer solution, 2.2 KHz of a 2.5 KHz sweep width, 0.8 sec acquisition time, 0.7 sec pulse delay, 45 μsec 90° r.f. pulse, 10 K transients, 1.0 sec exponential sensitivity enhancement.

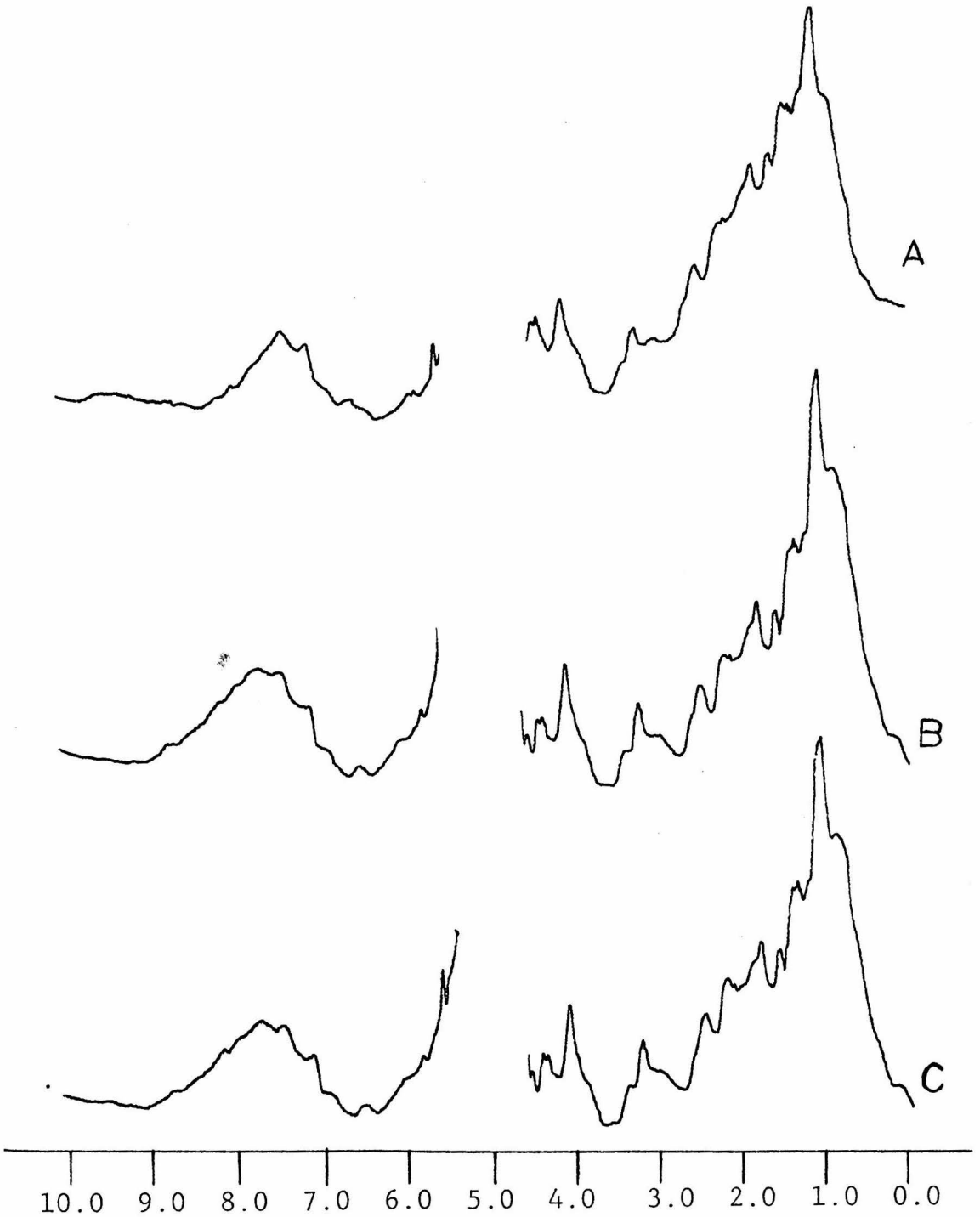
A
B
C
10.0
9.0
8.0
7.0
6.0
5.0
4.0
3.0
2.0
1.0
0.0

DNTP-GABA. The proton NMR spectra of the Fv fragment of MOPC-315 with varying amounts of DNTP-GABA are shown in Figure 14. The addition of two equivalents of DNTP-GABA causes very little change in the NMR spectra of the Fv fragment, but the addition of about six equivalents of DNTP-GABA to Fv fragment produces two new "aliphatic" peaks at δ3.1 ppm and δ2.0 ppm. A new aromatic peak also appears at δ8.5 ppm

CHF_2-GABA. When CHF_2-GABA is bound to MOPC-315 7S immunoglobulin it gives a very broad absorption (180 ± 20 Hz) that is shifted 1.8-2.1 ppm downfield from its absorption in buffer with no protein. On decoupling the peak width decreases to 125 ± 15 Hz. It was hoped that the variation in peak width upon changing the frequency offset of the decoupler could be used to determine the proton chemical shift (Δ) of the benzyl protons due to binding, but low signal to noise in a reasonable period at time due to the broadness of the bound peak prompted a switch to the Fv fragment.

CHF_2-GABA bound to the Fv fragment is in slow exchange on the chemical shift time scale with CHF_2-GABA free in solution. The bound peak occurs 1.8-2.0 ppm downfield from the center of the doublet of the excess unbound hapten. The single broad absorption (probably a poorly resolved doublet) of the bound peak was a little

Figure 14

^{1}H NMR spectra at 100.1 MHz of MOPC-315 Fv fragment plus increasing amounts of DNTP-GABA.

A. 5.3×10^{-4} M MOPC-315 Fv fragment

B. 5.3×10^{-4} M MOPC-315 Fv plus 1.0×10^{-3} M DNTP-GABA

C. 5.3×10^{-4} M MOPC-315 Fv plus 3.0×10^{-3} M DNTP-GABA.

All spectra were taken in 100% D_2O buffer solution and represent 1.1 KHz of a 2.5 KHz sweep width, 0.8 sec acquisition time, 1.2 sec pulse delay, 0.8 sec exponential sensitivity enhancement, 45 μsec 90° r.f. pulse width, 4 K transients, and 8 K Fourier transform.

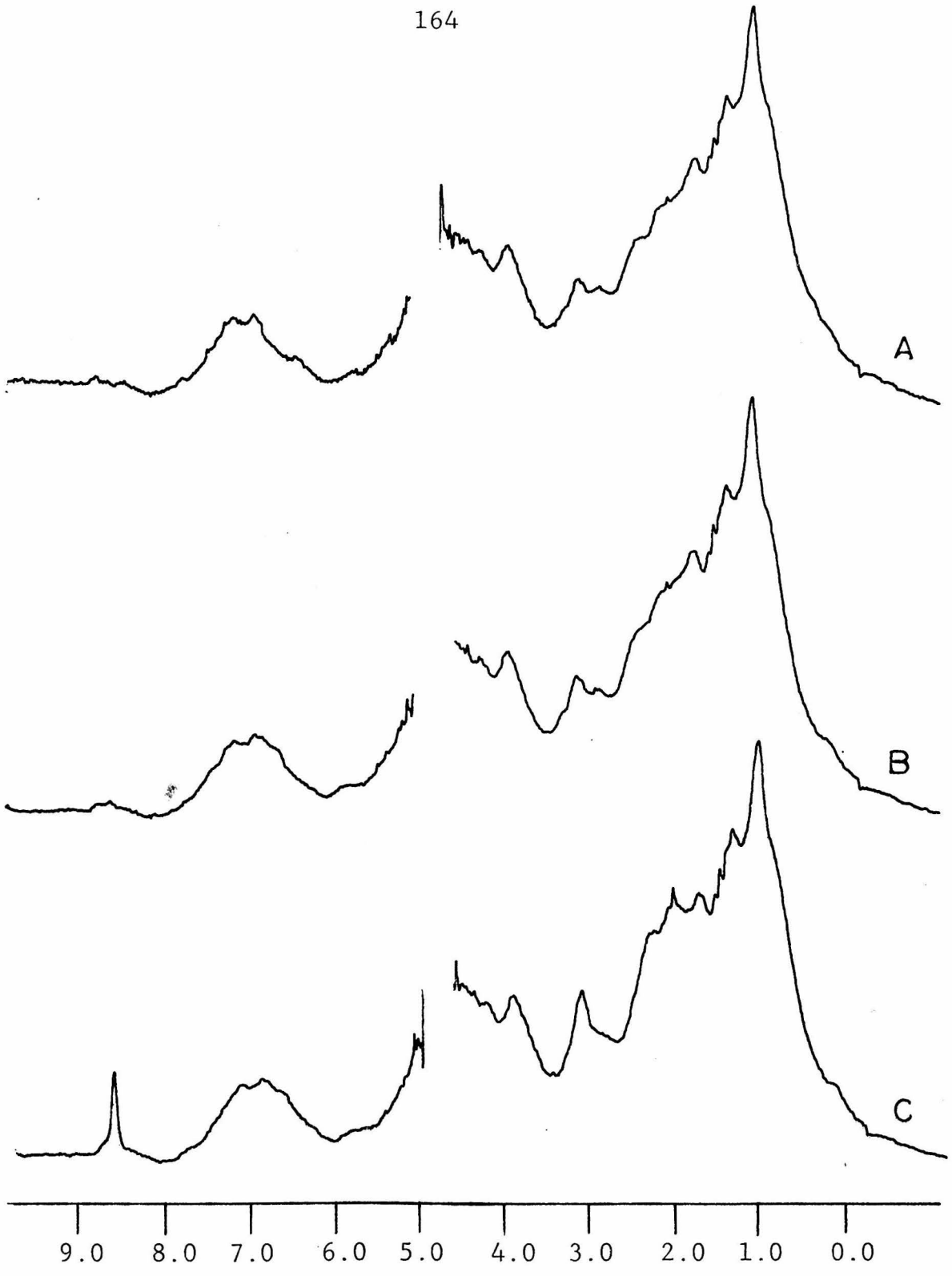
A
B
C
9.0
8.0
7.0
6.0
5.0
4.0
3.0
2.0
1.0
0.0

narrower than when this hapten is bound to the 7S monomer having a peak width of 120 ± 5 Hz undecoupled and 75 ± 5 Hz decoupled.

The alteration in peak width of CHF_2-GABA bound to the Fv fragment of MOPC-315 when different regions of the proton spectra were saturated is shown in Figure 15. The minimum peak width was obtained when protons at δ5.4-6.1 ppm were decoupled. This is about 1.2 ppm upfield from the position of the proton triplet for this hapten with no protein (δ6.9 ppm).

Fluorine Chemical Shifts in D_2O.

DNTP-GABA. The chemical shift, Δ, of DNTP-GABA bound to MOPC-315 Fv fragment is 178 ± 3 Hz (1.89 ppm) in deuterium oxide buffer and 168 ± 5 Hz (1.79 ppm) in water buffer. This difference in chemical shift is due to a 13 Hz upfield shift of the free hapten when placed in deuterium oxide buffer as referenced to an external standard. The position of the NMR absorption due to hapten bound to the protein is essentially the same in both solvents as referenced to an external standard.

NTP-GABA. The chemical shift of this hapten in deuterium oxide buffer is shifted about 16 Hz upfield from this hapten in water buffer as referenced to an external standard. The position of the NMR absorption of NTP-GABA

Figure 15

Change in line width (corrected for sensitivity enhancement) of the fluorine NMR spectra of CHF_2-GABA bound to the Fv fragment of MOPC-315 when different regions of the proton spectra are saturated with a second radio frequency from the decoupler.

□ , decoupling power $\gamma H_2/2\pi$ = 4.2 J.

Δ , decoupling power $\gamma H_2/2\pi$ = 2.0 J.

○ , decoupling power $\gamma H_2/2\pi$ = 0.93 J.

Spectra were taken of a 2.5 ml sample containing 5.2×10^{-4} M CHF_2-GABA; and 7.3×10^{-4} M Fv fragment of MOPC-315. Each point represents a spectrum taken with 3.0 KHz sweep width, 0.3 sec acquisition time, 0.6 sec pulse delay, 70 μsec 90° r.f. pulse, 0.03 sec sensitivity enhancement, about 8 K transients with an 8 K Fourier transform, D_2O lock, temperature 24.5 C. Decoupler was on only during the acquisition time. Decoupler offsets are given in ppm downfield from TMS. Estimated error in line width measurements was about ± 5 Hz.

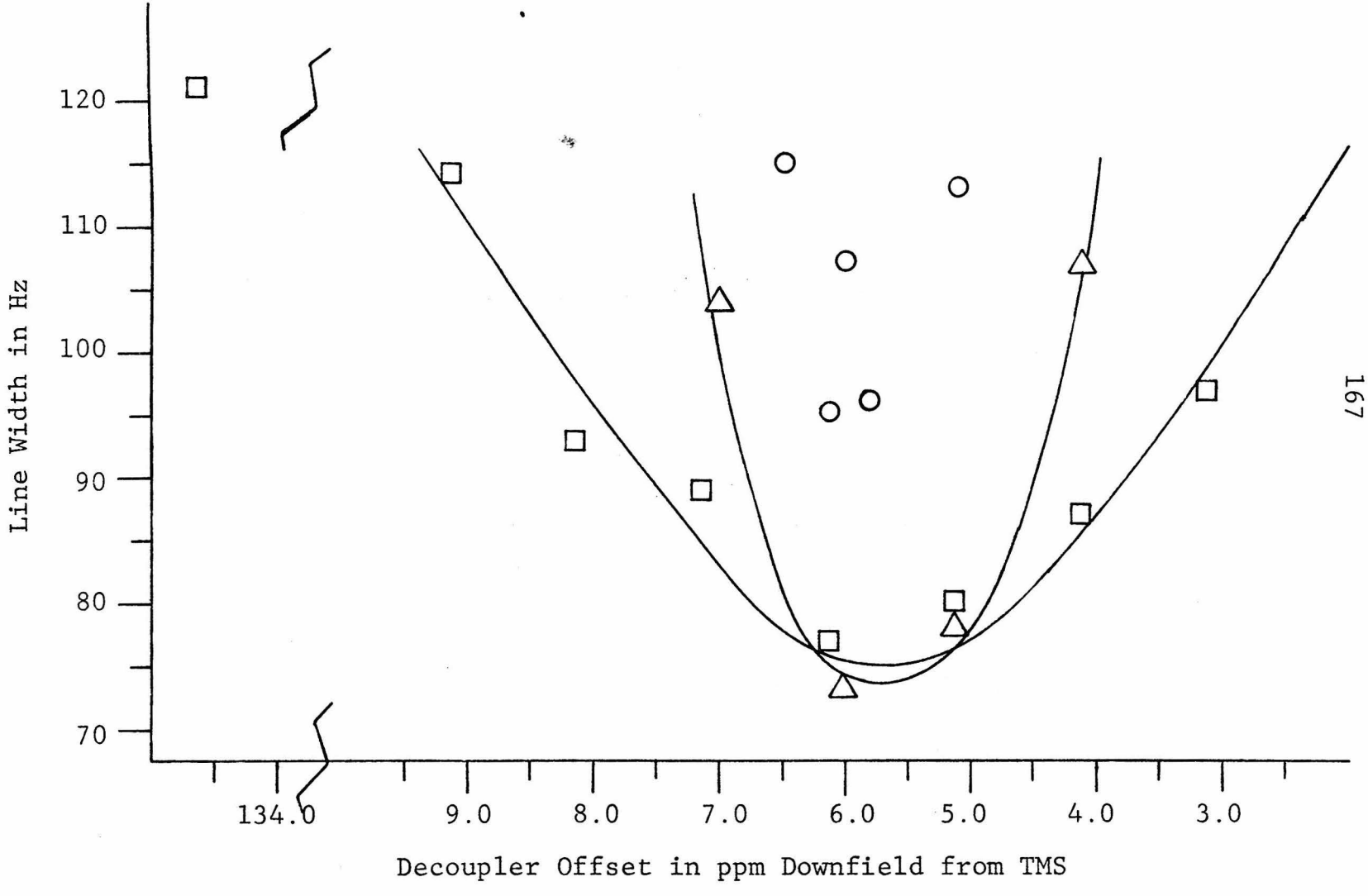
Line Width in Hz
120
110
100
90
80
70
134.0
9.0
8.0
7.0
6.0
5.0
4.0
3.0
Decoupler Offset in ppm Downfield from TMS

with protein also seems to be shifted slightly upfield in deuterium oxide buffer versus water buffer. However, the total chemical shift, Δ, and the position of the trifluoromethyl group when 100% bound to the protein has not been determined.

DISCUSSION

pH Studies

NTP-GABA. The variation in the observed chemical shift, δ, of the fluorine nuclei of NTP-GABA binding to MOPC-315 7S protein (under conditions where 86% of the total hapten is bound at pH 7.5) is shown in Figure 6. As the pH increases above 8.5 the chemical shift, δ, begins to decrease until at pH 10.6 its chemical shift is very close to that of the free hapten. This change in δ can be caused by a decrease in the amount of hapten bound and/or a change in the total chemical shift, Δ.

The observed chemical shift, δ, plotted in Figure 6 is related to the mole fraction of hapten bound, [AbHap]/[Hap_o], and the total chemical shift, Δ. Δ is the difference in ppm between the NMR absorption of the hapten bound and free, corrected for bulk magnetic susceptibility (Gammon et al., 1972). Δ is sensitive to the difference in the bound and free microenvironment experienced by the trifluoromethyl group of the hapten. Therefore, the observed change in δ can be due to a decrease in protein

hapten binding affinity and/or a change in the Δ (environment of the trifluoromethyl group).

The deprotonation of a group intimately involved in binding to the trifluoromethyl group should cause a change in Δ and in binding affinity, whereas, the titration of a group not directly involved in binding the trifluoromethyl group can affect the binding affinity without causing a change in chemical shift, Δ. A change in Δ, however, does not necessarily mean that an interacting group is being titrated.

To help differentiate between changes in binding affinity and chemical shift at these high pH values the binding affinity was measured at pH 9.3 and 10.0 by fluorescence quenching. At pH 10.0 MOPC-315 7S immunoglobulin shows essentially the same decrease in fluorescence as do the "Fc" fragments from pepsin digest used to correct for non-specific quenching. The binding affinity determined by fluorescence quenching at pH 9.3 was approximately $1.5 \times 10^4\ M^{-1}$. (This binding affinity is the average for the total number of sites present in solution, and because of the way the experiment was run could not differentiate between fewer binding sites having the original binding affinity and an equal but weaker binding by all sites.)

This binding affinity (at pH 9.3) was used to calculate δ (0.38 ppm) using the concentration of hapten and protein shown in Figure 6 and the Δ observed at neutral pH (Kooistra and Richards, 1977). This calculated value of δ is within experimental error of 0.36 ppm determined from Figure 6. Thus, no change in Δ is needed to account for the observed shifts in δ at high pH values.

Since the binding at pH 10 is very small as evidenced by the small chemical shift and by the lack of binding seen by fluorescence quenching, the deprotonated form of the immunoglobulin has very little if any hapten binding acitivity. Therefore, one reason no new value for the total chemical shift, Δ, is seen is because there is very little, if any hapten bound to this deprotonated form of the immunoglobulin.

Since we only see hapten bound to the protonated form of the 7S monomer the pH plot in Figure 6 can be related to a plot of mole fraction of NTP-GABA bound (a δ value of 0.62 ppm (Δ) represents all hapten bound). With this assumption it is possible to calculate approximate association constants at different pH values. A plot of log K_a versus pH is concave downward with a pK_a value for the protein of about 8.5-9.0. The downward slope is between 1.7 and 2.0 indicating that more than one group may be involved, but at the higher pH values some irreversible

denaturization is possible causing a steeper slope. The dilution effect of the titration itself and the possibility of a small change in the bulk magnetic susceptibility with pH may also affect the downward slope.

The structural model of the binding site of MOPC-315 proposed by Padlan et al. (1976) and modified by Dwek et al. (1977) shows several trysines, an aspartic acid, a histidine, lysine and arginine near the binding pocket. Which group or groups are responsible for this reversible loss of binding will have to await further studies with chemically modified immunoglobulin to show the importance of specific groups such as, nitration of tyrosine 34 (H) (Dwek et al., 1977), glyoxalation of arginine and maleylation of lysine (Klostergaard et al., 1977a and b). The "irreversible" titration above 11 may be due to the ionization of some or all of the tyrosines buried in the binding pocket causing a complete disruption of the binding pocket, however, this is strictly speculative.

The variation of the observed chemical shift, δ, of the fluorine nuclei of NTP-GABA binding to MOPC-315 7S protein when the pH is lowered is also shown in Figure 11. The increase in δ as the pH drops below 5 is probably caused by protonation of the carboxylate group of the hapten. As this carboxylate group is protonated the

solubility of the hapten in water decreases and since all the free ligand has precipitated the only hapten in solution is bound to the protein. The observed chemical shift, δ, becomes essentially equal to the total chemical shift, Δ. In actuality things may be a little more subtle; there may also be a net increase in the total amount of hapten bound due to an increase in binding affinity. Since binding affinities are really a measure of the difference in the solvent "binding" (solubility) and the binding by the immunglobulin the protonated form of the hapten may have a higher binding affinity than the ionized form. There is about a 15 to 20% decrease in peak area as the pH drops below five but some of the decrease may also be due to precipitating protein containing bound hapten.

A further decrease in pH below 3.5 leads to a decrease in the observed chemical shift, δ. Since protein is also thought to be precipitating at these low pH values it becomes very difficult to do any kind of binding study to determine if this decrease in δ is caused by a change in Δ and/or binding affinity.

One possible explanation for this decrease in chemical shift at very low pH values may be due to a loss of specific binding sites because of precipitation of protein and an exchange between hapten specifically bound to the

remaining protein and hapten that is bound to low affinity binding sites (hapten "precipitating" into hydrophobic pockets on the protein) on the protein. If these low affinity pockets have solution-like environment or the trifluoromethyl group is still exposed to solvent then its chemical shift will be the same as free hapten in buffer. Evidence for this type of non specific binding has been seen before (Kooistra et al., 1977).

The total amount of hapten in solution, determined from the area under the single absorption peak (any precipitated hapten should have a very broad NMR absorption and would be hidden in the baseline) decreases by about 15-20% as the pH is lowered past 5 but then it remains fairly constant. However, even when the pH is raised back to 7.5 the chemical shift, δ, and peak area stay about the same as they were at pH 2.3. A fairly similar observation is made for DNTP-GABA binding to MOPC-315 (Figure 3) where the amount of ligand bound when the solution is neutralized is similar to the amount bound at the lower pH, and the size of the free ligand though broader has the same area as it did orginally. These observations suggest that the precipitated immunoglobulin may contain bound hapten, and that it does not rapidly renature or release this hapten when the pH is made neutral.

DNTP-GABA. The ^{19}F NMR spectra of DNTP-GABA bound to MOPC-315 7S and Fv fragment shows very little change as the pH is varied between 5 and 10 (Figures 2-5).

As the pH is lowered past 5, the unbound hapten peak disappears due to hapten precipitation, but the bound peak (the downfield peak) remains essentially the same until around pH 3.5. Below pH 4.0 even the bound peak slowly decreases in size. As the bound peak disappears there is no apparent change in the chemical shift nor do any new peaks appear, however, there does appear to be some broadening. This broadening is thought to be due to low affinity binding by the "insoluble" hapten.

Again the amount of binding seen when the NMR solution was neutralized is essentially the same as the amount that was bound at the lower pH value. This indicates that this acid denatured and/or precipitated protein is not reversible, and since the free peak of the neutralized protein solution has essentially the same area, though considerably broader, and not larger to account for the smaller area of the bound peak it seems that the precipitated protein probably contains bound hapten. The precipitated protein that is still present in neutralized sample may cause the increased broadness of the free peak (Figure 3) by affecting the viscosity and/or having some low affinity binding sites for the hapten.

When the pH is increased from neutral the ^{19}F NMR spectra of DNTP-GABA bound to MOPC-315 7S and Fv fragment remains relatively constant until pH values above 10. At pH values above 10 the bound peak (the downfield peak) begins to decrease with a concomitant increase in the size of the free ligand peak (Figures 2 and 4). The decrease in the size of the bound peak is better than 90% reversible at pH 10.56 but not at pH values above 11 (Figure 2).

Since, the pK_a value of the reversible loss in binding and the irreversible denaturation are so close together a quantitative study of pH versus binding would be very difficult. However, in light of the pH results, from NTP-GABA binding to MOPC-315 a couple of conclusions can be infered. Since no new peaks are seen (of course, the possibility of moderately strong binding by the titrated form with a chemical shift very close to the free ligand is possible) it appears that the "reversible" decrease in the size of the bound peak is probably due to the formation of a very low binding deprotonated form of the protein as was observed for NTP-GABA. The exchange rate of DNTP-GABA remains in slow exchange on the NMR chemical shift time scale indicating that the pK_a of the hapten protein complex is much higher, so that there is very little titration of this complex to increase the off rate.

A comparison of Figures 2 and 4 and 3 and 5 illustrates that the pH profile of DNTP-GABA binding to MOPC-315 7S or Fv proteins are essentially the same except for a slightly slower decrease in the bound peak at low pH values. This small difference is probably due to differences in solubility, or due to the lower protein concentration used in Fv experiments. This again shows the relative independence of the binding pocket on the amount of constant region attached to it, except maybe for solubility as was seen with chemical shift, binding affinity, binding kinetics (Kooistra and Richards, 1977 and Kooistra et al., 1977), and now the variation of binding with pH.

The apparent difference in the observed "pK_a" values for DNTP-GABA and NTP-GABA binding to MOPC-315 7S immunoglobulin at high pH is probably due to differences in the binding affinity of these two haptens (Kooistra and Richards, 1977) and not because different groups are being titrated on the protein.

Assignment of Chemical Shifts

Proton NMR. As a further study into the molecular interaction which occurs between MOPC-315 and bound hapten an attempt was made to compare the chemical shifts of a fluorine and a hydrogen nuclei bound in the same microenvironment. Since fluorine has occupied p orbitals, molecular interactions that affect the symmetry of these

orbitals can cause very large chemical shifts, because they change the angular momentum of these orbitals. Hydrogen atoms on the other hand, have only a single s electron which has no angular momentum. Because of this difference in electronic structure the chemical shift induced by non-covalent bonding except, for ring currents, which do not disrupt the electronic structure of the molecule (Millet and Raftery, 1972), will cause much larger shifts for fluorine than protons.

Studies with a variety of different nitrophenyl haptens containing a trifluoromethyl label showed that the chemical shift, Δ, of the fluorine nuclei caused by immunoglobulin binding (7S, Fab', and Fv proteins of MOPC-315) was dependent only on the orientation of the trifluoromethyl group relative to the alkyl side chain. The binding affinity of the hapten and the amount of constant region attached to the binding site had no effect on the total chemical shift, Δ, observed (Kooistra and Richards, 1977). Since Δ is sensitive to the difference in the microenvironment experienced by the hapten bound and free in solution, this semblance in chemical shift indicates an identity in the microenvironment experienced by different labelled haptens. Therefore, the substitution of a methyl group for a trifluoromethyl group may affect the binding affinity, but both groups should

still experience the same microenvironment.

It was not possible to determine the position of hapten protons bound to the protein until a large excess of hapten to protein was used. However, the results seen at this high concentration of hapten are consistent with an upfield shift for the methyl group of DNMP-GABA.

The proton NMR spectra of varying amounts of DNMP-GABA to MOPC-315 Fv fragment are shown in Figures 12 and 13. No discernable differences in the aliphatic region between the protein and the protein with DNMP-GABA are seen until a fairly large excess of hapten is added, even when the proton spectra were taken at 220 MHz. A more detailed analysis was done using a computer program to subtract a spectra of the Fv fragment of MOPC-315 with no hapten from a spectra of the Fv fragment plus two equivalents of DNTP-GABA, but the small broad peaks could have arisen from hapten, protein, or from phasing errors.

To differentiate the peak due to the methyl group of DNTP-GABA from other hapten protons and chemically shifted protein absorptions a similar study was done using DNTP-GABA as the ligand. This ligand has essentially the same proton NMR spectra as DNMP-GABA, except, it has a trifluoro-methyl group in place of a methyl group. However, the proton NMR spectra of this ligand bound to the Fv fragment

of MOPC-315 did not show any discernable changes from the protein with no ligand, either, until a large excess was used (Figure 14).

It was hoped that a comparison of the proton NMR spectra of DNMP-GABA bound to the Fv fragment with the protein NMR spectra of DNTP-GABA would show one extra peak due to the methyl group of DNMP-GABA. However, no discernable differences could be seen until a large excess of hapten over protein was used and then the spectra of DNTP-GABA plus the Fv fragment showed two new peaks (δ8.50 and δ2.0 ppm) not seen with DNMP-GABA. These spectra with DNMP-GABA did show one larger peak at δ2.2 ppm. These results are not only somewhat confusing but also somewhat meaningless since they only appear when a large excess of hapten is used.

The δ2.2 ppm peak is probably the methyl group of DNMP-GABA, but it may represent the unbound excess hapten. The small upfield shift of this methyl peak in protein spectra when compared to spectra taken of this hapten in d_6 acetone may be due to bulk magnetic susceptibility and/or about 10% of a larger upfield shift if the hapten is in fast exchange. The two peaks at δ2.0 ppm and δ8.5 ppm that are seen for protein spectra with DNTP-GABA and not with DNMP-GABA probably occur because of differences in the exchange rates of these two haptens upon binding

which may result in different peak widths and maybe even different observed shifts if one of these protons are in fast exchange on one hapten and slow exchange on the other.

CHF_2-GABA. Because of the difficulty in resolving the hapten proton NMR resonances among the protein protons, CHF_2-GABA was used to locate the proton shift by using the decoupler while observing the fluorine NMR of this hapten bound to MOPC-315 protein. Initial studies with this hapten bound to the 7S monomer of MOPC-315 gave inconclusive results because of the broadness of the bound hapten signal and the decrease in signal due to NOE which resulted in very poor signal to noise in a reasonable time.

Better results were obtained when the Fv fragment of MOPC-315 was used. Figure 15 shows the variation in the line width at half peak height of the fluorine NMR absorption of CHF_2-GABA bound to MOPC-315 as different regions of the proton spectra were saturated using different amounts of decoupler power. The complex change in line width with offset of the saturating field when $\gamma H_2/2\pi$ is 0.93 J_{HF} probably occurs because the power band width is less than the coupling constant, which can cause fairly complicated results (Freeman and Whiffen, 1962).

The minimum line width in the fluorine NMR of this bound hapten occurs when protons at δ5.4-6.1 ppm are saturated. Since the center of the proton triplet when the hapten is in buffer in the absence of protein is at δ6.93 ppm this amounts to a 0.8-1.5 ppm upfield shift induced by binding. The fluorine nuclei, on the other hand, shift 1.8-2.0 ppm downfield.

If the CHF_2 group rotates freely, so that the fluorine and the proton experience identical microenvironment these data indicate that the major source of chemical shift, Δ, of the bound fluorine nuclei is not due to ring currents. If ring currents were the major cause of the fluorine chemical shift, Δ, the chemical shift of the fluorine and proton would be approximately equal in magnitude and direction.

Van der Waals' interactions are usually the major cause to media induced chemical shift, Δ, for the fluorine and is about 15 times larger for the fluorines than for the proton in fluoroform (Petrakis and Bernstein, 1963). Downfield chemical shift due to van der Waals' interaction usually represent an increase in the polarizability and/or a decrease in internuclear distances (Emsley and Phillips, 1971) between the fluorine nuclei and molecules in their surrounding environment. Fluorine nuclei are about three and a half times more sensitive to electric

fields from polar molecules then protons, but these electric fields can cause protons and fluorine nuclei to be shifted in opposite directions (Petrakis and Bernstein, 1963). Hydrogen bonding usually causes downfield shifts for both fluorine ($\sim$ 1.22 ppm) and protons ($\sim$ 0.5 ppm) (Doddrell et al., 1969 and Laszlo, 1967). However, the proton and fluorines of the CHF_2 group would hydrogen bind to different types of groups, the proton to a proton acceptor and the fluorine to a proton donor group.

Not only can these medium effects cause chemical shifts, but interaction at the phenyl ring, such as ring stacking or charge transfer, can also cause chemical shifts by affecting the bond character of the fluorine and proton nuclei.

Because of the entanglement of these different sources of chemical shift it is very difficult to speculate on the cause of the observed chemical shifts, especially for fluorine nuclei. Dwek et al. (1977) has attributed the source of large upfield proton shifts on hapten binding to MOPC-315 as due to ring current shifts from aromatic amino acid side chains. Since most non-covalent interactions would cause the fluorine nuclei to shift more than three and a half times the proton shift it is possible that ring current can be the major source of the upfield proton chemical shift.

NOE. As mentioned in the theory section at slow correlation times H-H and H-F dipolar relaxations can become more efficient than F-F dipolar relaxation and the transfer of decoupling power between protons not directly involved in dipolar coupling with the fluorine can cause non-specific NOE's. These conditions make interpretation of NOE results like those in Figures 7-11 less than straightforward. However, the data can be analyzed under several different constrictive assumptions.

It was hoped that by pulsing the decoupler for only a short time ($\sim T_1$ of the fluorines) it would be possible to eliminate non-specific effects. Therefore, each downward peak would represent groups of protons near the trifluoromethyl group of the bound hapten.

If this solution is correct then the sum of the downward peaks should be approximately equal to the total NOE observed under high power broad band decoupling. While at first glance the sum of the downward peaks in the pulse experiments does seem to be approximately equal to the total NOE, the decoupler had only enough time[7] ($\sim T_1$) to change the equilibrium value of the fluorine nuclei by

---

[7] Since these T_1 measurements were made with the decoupler off they may or may not be true exponential relaxation times (Hull and Sykes, 1975a).

about 67%. Therefore, the NOE values shown in Figures 2-4 only represent about 67% of the total possible NOE for each region of proton irradiation. (Stronger decoupling power, with the decoupler on continuously, while providing more saturation also lead to a loss of selectivity.) Therefore, it seems that even in these pulse experiments nonselective NOE's, from non-interacting protons, can occur.

Another possibility is that each of these downward peaks represents not only an interaction directly with the trifluoromethyl group but also indirect proton-proton interactions with each other. This solution would produce direct and indirect NOE's and could give individual NOE values that add to a sum larger than the total NOE.

A very plausible interpretation was recognized during calculations on the involvement of protons on the hapten. These calculations showed that most of the NOE could be due to a direct interaction between the aromatic protons on the hapten with the trifluoromethyl group, and that the other observed interactions are due mainly to non-specific interaction. (The size of these non-specific NOE peaks are probably proportional to the number and efficiency of the protons in that region to interact with the aromatic protons of the hapten.)

The effect of the aromatic protons of DNTP-GABA and NTP-GABA will be discussed separately. In the discussion of these data several internuclear distances have been calculated using bond lengths published by Sutton (1965) and assuming tetrahedryl symmetry for saturated atoms and trigonal planar symmetry for unsaturated atoms.

DNTP-GABA. Figures 7-9 show the NOE of the fluorines of DNTP-GABA bound to MOPC-315 Fv protein when various sections of the proton spectra are decoupled. These figures show that the largest interaction between the fluorines of the bound hapten are with protons with a chemical shift of about δ6.5 ppm. This NOE is thought to be due to the aromatic protons on the hapten.

In order to determine the relative importance of fluorine-proton relaxation there must be some knowledge of the internuclear distance and the rotational correlation time.

The internuclear distance between the fluorine atoms of the trifluoromethyl group is 2.20 Å. The distance of closest approach between the aromatic protons of the hapten and a fluorine on the trifluoromethyl group is about 2.3 Å and about 2.4 Å when the trifluoromethyl group is in the staggered position. While these two rotomers place one or two of the fluorines in very close contact

with the proton(s) the other fluorine(s) is much further away. Calculation of the average distance between all three fluorines and the two aromatic protons is much more difficult to do mathematically. However, Figure 8 shows not only the NOE of DNTP-GABA bound to the Fv fragment of MOPC-315 but also the NOE of the free hapten in buffer. The free hpaten shows two peaks of similar magnitude each representing approximately 12% of the total fluorine relaxation. The semblance of the NOE at δ8.5 ppm, due to the aromatic protons, and the NOE at δ5.0 ppm, due to the interaction of the trifluoromethyl group with the water protons, indicates that the average fluorine aromatic distance is approximately equal to the distance between the fluorine and the protons of the water solvent. This distance is probably close to the fluorine-proton van der Waals contact distance of 2.65 $\mathring{A}$ (Cruickshank et al., 1964). By making the following assumptions: (1) all fluorine relaxation occurs by dipolar mechanism between fluorines of the trifluoromethyl group (η^{FF}) or by fluorine-proton (ρ^{HF}) interaction; (2) a correlation time for the free hapten of less than 10^{-10} sec; (3) a fluorine-fluorine distance of 2.20 $\mathring{A}$; (4) that each fluorine can relax to two other fluorines, and (5) is close to a given aromatic proton 2/3's of the time; the average distance between the fluorine and the aromatic

protons can be calculated to be 2.66 Å from the NOE data in Figure 8.

Any other relaxation mechanism or lack of total saturation because of the courseness in the decoupler placement would lead to a shorter calculated internuclear distance.

The efficiency of proton-fluorine dipolar relaxation relative to fluorine-fluorine relaxation increases as the rotational correlation time increases. Thus, while the two aromatic protons only account for 12% of the relaxation in the free molecule these protons can account for a much higher percentage of the relaxation when the hapten is bound to the protein. Therefore, a fairly accurate knowledge of the protein correlation time is also needed for a more thorough investigation of the NOE data.

The rotational correlation time of the protein/hapten complex is related to T_1 and T_2. The rotational correlation time of the bound hapten can be calculated from the T_1 and T_2 relaxation time by (1) using the above calculated internuclear distances, (2) the "like spin" dipolar formulation presented by Solomon (1955) for the fluorine-fluorine contribution to $1/T_1(\eta^{FF})$ and $1/T_2$, and (3) the unlike spin formulas (Doddrell et al., 1971) for the proton-fluorine contributions to $1/T_1(\rho^{HF})$ and $1/T_2$. The 24 Hz intrinsic line width of DNTP-GABA bound to the Fv fragment (Kooistra et al., 1977) corresponds

to a rotational correlation time of 1.8×10^{-8} sec. This correlation time gives a calculated T_1 of 0.30 sec versus the observed valued of 0.24 ± 0.5 sec for the protein hapten solution used in the NOE experiment shown in Figure 3. The closeness of the observed and calculated T_1 values indicates that internal rotation is very slow (greater then the protein correlation time), and that these two aromatic protons account for most of the fluorine cross relaxation. Since the three fluorines only produce one signal the three fluorines must experience the same environment so there is probably some internal motion of the trifluoromethyl group on the bound hapten. This places the lower limit to internal rotation at the milli second level, which is much slower than the isotropic motion of the protein.

This correlation time is longer than that calculated by Dwek et al. (1975) of 7×10^{-9} sec, but is consistent with the 7×10^{-8} sec correlation time used by Hull and Sykes (1975a and b) for alkaline phosphatase (86,000 M.W.). (Correlation time is directly proportional to molecular weight viscosity and molecular shape being equal.) The 0.1 NOE observed under high power noise decoupling requires a correlation time greater than 1×10^{-8} sec.

At this correlation time (1.8×10^{-8} sec) fluorine relaxation to the two aromatic protons is calculated to be about three times more efficient than the fluorine-fluorine relaxation, and the predicted NOE is about 0.23, which is within the experimental error of these calculations to the observed value of 0.1-0.13. This small difference may also be due to slight errors in bond lengths and/or the presence of other protons at a longer distance which account for minor relaxation pathway.

These calculations may seem somewhat circuitous since we used a set of internuclear distances to predict a correlation time, and then found that this correlation time predicted that relaxation occurs by the pathway initially assumed. However, while the T_1 contribution due to fluorine-fluorine relative to fluorine-proton relaxation will change drastically with correlation time, the contribution to T_2 relaxation from these two relaxation pathways stays relatively constant. In fact, because of the difference in internuclear distance fluorine-proton relaxation only accounts for 11% of the line width, so that, an error in the number of protons active in dipolar relaxation would only cause a relatively small error in the calculation of the correlation time. Another source of error may be due to other relaxation mechanisms such as chemical shift anistropy which may add about 5 Hz to

the line width (Hull and Sykes, 1975b).

This analysis indicates that the major source of NOE for DNTP-GABA bound to MOPC-315 Fv fragment (at 6.5 ppm) is probably due to the two aromatic protons on the hapten. This places these two protons 2 ppm upfield from their position on the hapten in the absence of protein. Dwek et al. (1977) saw a similar upfield shift for the ring protons of DNP-aspartate. Their data, however, would predict two different absorptions at δ6.2 ppm and δ6.8 ppm, which straddles our single NOE peak. There are three possible reasons why only one absorption is seen in the NOE studies: (1) The power band width of the decoupler does not have the resolution to separate these two peaks. (2) Saturation of non-specific protein aromatic protons can distribute the decoupler energy to both hapten protons decreasing decoupler resolution, and/or (3) the exchange process of hapten binding may average these two protons.

NTP-GABA. This hapten has only one aromatic proton next to the trifluoromethyl group, but it also contains an amine proton that can, depending on the rotational orientation of the nitrogen, interact strongly with the trifluoromethyl group.

The NOE of the free hapten in buffer shows a peak at δ6.5 ppm (Figure 10) which is probably due to cross relaxation between the fluorine and this amine proton. When this hapten is bound to the Fv fragment of MOPC-315 it shows three regions of cross relaxation (downward NOE peaks) in water solution but only two in deuterium oxide solution, indicating the involvement of an exchangeable proton, such as an amine proton.

However, if this proton was involved in an effective dipolar relaxation mechanism with the fluorines of the bound hapten then the total high power noise decoupled NOE in water should be larger than the NOE in deuterium oxide solution, and the T_1 in deuterium oxide solution should be larger. The total NOE in water (0.50) and deuterium oxide (0.49) solution are the same and so are the T_1 values:[8] 0.16 sec (D_2O) and 0.18 sec (H_2O). (A deuterium nuclei is only about 0.06% as effective as a proton in causing dipolar relaxation (Noggle and Schirmer 1971). If all three regions of cross relaxation seen in Figure 10 are due to direct interactions, then they each represent 1/6 of the total fluorine relaxation (since the total NOE is only one-half). If there is equal con-

[8]These T_1 values are not extrapolated to 100% bound, but are probably within experimental error of the true value.

tribution from each downward going peak and a correlation time similar to that found for bound DNTP-GABA in water solution, then in deuterium oxide solution the two remaining peaks should each represent 1/5 of the total relaxation and total NOE should be 0.6 instead of 0.5. These results indicate that the amine proton is not directly involved in cross relaxation with the fluorines on the trifluoromethyl group and that it may be rotated away from the trifluoromethyl group. However, they are fairly close to the experimental error in the NOE measurement. Another source of error may be because the mole fraction of bound hapten was higher in the deuterium oxide solvent spectra than in the water solvent spectra. While no major effects were seen in NOE's from spectra taken at different hapten to protein ratios this small change may be possible. In fact there was a small increase in the size of the downward NOE peaks seen in the selective NOE experiment in D_2O ([AbHap]/[Hap_o] $\sim$ 80%, Figure 11) when compared to the water solvent study ([AbHap]/[Hap_o] $\sim$ 70%, Figure 10). Going from water to deuterium oxide causes about a 10 Hz increase in chemical shift.[9] This

[9]This change in Δ was observed directly for DNTP-GABA and also seemed to be present in NTP-GABA binding though a complete binding study was not done.

shift seems to be due mostly to an upfield shift of the free peak with no change in the position of the bound hapten peak, as referenced to an external standard. The effect of changing solvents on the structure of the binding pocket is not known. A few more careful experiments along this line should be able to determine the orientation of the amine proton of the hapten in the immunoglobulin pocket.

The intrinsic line width of NTP-GABA bound to the Fv fragment of MOPC-315 is essentially the same as the bound line width of DNTP-GABA (Kooistra et al., 1977). Since fluorine-fluorine dipolar relaxation is the major source of T_2 relaxation this indicates that both haptens experience similar isotropic motion when bound to the Fv fragment, as expected.

The T_1 relaxation, which depends heavily on the number of protons available for dipolar relaxation, is less for NTP-GABA (0.18 sec) than for DNTP-GABA (0.24 sec) indicating more protons interacting with the trifluoromethyl group. However, the total NOE for bound NTP-GABA is smaller than the total NOE for bound DNTP-GABA. This is opposite to the expected change in NOE if the shorter T_1 was caused by the interaction of the trifluoromethyl group with more protons.

This apparent mismatch of NOE, T_1, and T_2 data indicates the presence of non-dipolar relaxation mechanisms and/or the presence of internal rotation by the trifluoromethyl group. The effect of internal rotation is fairly complex. Internal motion changes the simple spectral density function given earlier into one that is the sum of three simple spectral density functions each having a correlation time that is dependent on the combination of the internal and over-all reorientation. These new spectral density functions are each modified further depending on the angle between the vector connecting the nuclei and the axis of rotation (Hull and Sykes, 1974).

Normally internal rotation will tend to increase both T_1 and T_2 (Hull and Sykes, 1974). T_1 will usually increase because ρ^{HF} decreases as internal motion increases, but for very slow internal rotation ($> 10^{-8}$ sec) the decrease in ρ^{HF} will be small and η^{FF} will increase causing an overall decrease in the value of T_1 (Hull and Sykes, 1975a), especially since the vector connecting fluorine nuclei vector is 90° to the axes of rotation. Internal rotation in this range will also tend to decrease the maximum NOE possible (closer to one) (Hull and Sykes, 1975a).

A quantitative analysis is beyond the scope of this study, however, a qualitative analysis can be made with reference to results illustrated in Figure 8 of Hull and Sykes (1975a). This figure shows that ρ^{FH} decreases slowly and η^{FF} (same as η^{HH} in this figure) and σ^{FH} (which is negative) both increase fairly rapidly as the correlation time due to internal rotation decreases towards 10^{-9} sec.

As η^{FF} increases (due to slow internal rotation) it will become a more important relaxation pathway than ρ^{HF} causing a decrease in T_1 and a smaller NOE. This internal rotation will also cause $|\sigma^{FH}|$ to become less than ρ^{HF} also reducing the NOE. However, because of the difference in the proton-fluorine versus fluorine-fluorine internuclear distance η^{FF} will increase faster than $|\sigma^{HF}|$ will decrease, so that, the maximum possible NOE (σ^{HF}/ρ^{HF}) should not change very much for slow rates of internal rotation. The 0.50 total NOE observed, therefore, probably indicates that $\eta^{FF} \sim \rho^{HF}$. $\eta^{FF} \sim \rho^{HF}$ means that half of the spin lattice relaxation, T_1, takes place by dipolar relaxation by fluorine-fluorine and half by fluorine-proton interactions.

The correlation time for the internal motion must be fairly large ($\sim 10^{-8}$ sec) otherwise the line width ($1/(\pi T_2)$) of bound TNP-GABA would be smaller than the line width of bound DNTP-GABA (Hull and Sykes, 1974) and the total NOE would also be much smaller (Hull and Sykes, 1975a).

The total number of protons interacting with the trifluoromethyl group is probably about 2 ± 1 (assuming all fluorine-proton distances are about 2.66 Å). More protons than this and the observed T_1 and T_2 could have been explained without internal rotation, and if there is no internal rotation the total NOE seen by this number protons would be much larger than the 0.5 observed. Fewer protons than two would require η^{FF} to be greater than ρ^{FH} and the total NOE would be smaller than the 0.5 observed.

Since none of the selective NOE peaks are large enough to account for the total NOE (even after correcting for only seeing about 67% of the total NOE because the decoupler was pulsed), none of the downward NOE peaks can represent more than one proton. Therefore, the aromatic protons on the hapten probably cause the NOE observed when protons at δ6.7 ppm are saturated (Figures 10 and 11). This indicates that the aromatic proton next to the trifluoromethyl group is shifted about 1.5 ppm upfield on

binding, in agreement with the shifts observed for DNTP-GABA and those reported by Dwek et al. (1977).

Fluorine Chemical Shifts in Deuterium Oxide

Both NTP-GABA and DNTP-GABA show an upfield shift (16 and 13 Hz, respectively) in the ^{19}F NMR spectra taken in deuterium oxide buffer when compared to water buffer solutions. However, the ^{19}F NMR absorption of DNTP-GABA bound to the Fv fragment occurs in the same position in deuterium oxide and water buffer solutions. This indicates that hydrogen bonding is more important between the trifluoromethyl group of the hapten in solution than between this group and the protein when the hapten is bound. This agrees with the NOE data (Figures 8 and 9) which show no change when deuterium oxide or water is used as solvent.

Since the total chemical shift and/or position of the NTP-GABA peak when totally bound to the protein was not determined no conclusions on the importance of hydrogen bond can be made at this time.

The effect of substituting a deuterium for a protein in a hydrogen bond is fairly complicated even in simple systems. Deuterium forms weaker hydrogen bonds in some cases (Dahlgren and Long, 1960), but stronger hydrogen bonds in other systems (Creswell and Allred, 1962). The deuterium exchange that accompanies protein

solvation when deuterium oxide is used as solvent can effect chemical shifts directly if there is hydrogen bonding between the protein and the fluorine. However, deuterium exchange can also cause conformational change by changing the hydrogen bonding involved in secondary, tertiary, and quaternary structure, and these conformational changes can also cause chemical shifts.

CONCLUSION

The pH studies on the binding of DNTP-GABA and NTP-GABA to MOPC-315 protein show one or two ionizable groups on the protein with a pK_a between 8.5 and 9.0. The deprotonation of this group(s) causes a reversible loss in the protein's ability to bind hapten.

At pH values below 5 the hapten precipitates, but the intensity of the bound hapten peak in the NMR spectrum does not decrease until the pH is lowered below 3.5. This decrease in the NMR signal of the bound peak is thought to be due to precipitation of the immunoglobulin containing bound hapten.

The pH profile of DNTP-GABA binding to the Fv fragment of MOPC-315 is essentially the same for the 7S monomer. Indicating that the changes in binding are due to groups located within the variable region of the immunoglobulin.

Double resonance experiments show that the downfield shift experienced by fluorine nuclei para to the alkyl side chain are not caused solely by diamagnetic ring currents. In fact, the ring current's contribution to the fluorine chemical shift is thought in the upfield direction.

NOE data indicates that the aromatic protons on the hapten next to the trifluoromethyl group undergo an up-filed shift in agreement with observation by Dwek et al. (1977). These NOE data were also used to determined the rate of internal rotation by the bound trifluoromethyl group. The internal rotation of the trifluoromethyl group of DNTP-GABA seems to be much less than the tumbling rate of the protein (1.8×10^{-8} sec) while the trifluoro-methyl group of NTP-GABA appears to rotate with a correlation time around 10^{-8} sec.

Comparison of fluorine chemical shift and NOE of DNTP-GABA bound to the Fv fragment of MOPC-315 in water buffer with spectra in deuterium oxide buffer show that no important hydrogen bonds are formed between the fluorine and the binding site of the protein.

REFERENCES

Corey, E.J. and Suggs, J.W. (1975), Tet. Letters 2647.

Creswell, C.J. and Allred, A.L. (1962), J. Amer. Chem. Soc. 84, 3966.

Cruickshank, D.W.J., Jones, D.W., and Walker, G. (1964), J. Chem. Soc. (London), 1303.

Dahlgren, G., Jr. and Long, F.A. (1960), J. Amer. Chem. Soc. 82, 1303.

Doddrell, D., Glushko, V., and Allerhand, A. (1971), J. Chem. Phys. 56, 3683.

Doddrell, D., Wenkert, E., and Demarco, P.V. (1969), J. Mol. Spectrosc. 32, 163.

Dwek, R.A., Jones, R., Marsh, D., McLaughlin, A.C., Press, E.M., Price, N.C., and White, A.I. (1975), Phil. Trans. R. Soc. Lond. B. 272, 53.

Dwek, R.A., Wain-Hobson, S., Dower, S., Gettens, P., Sutton, B., Perkins, S.J., and Givol, D. (1977), Nature 266, 31.

Emsley, J.W. and Phillips, L. (1971), Progress in NMR Spectroscopy 7, 1.

Ernst, R.R. (1966), J. Chem. Phys. 45, 3845.

Freeman, R. and Hill, H.D.W. (1971), J. Chem. Phys. 54, 3367.

Freeman, R. and Whiffen, D.H. (1962), Proc. Phys. Soc. (London) 79, 794.

Gammon, K.L., Smallcombe, S.H., and Richards, J.H. (1972), J. Amer. Chem. Soc. 94, 4573.

Gerig, J.T. (1977), J. Amer. Chem. Soc. 99, 1721.

Harrison, I.T., Lewis, B., Nelson, P., Books, W., Roszkowski, A., Tomolonis, A., and Freed, J.H. (1970), J. Med. Chem. 13, 203.

Hull, W.E. and Sykes, B.D. (1974), Biochem. 13, 3431.

Hull, E.W. and Sykes, B.D. (1975a), J. Chem. Phys. 63, 867.

Hull, W.E. and Sykes, B.D. (1975b), J. Mol. Biol. 98, 121.

Klostergaard, J., Grossberg, A.L., Krausz, L.M., and Pressman, D. (1977a), Immunochem. 14, 37.

Klostergaard, J., Krausz, L.M., Grossberg, A.L., and Pressman, D. (1977b), Immunochem. 14, 107.

Kooistra, D.A. and Richards, J.H. (1977), Biochemistry, in press. Also see part II of this thesis.

Kooistra, D.A., Smallcombe, S.H., and Richards, J.H. (1977), Biochemistry, submitted, also see part III of this thesis.

Laszlo, P. (1967), Prog. in NMR Spectro. 3, 231.

Millett, F. and Raftery, M.A. (1972), Biochem. Biophys. Res. Comm. 47, 625.

Noggle, J.H. and Schirmer, R.E. (1971), "The Nuclear Overhauser Effect," Academic Press, New York, NY.

Pachler, K.G.R. (1972), J. Mag. Res. 7, 442.

Padlan, E.A., Davies, R.D., Pecht, I, Givol, D. and Wright, C. (1976), Cold Springs Harbor Symp. Quant. Biol. 41, 627.

Petrakis, L. and Bernstein, H.J. (1963), J. Chem. Phys. 38, 1562.

Solomon, I. (1955), Phys. Review 99, 559.

Sutton, L.E. (ed.) (1965), "Tables of Interatomic Distance and Configuration in Molecules and Ions" The Chemical Society, Burlington House, London, England.

Zweifel, G. and Brown, H.C. (1963), Organic Reactions 13, 1.